Kardiorenální problematika v experimentu, modely

Matúš Miklovič

KLINICKÁ FYZIOLOGIE KARDIOVASKULÁRNÍHO A RENÁLNÍHO SYSTÉMU – OD TEORIE K PRAXI

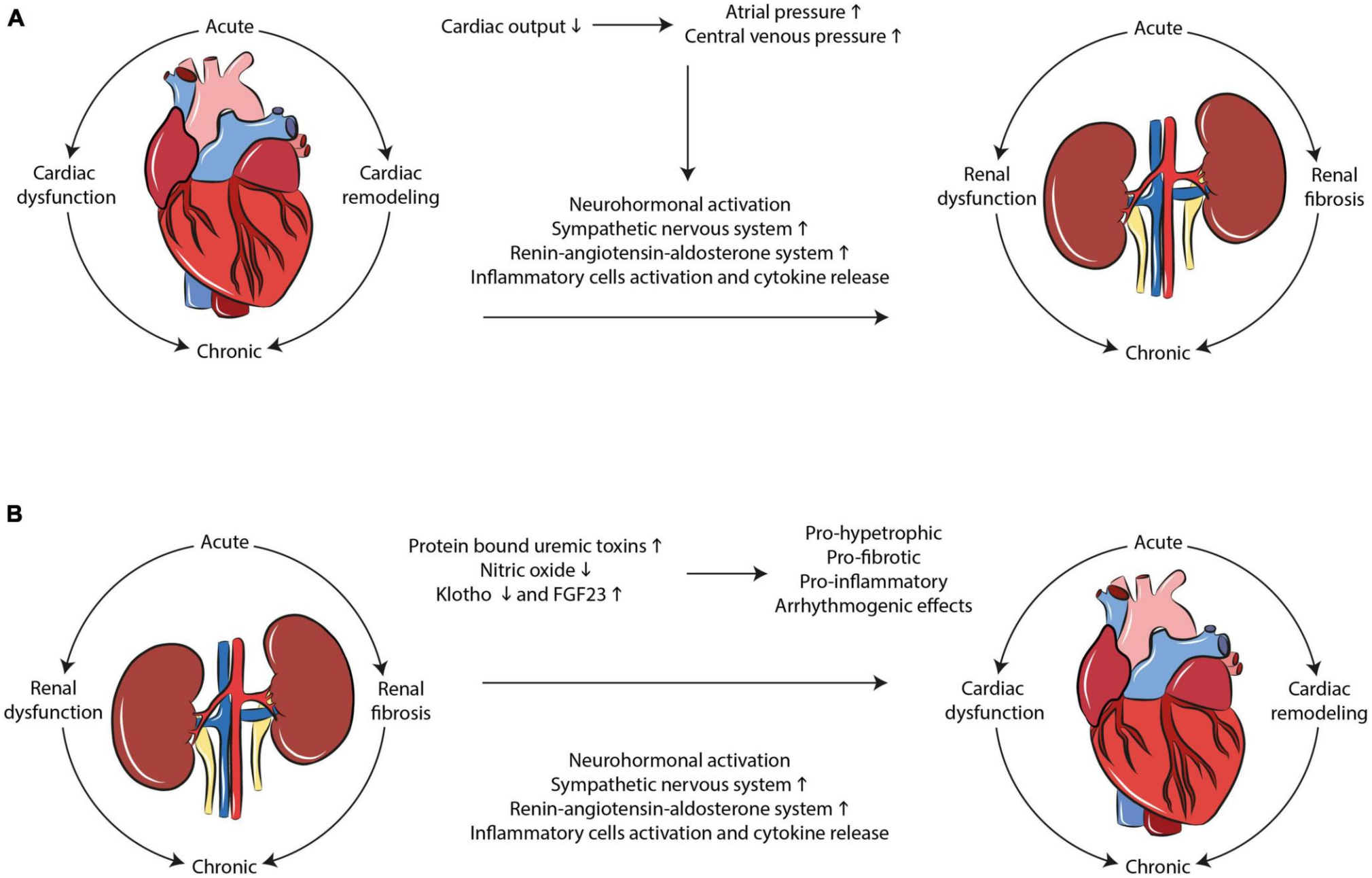

Gabbin B, Meraviglia V, Mummery CL, Rabelink TJ, van Meer BJ, van den Berg CW and Bellin M (2022) Toward Human Models of Cardiorenal Syndrome *in vitro*. *Front. Cardiovasc. Med.* 9:889553. doi: 10.3389/fcvm.2022.889553

CRS Type I (Acute cardiorenal syndrome)
Abrupt worsening of cardiac function leading to acute kidney injury

CRS Type II (Chronic cardiorenal syndrome)
Chronic abnormalities in cardiac function (e.g. chronic congestive heart failure) causing progressive and permanent chronic kidney disease

CRS Type III (Acute renocardiac syndrome)
Abrupt worsening of renal function (e.g. acute kidney ischaemia or glomerulonephritis) causing acute cardiac disorders (e.g. heart failure, arrhythmia, ischemia)

CRS Type IV (Chronic renocardiac syndrome)
Chronic kidney disease (e.g. chronic glomerular disease) contributing to decreased cardiac function, cardiac hypertrophy and/or increased risk of adverse cardiovascular events

CRS Type V (Secondary cardiorenal syndrome)
Systemic condition (e.g. DM, sepsis) causing both cardiac and renal dysfunction

Experimentálne modely a klinická translácia

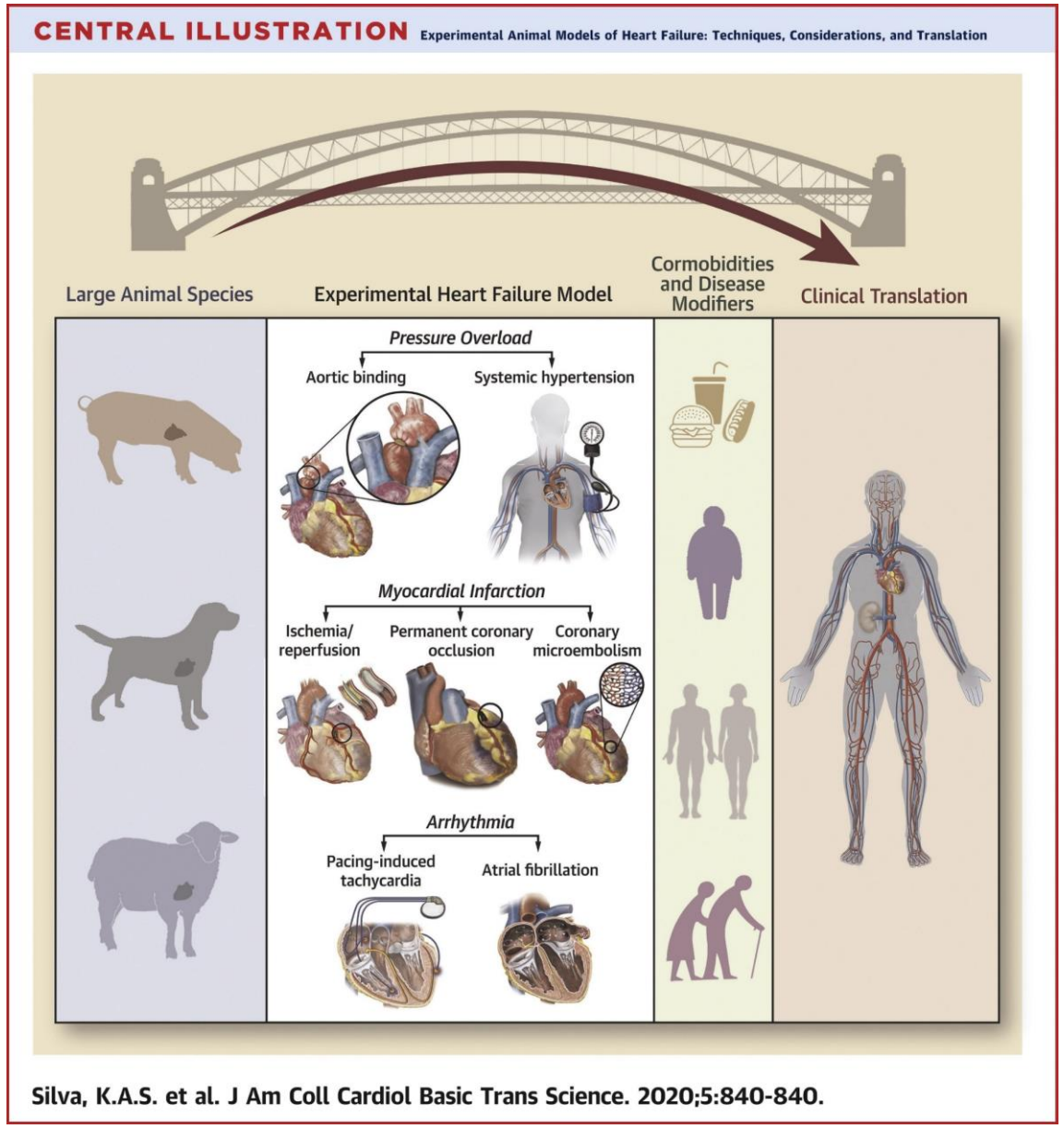

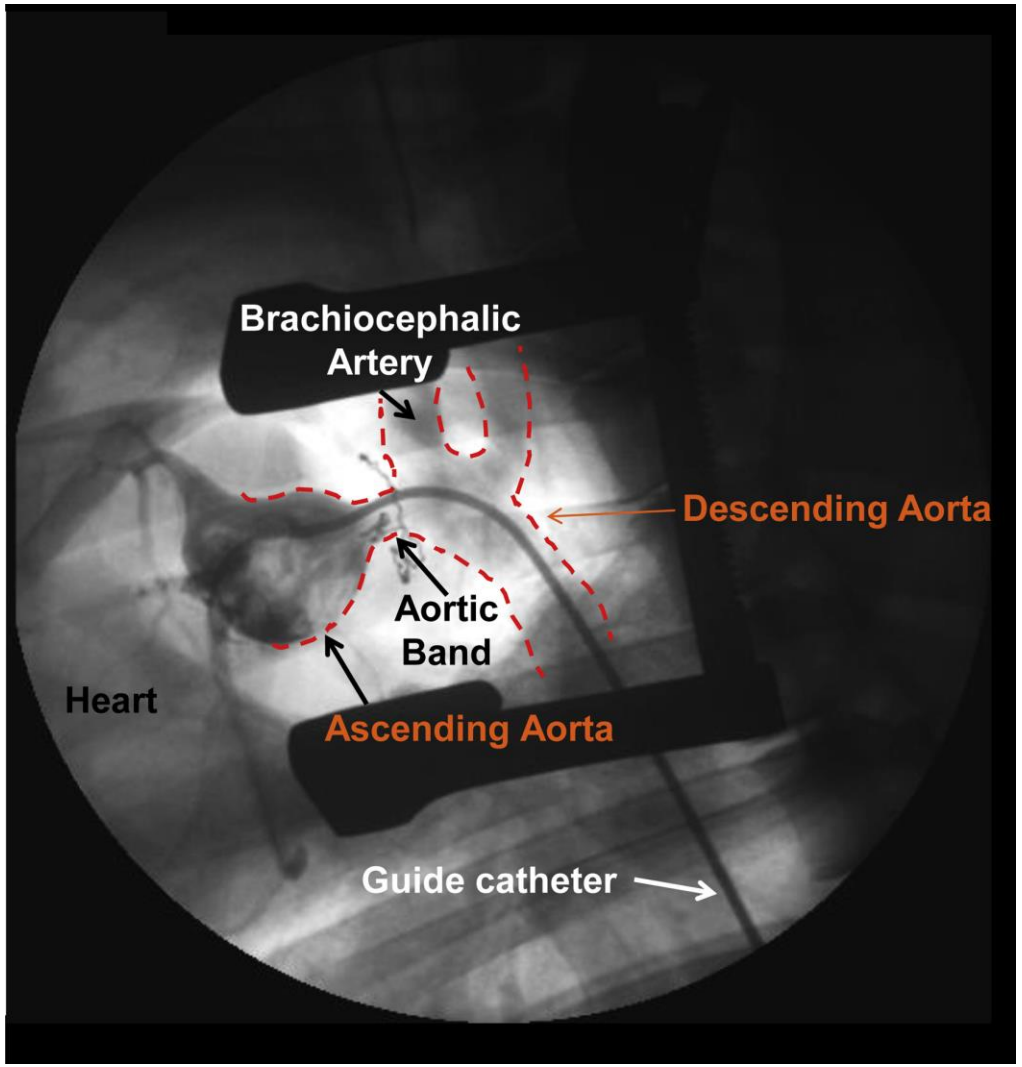

Silva, K. A. S., & Emter, C. A. (2020). Large Animal Models of Heart Failure: A Translational Bridge to Clinical Success. *JACC. Basic to translational science*, *5*(8), 840–856. https://doi.org/10.1016/j.jacbts.2020.04.011

Výber vhodného experimentálneho modelu

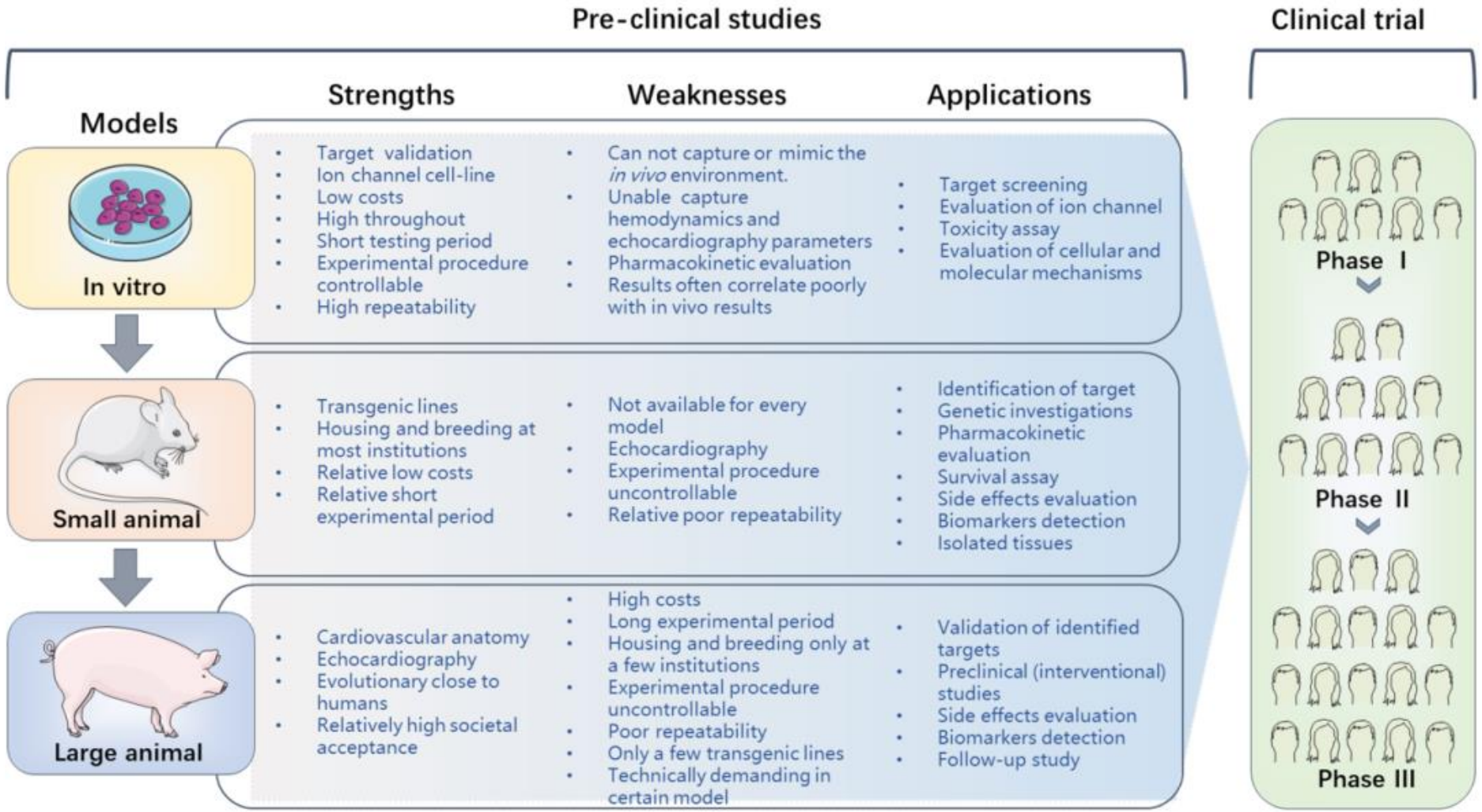

Yin wu, Liang Cao, Zeyu Cao, et al. Insights in animal models for translational cardiovascular research ： A pharmaceutical industry perspective. *Authorea.* April 22, 2021

Rozdelenie modelov podľa spôsobu navodenia HF

- Operačný zákrok (ACF, IM, TAC, 2K1C, 5/6 nefraktómia)
- Injekčné podanie: cytotoxické antracyklínové ATB (doxorubicin), L-NAME
- Orálne podanie (L-NAME, adenín-CKD)
- Spontánne nadobudnuté (vrátane genetických modifikácií)
- Kombináciou (IM+ monocrotaline)

Modely HF a ich limitácie

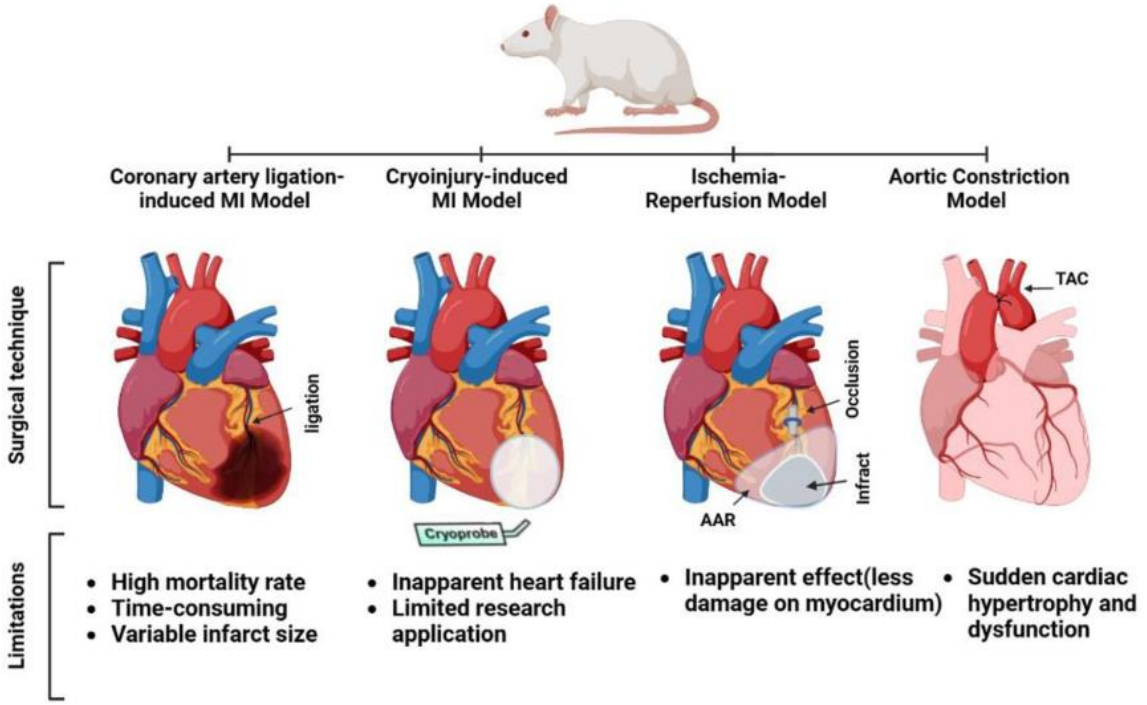

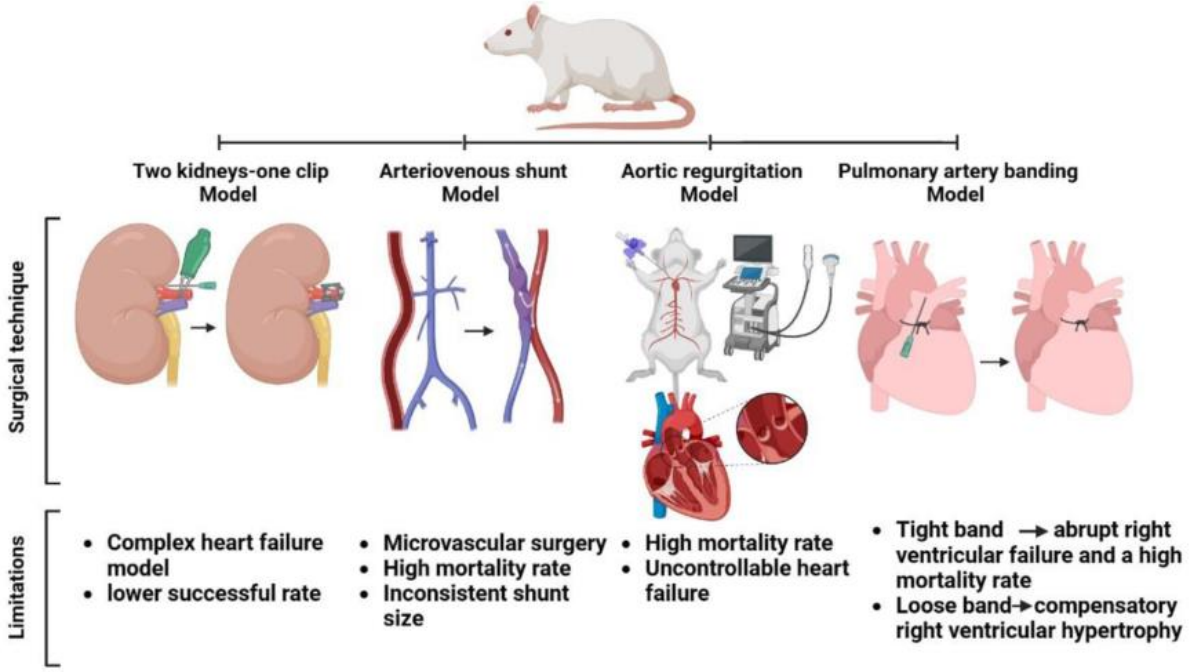

Farag, A., Mandour, A. S., Hendawy, H., Elhaieg, A., Elfadadny, A., & Tanaka, R. (2023). A review on experimental surgical models and anesthetic protocols of heart failure in rats. *Frontiers in veterinary science*, *10*, 1103229. https://doi.org/10.3389/fvets.2023.1103229

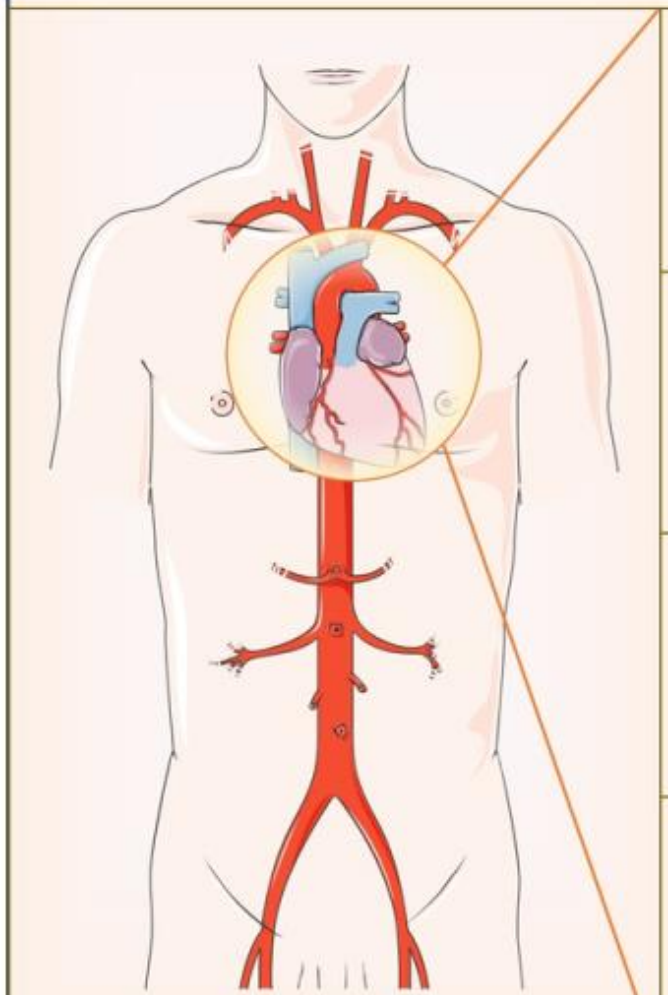

Major Causes of Heart Failure		Application of selected animal models for HF research					
	Heart Failure Stimulus						
 Ischemia	Coronary artery occlusion	✓	✓	✓	✓	✓	
	Ischemia-reperfusion	✓	✓	✓	✓	✓	
	Coronary microembolization	✗	✗	✓	✓	✓	
 Hypertension	Transgenic animal	✓	✓	✗	✗	✗	
	Renal artery stenosis	✓	✓	✓	✓	✓	
	Pulmonary arterial hypertension	✓	✓	✓	✓	✓	
 DCM	Chemical induced	✓	✓	✓	✓	✓	
	Rapid ventricular pacing	✗	✗	✓	✓	✓	
	Transgenic animal	✓	✓	✗	✗	✗	
 Valve disease	Transverse aortic constriction	✓	✓	✓	✓	✓	
	Chordae tendineae cutting	✗	✗	✓	✗	✓	

Ziyin wu, Liang Cao, Zeyu Cao, et al. Insights in animal models for translational cardiovascular research ： A pharmaceutical industry perspective. *Authorea.* April 22, 2021.
DOI: 10.22541/au.161909759.96594467/v1

Volume overload – ACF model

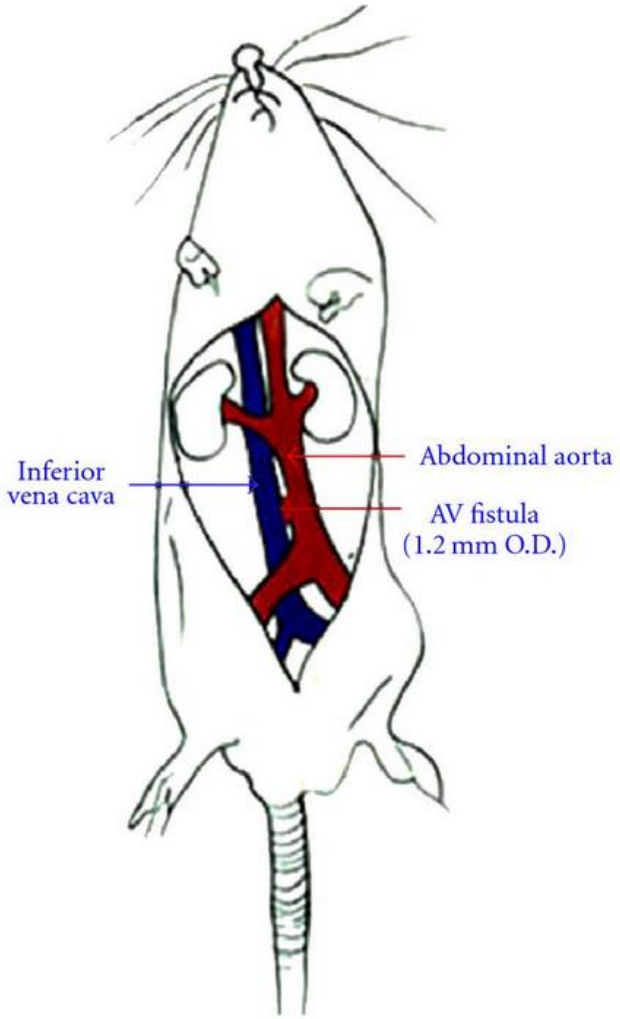

Abassi et al., 2011

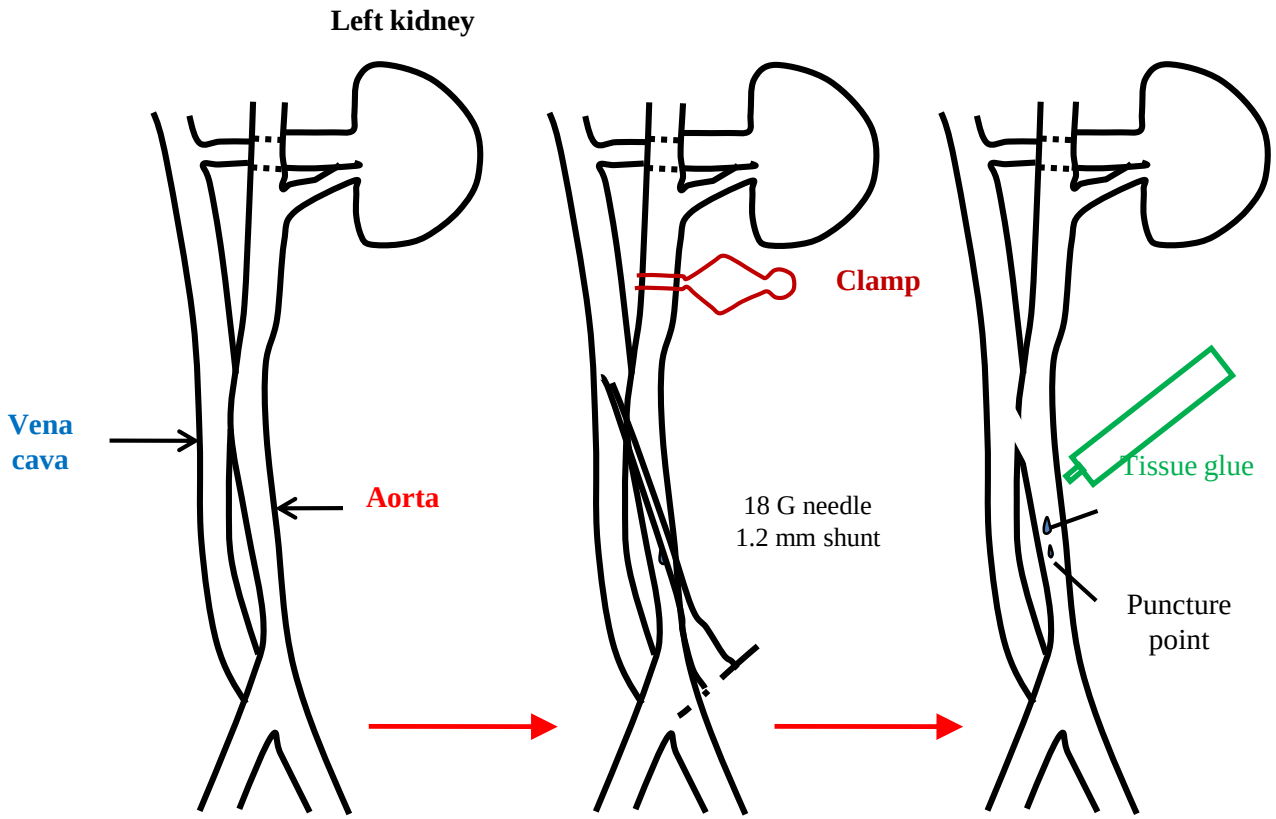

Garcia, R., & Diebold, S. (1990). Simple, rapid, and effective method of producing aortocaval shunts in the rat. *Cardiovascular research*, *24*(5), 430–432. https://doi.org/10.1093/cvr/24.5.430

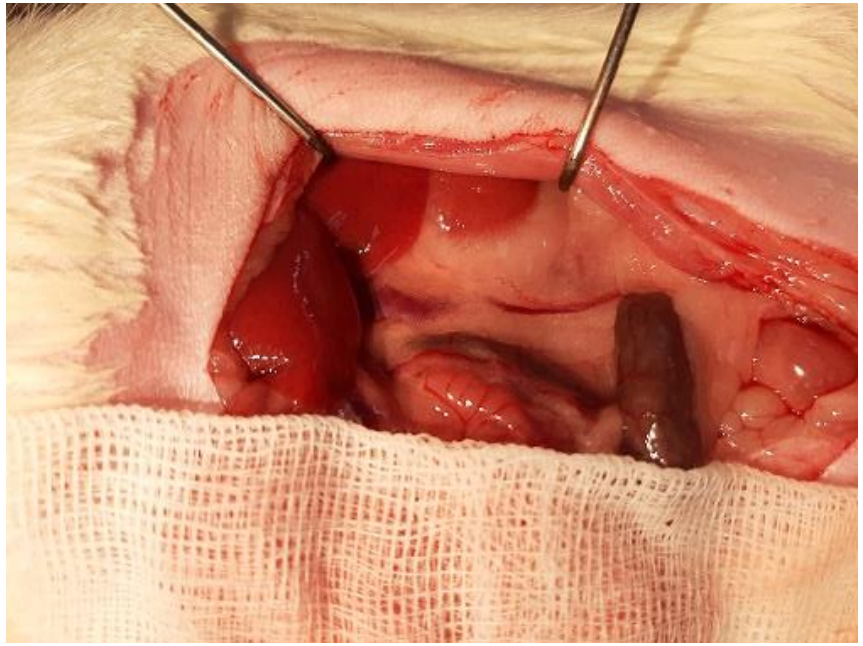

Sham-operated rats

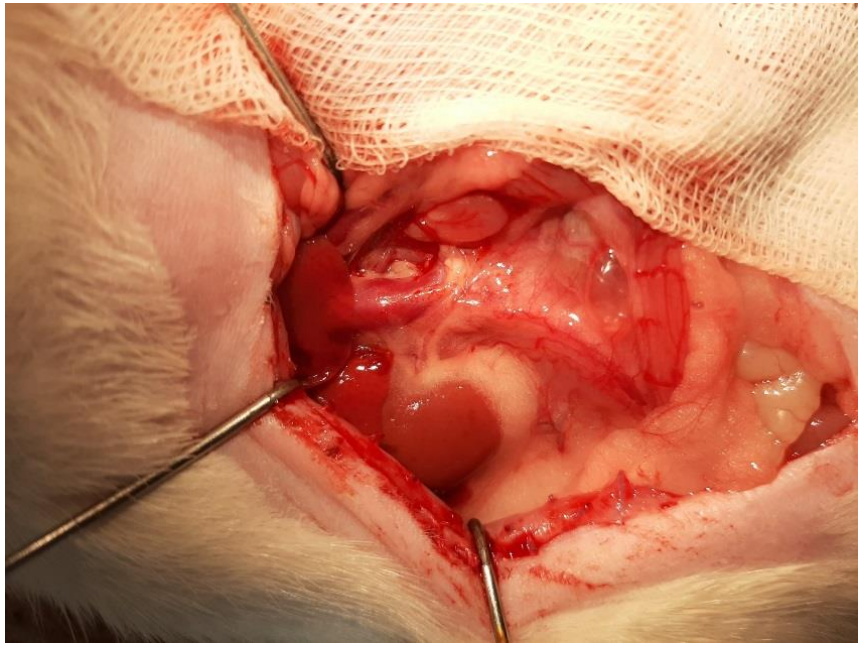

ACF rats (1 week)

Sham-operated HanSD

Heart weight (mg)/Body weight (g)
2.97 ± 0.04

ACF HanSD

Heart weight (mg)/Body weight (g)
3.86 ± 0.11

Sham-operated TGR

Heart weight (mg)/Body weight (g)
3.68 ± 0.04

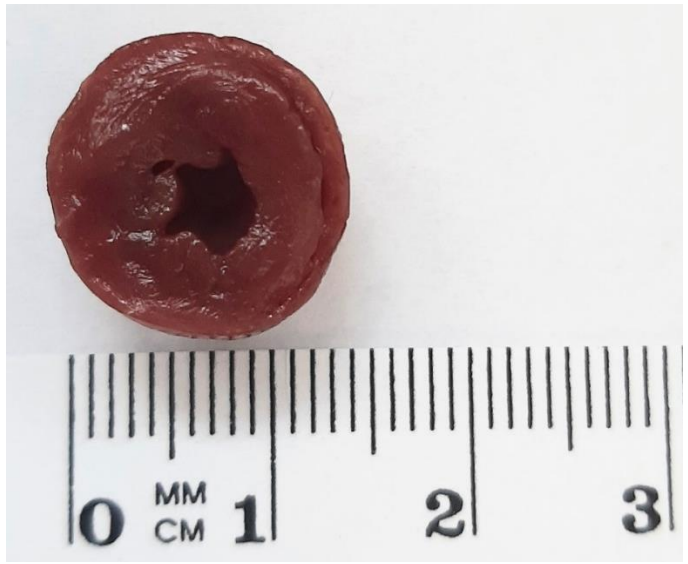

ACF TGR

Heart weight (mg)/Body weight (g)
4.42 ± 0.07

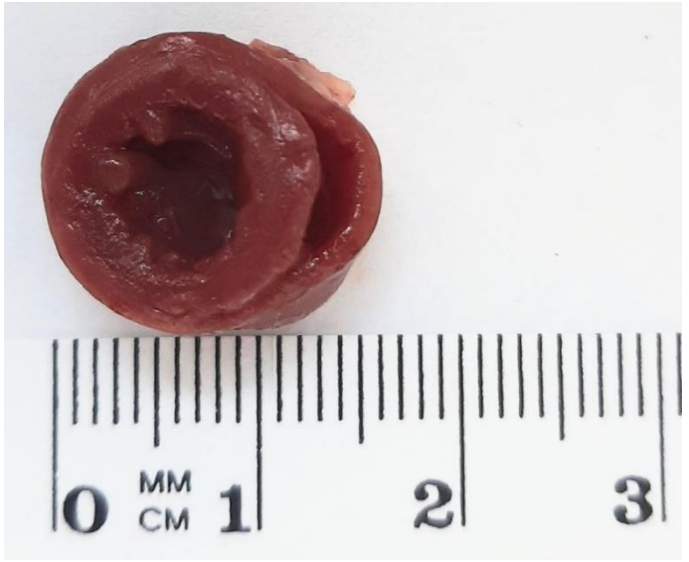

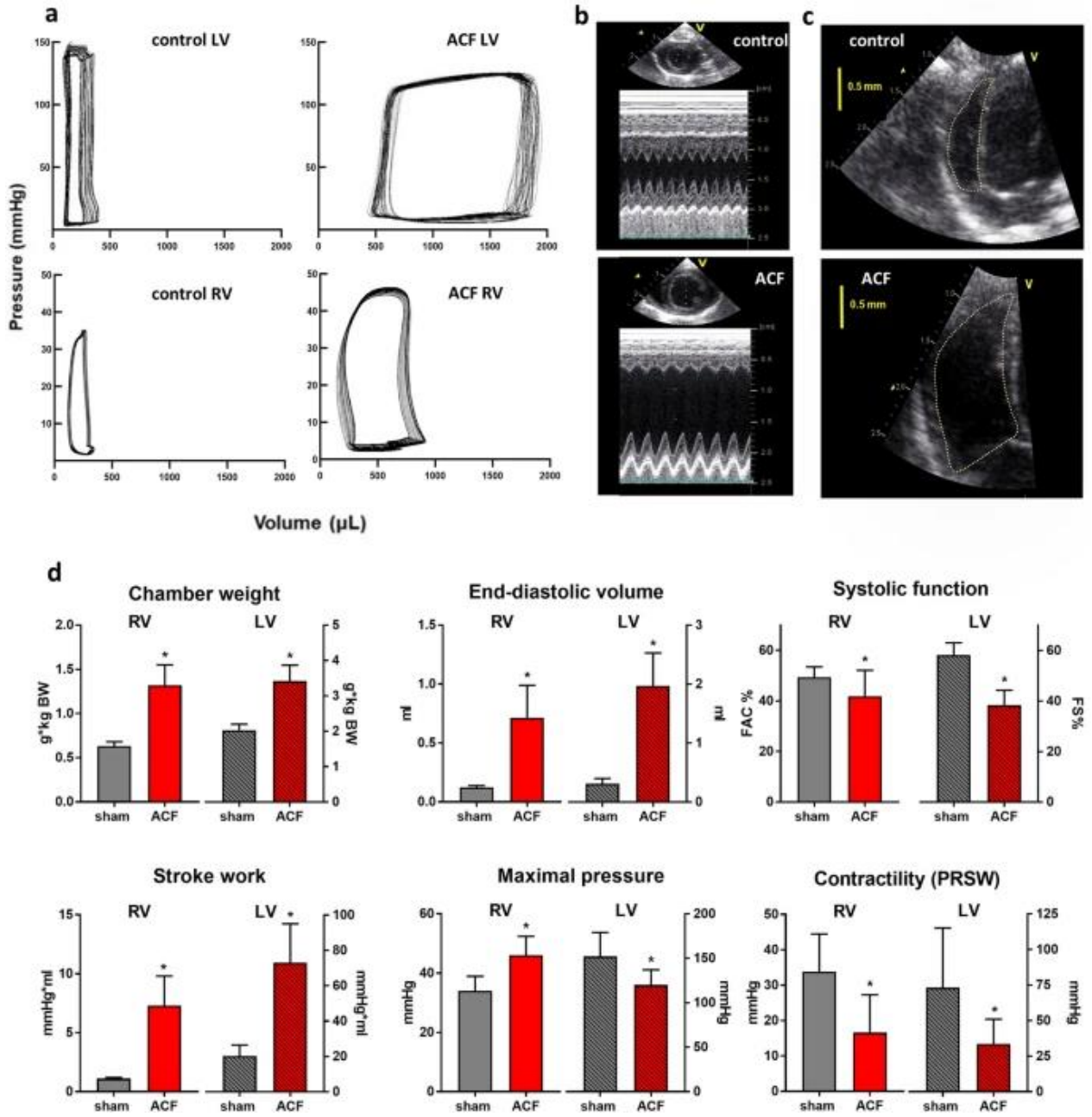

Havlenova, T., Skaroupkova, P., Miklovic, M. *et al.* Right versus left ventricular remodeling in heart failure due to chronic volume overload. *Sci Rep* **11**, 17136 (2021). https://doi.org/10.1038/s41598-021-96618-8

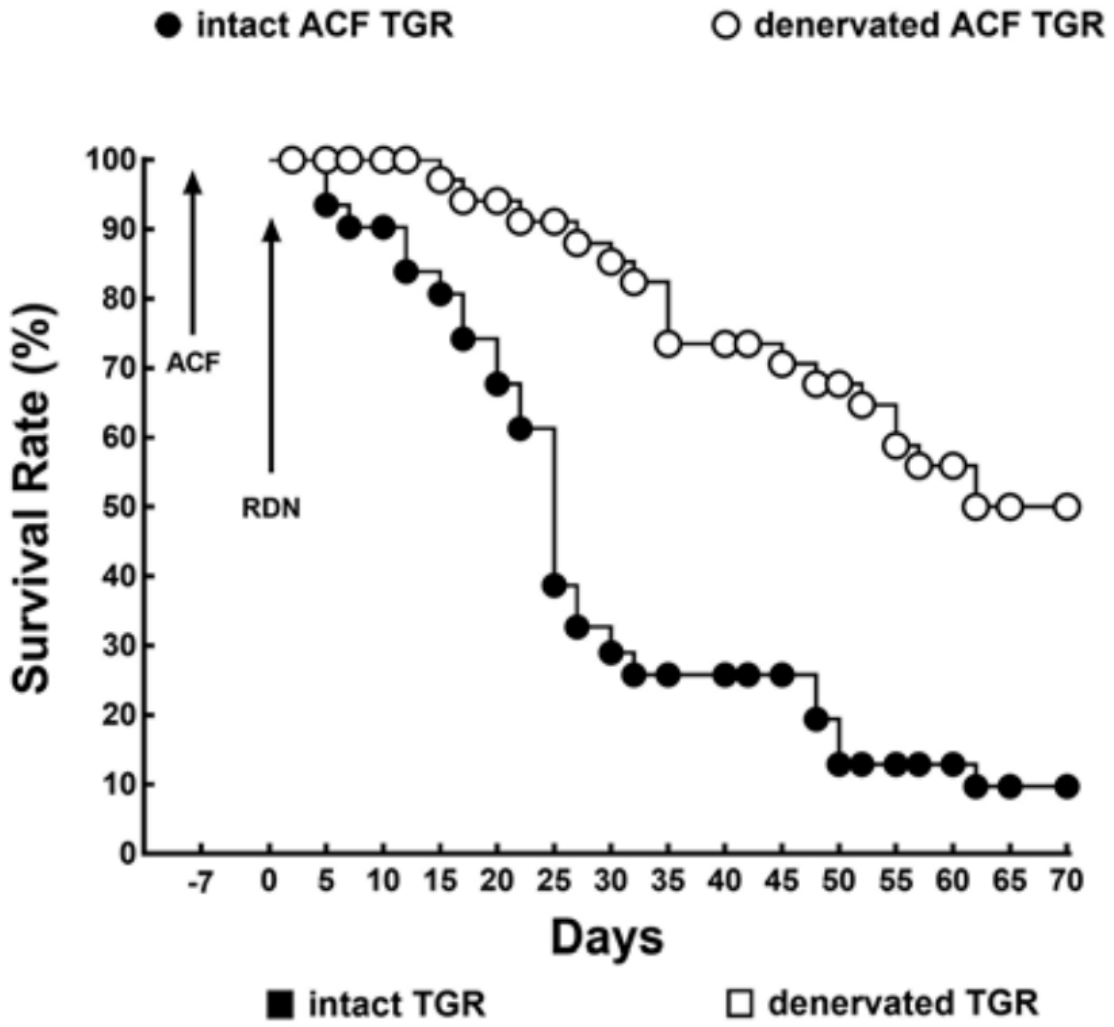

Honetschlagerová Z, et al. : Renal Sympathetic Denervation Attenuates Congestive Heart Failure in Angiotensin II-Dependent Hypertension: Studies with Ren-2 Transgenic Hypertensive Rats with Aortocaval Fistula. Kidney Blood Press Res 2021;46:95-113. doi: 10.1159/000513071

Ren-2 transgenic hypertensive rats (TGR)

+

Aorto-caval fistula (ACF)

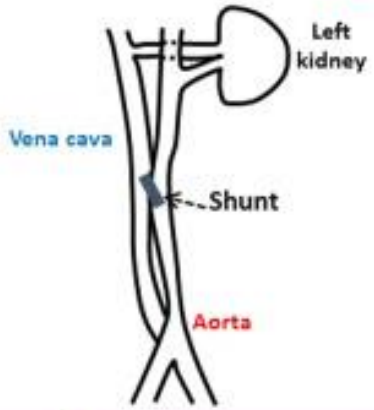

=

ACF TGR
model of combined
AGN II-dependent hypertension
+
heart failure

Basal values

1 week after ACF induction or sham-operation

ACF TGR vs. Sham-operated TGR

Renal Blood Flow (RBF)	↓
Urine Flow (UF)	↓
Absolute Sodium Excretion ($U_{Na}V$)	↓

Effects of stepwise changes in renal arterial pressure

	Sham-operated TGR	ACF TGR
RBF	↓↓	↔
UF	↓↓↓↓	↓↓
$U_{Na}V$	↓↓↓↓	↓↓

Conclusion: ACF TGR displayed well-maintained RBF autoregulatory capacity and better slope of the pressure-natriuresis relationship as compared with sham-operated TGR.

Honetschlägerová, Z., Sadowski, J., Kompanowska-Jezierska, E., Maxová, H., Táborský, M., Kujal, P., & Červenka, L. (2023). Impaired renal autoregulation and pressure-natriuresis: any role in the development of heart failure in normotensive and angiotensin II-dependent hypertensive rats?. *Hypertension research : official journal of the Japanese Society of Hypertension*, *46*(10), 2340–2355. https://doi.org/10.1038/s41440-023-01401-z

Pressure-overload model

- Cyp1a1-Ren2 rats with I3C

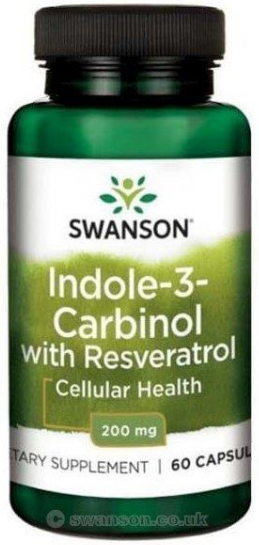

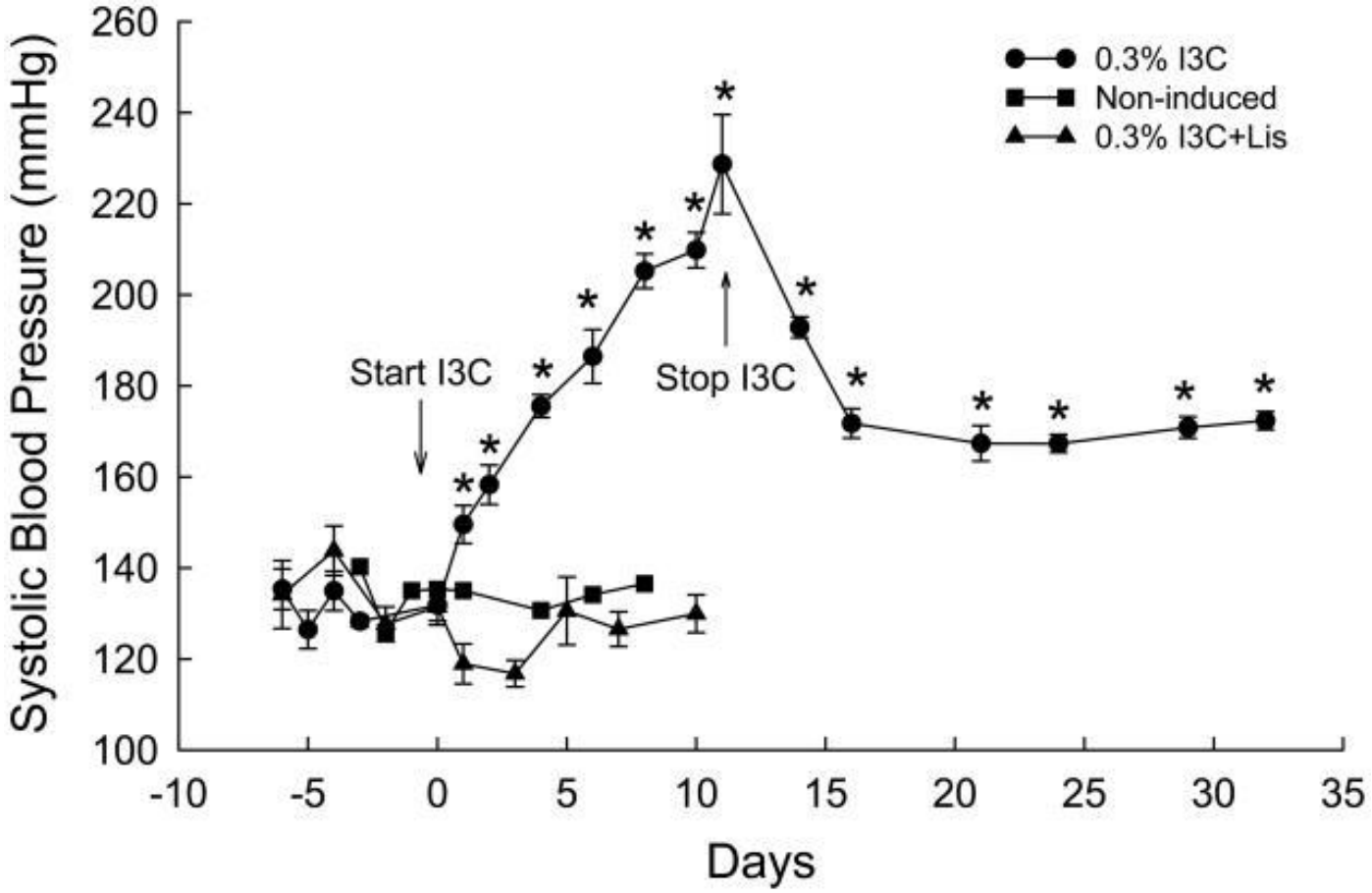

Howard CG, Mullins JJ, Mitchell KD. Transient induction of ANG II-dependent malignant hypertension causes sustained elevation of blood pressure and augmentation of the pressor response to ANG II in CYP1A1-REN2 transgenic rats. Am J Med Sci. 2010 Jun;339(6):543-8. doi: 10.1097/MAJ.0b013e3181d82a62. PMID: 20375689; PMCID: PMC2882982.

Effects of early treatment

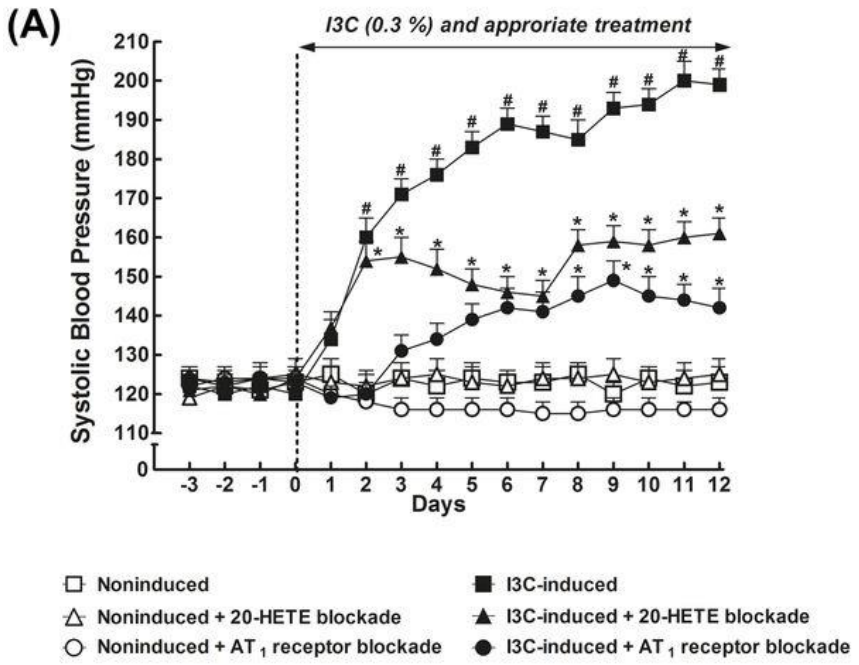

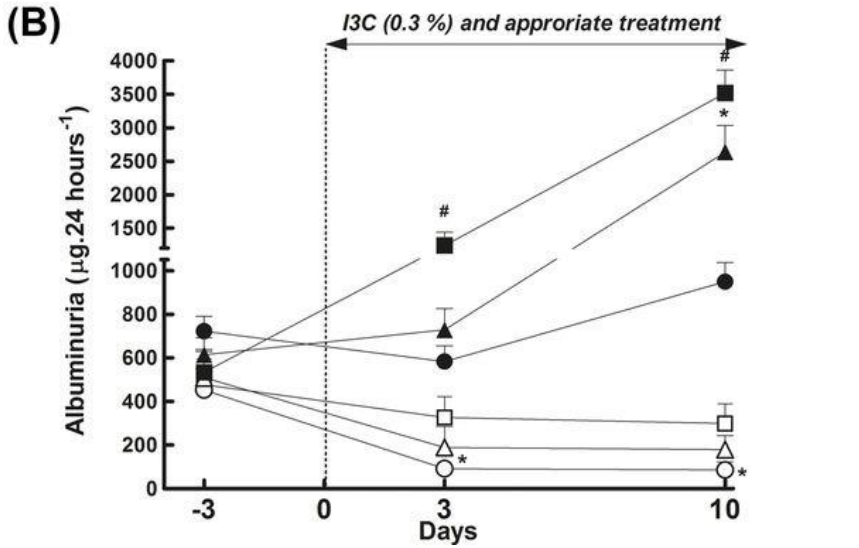

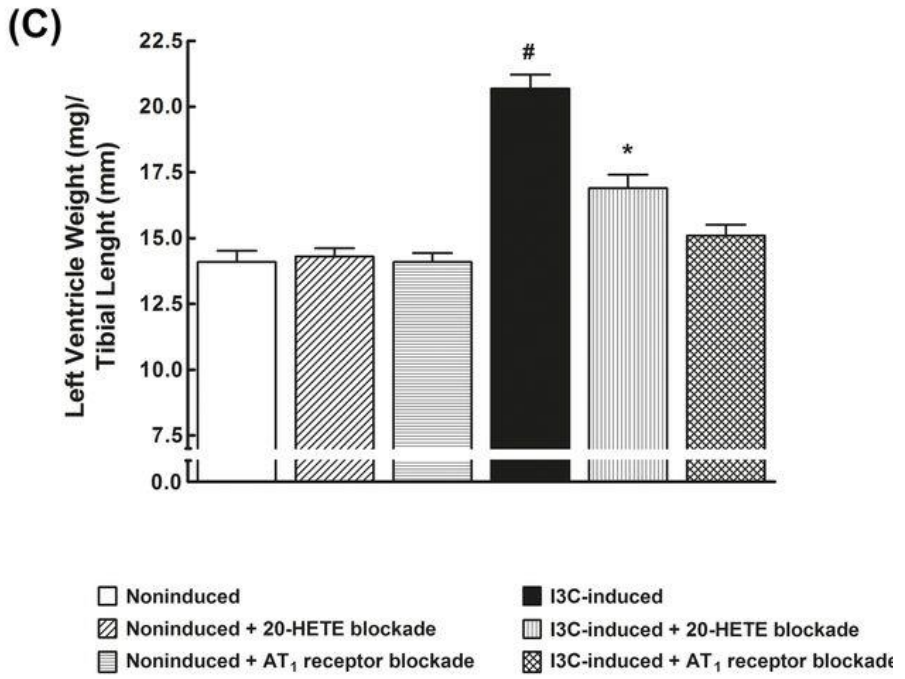

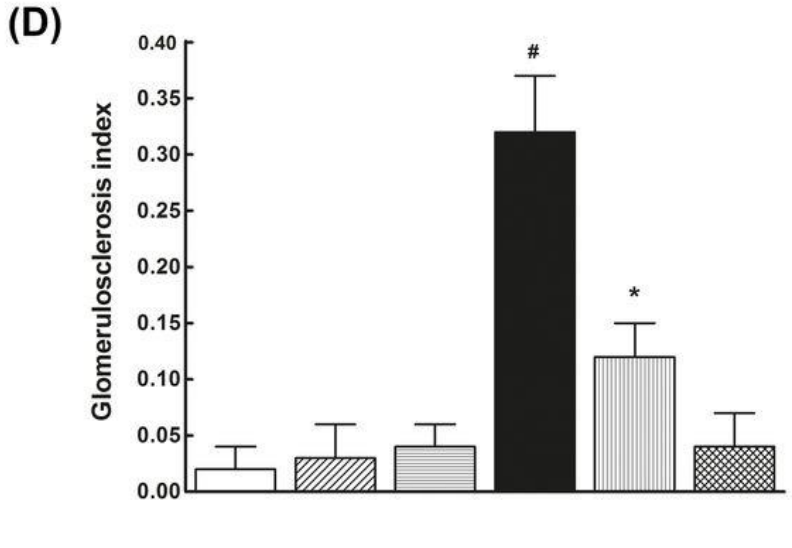

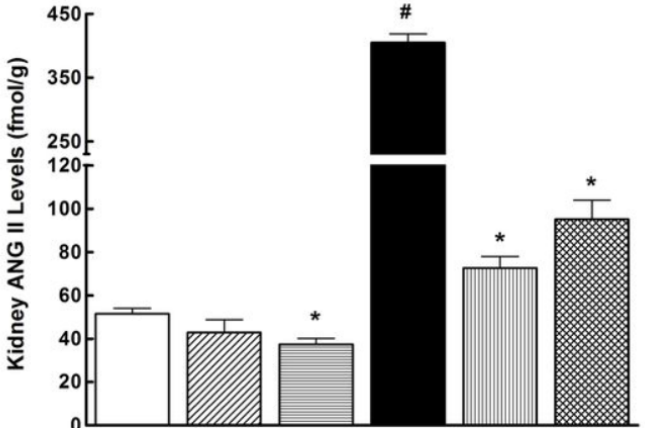

Sedláková L, Kikerlová S, Husková Z, Červenková L, Chábová VČ, Zicha J, Falck JR, Imig JD, Kompanowska-Jezierska E, Sadowski J, Krátký V, Červenka L, Kopkan L. 20-Hydroxyeicosatetraenoic acid antagonist attenuates the development of malignant hypertension and reverses it once established: a study in Cyp1a1-Ren-2 transgenic rats. Biosci Rep. 2018 Sep 12;38(5):BSR20171496. doi: 10.1042/BSR20171496. PMID: 30054426; PMCID: PMC6131326.

Pressure-overload model HF

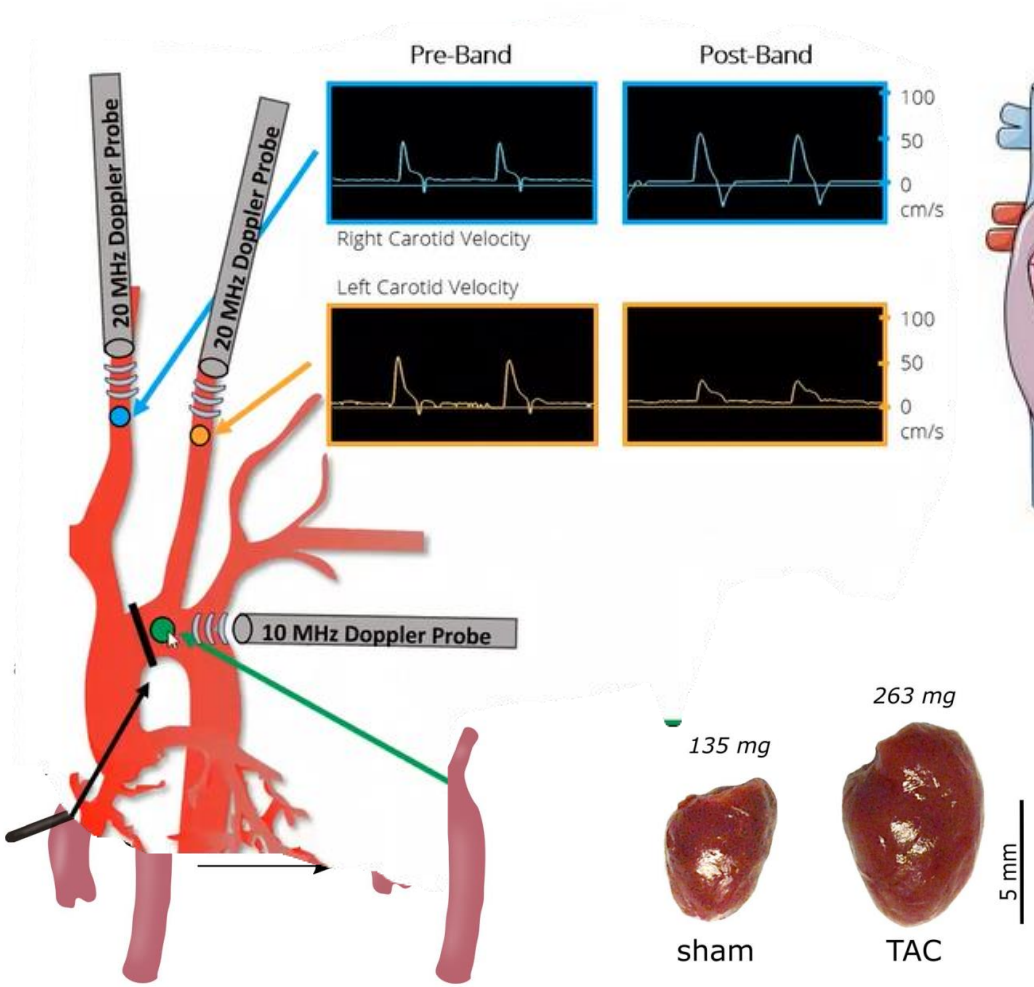

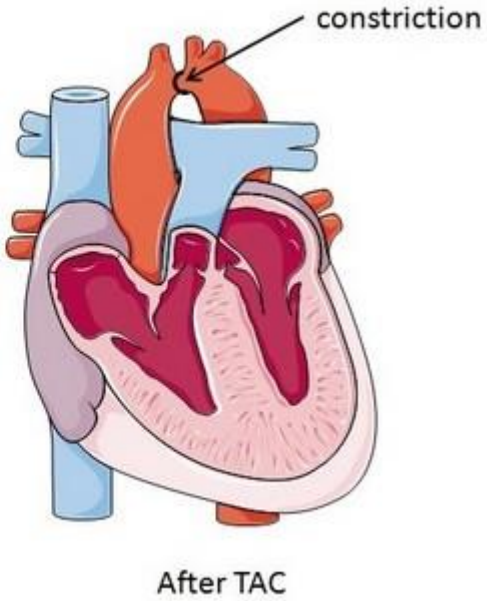

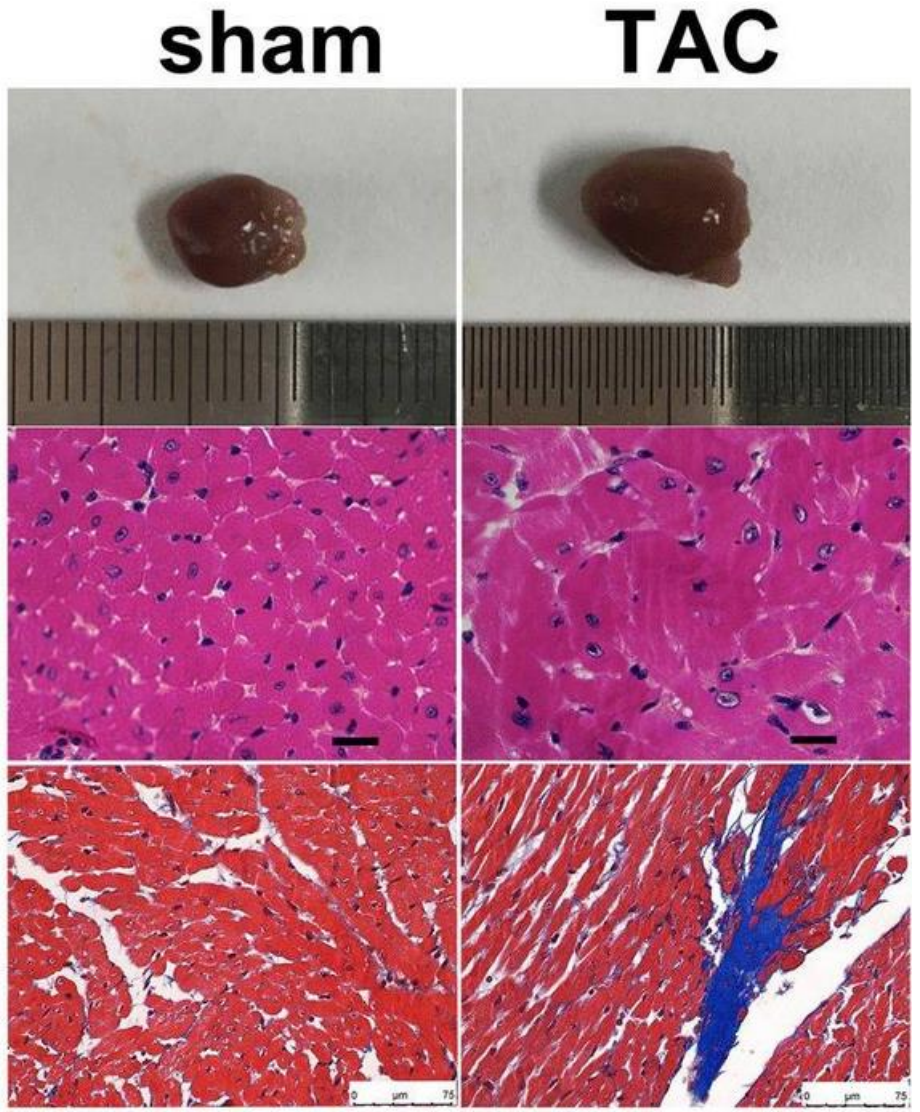

Bacmeister, L., Schwarzl, M., Warnke, S. *et al.* Inflammation and fibrosis in murine models of heart failure. *Basic Res Cardiol* **114**, 19 (2019). https://doi.org/10.1007/s00395-019-0722-5

Han X, Wang Y, Fu M, Song Y, Wang J, Cui X, Fan Y, Cao J, Luo J, Sun A, Zou Y, Hu K, Zhou J, Ge J. Effects of Adiponectin on Diastolic Function in Mice Underwent Transverse Aorta Constriction. J Cardiovasc Transl Res. 2020 Apr;13(2):225-237. doi: 10.1007/s12265-019-09913-1. Epub 2019 Oct 16. PMID: 31621035; PMCID: PMC7166206.

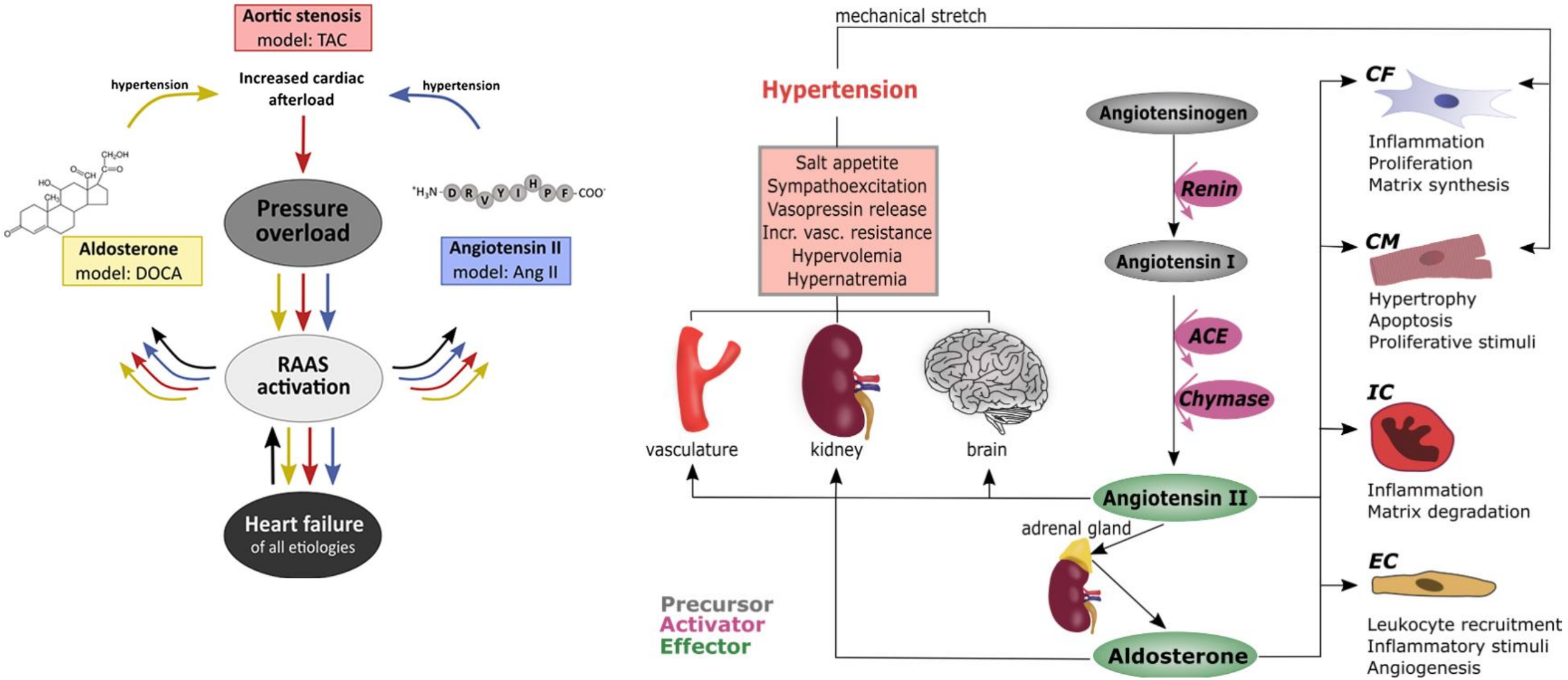

Bacmeister, L., Schwarzl, M., Warnke, S. *et al.* Inflammation and fibrosis in murine models of heart failure. *Basic Res Cardiol* **114**, 19 (2019). https://doi.org/10.1007/s00395-019-0722-5

Pressure-overload model HF

- 5/6 nephractomy model of HF

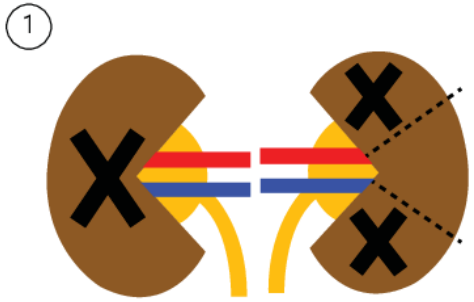

Sub-total (5/6) nephrectomy

Unilateral ureteral obstruction

Comparison of the Surgical Resection and Infarct 5/6 Nephrectomy Rat Models of Chronic Kidney Disease

Rabe, Michael and Franz Schaefer. "Non-Transgenic Mouse Models of Kidney Disease." Nephron 133 (2016): 53 - 61.

METHODS

5/6 Nephrectomy by Surgical Pole Removal

5/6 Nephrectomy by Pole Infarction

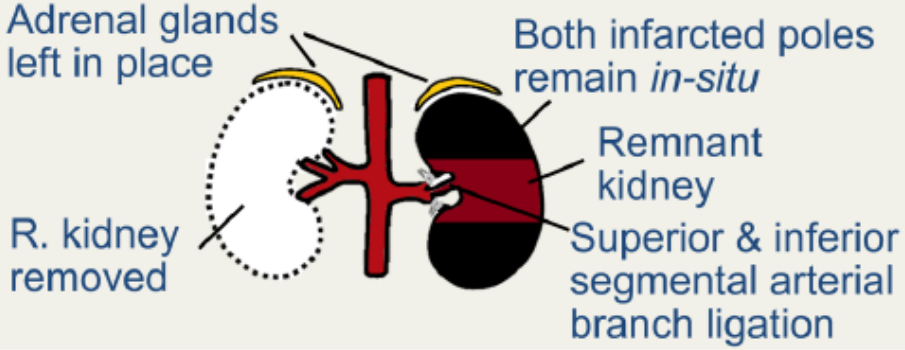

OUTCOME

Phenotypic Similarities Between Models

- Loss of nephrons upon surgery
- Compensatory remodeling
- Uremia, fibrosis and glomerular injury
- Ultimately develop renal failure

Phenotypic Differences Between Models

- Infarction model has relatively more RAAS activation.
- Infarction model spontaneously develops greater increases in mean arterial pressure.

CONCLUSION These models have much in common but also have significant differences and thereby model unique aspects of human CKD.

Adam, R. J., Williams, A. C., & Kriegel, A. J. (2022). Comparison of the surgical resection and infarct 5/6 nephrectomy rat models of chronic kidney disease. *American journal of physiology. Renal physiology*, *322*(6), F639–F654. https://doi.org/10.1152/ajprenal.00398.2021

Pressure-overload model HF

- 2K1C a 1K1C

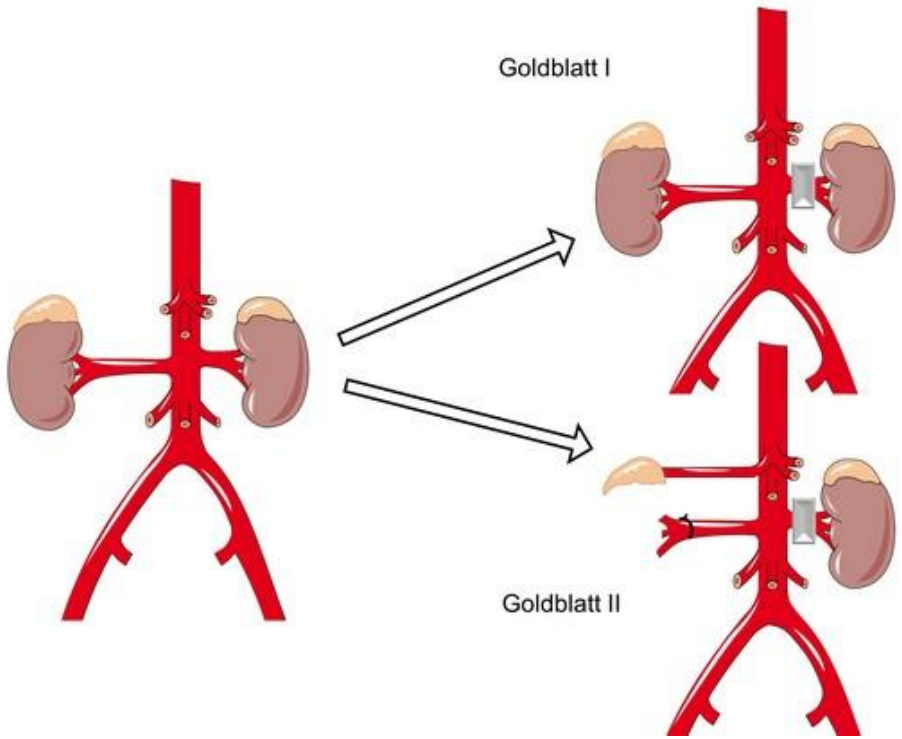

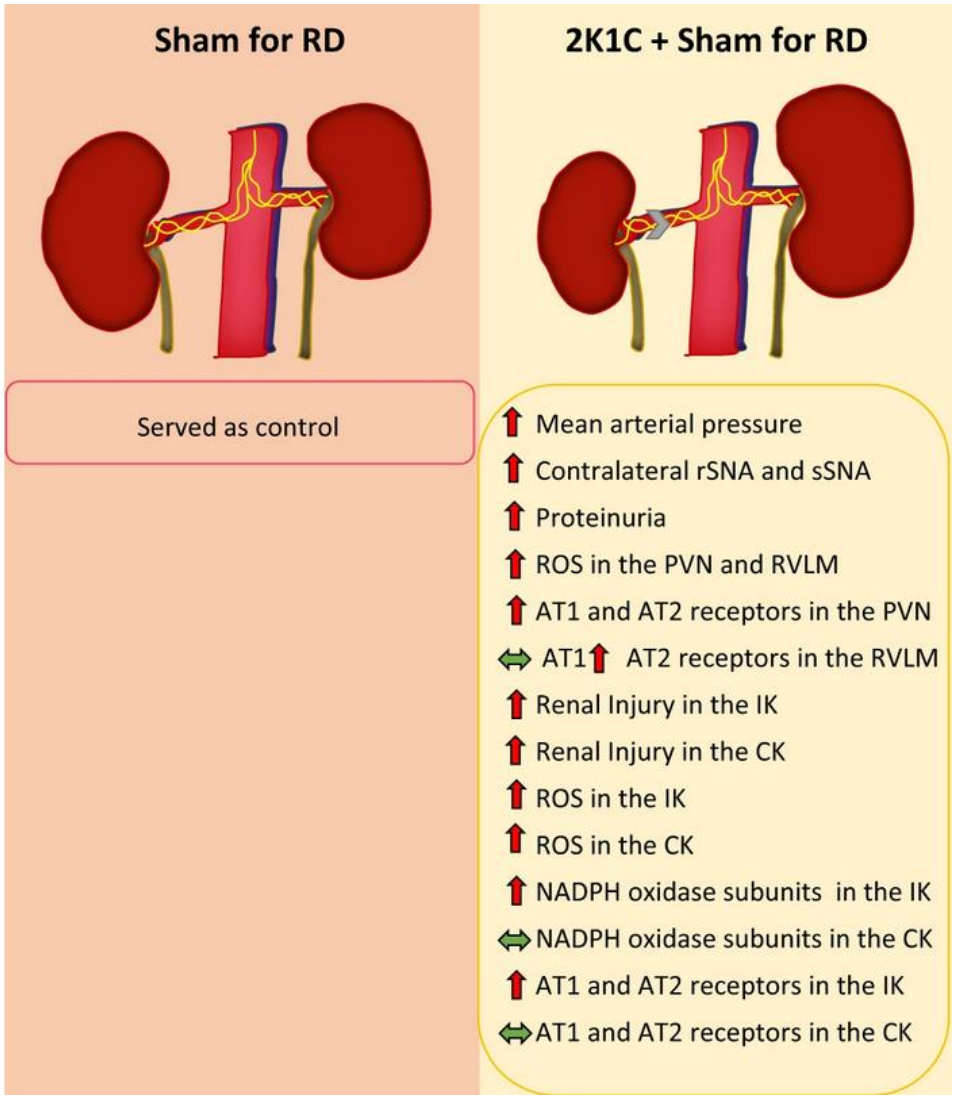

https://www.unil.ch/caf/en/home/menuinst/services/surgical-models.html

Carlström, M., Braga, V.A. í. *Hypertens Res* **42**, 754–757 (2019). https://doi.org/10.1038/s41440-019-0233-7

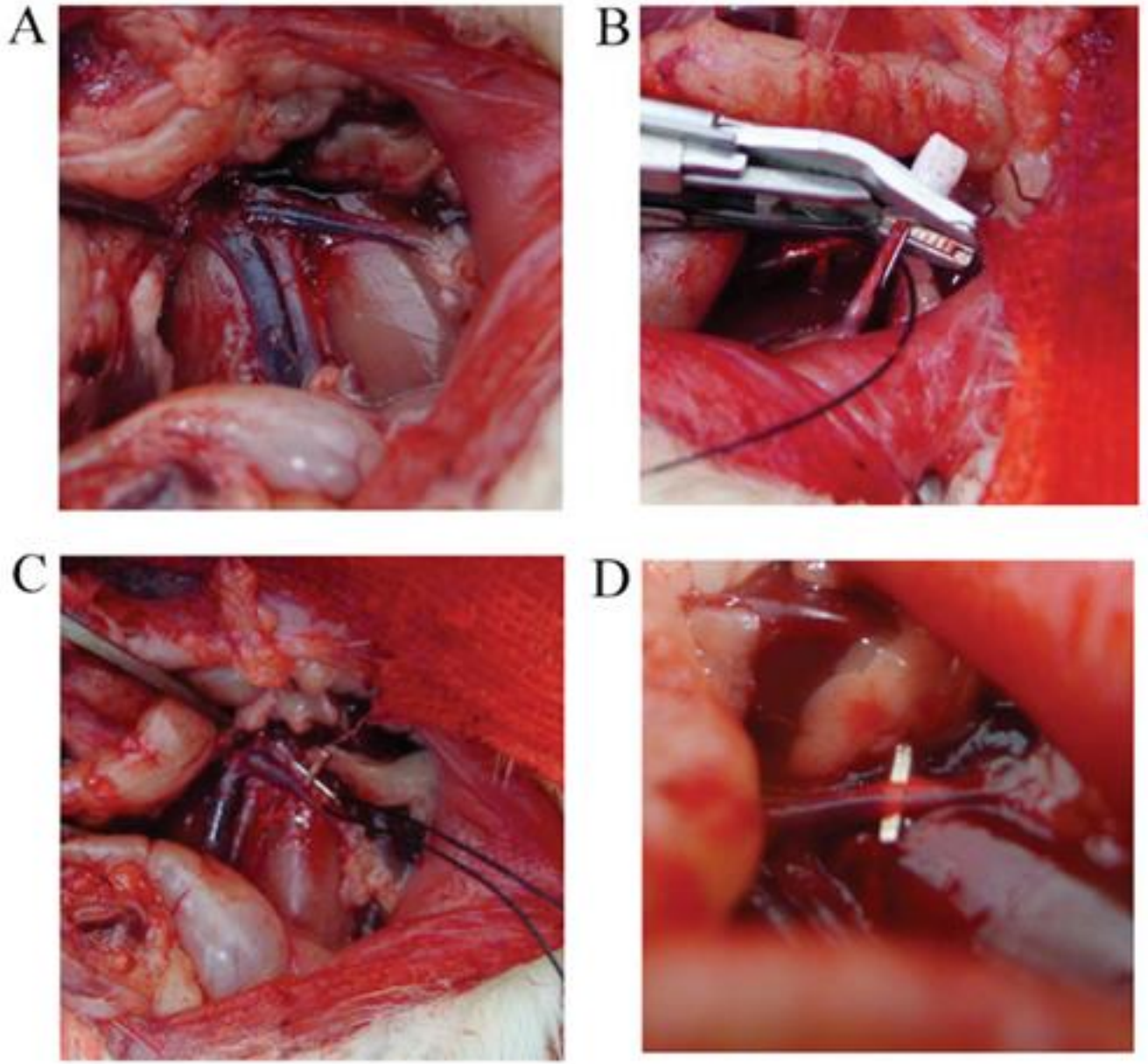

https://www.creative-bioarray.com/services/two-kidney-one-clip-2k1c-renovascular-hypertension-model.htm

Pressure-overload model HF

- L-NAME

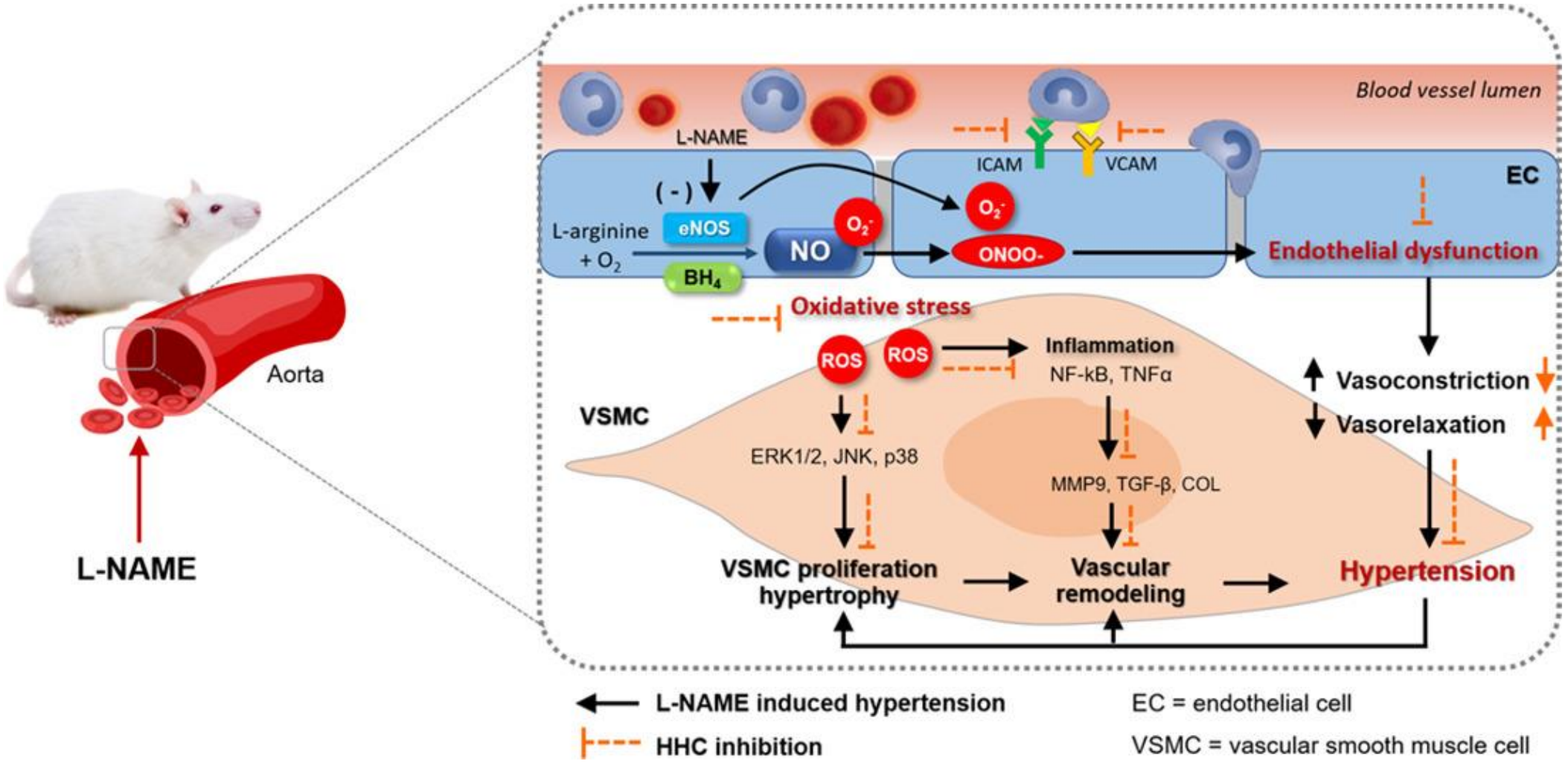

Panthiya, L., Tocharus, J., Onsa-Ard, A., Chaichompoo, W., Suksamrarn, A., & Tocharus, C. (2022). Hexahydrocurcumin ameliorates hypertensive and vascular remodeling in L-NAME-induced rats. *Biochimica et biophysica acta. Molecular basis of disease*, *1868*(3), 166317. https://doi.org/10.1016/j.bbadis.2021.166317

Infarktový model HF

- IM/R
- IM

- IM+sugen
- IM+monocrotaline /hypoxia

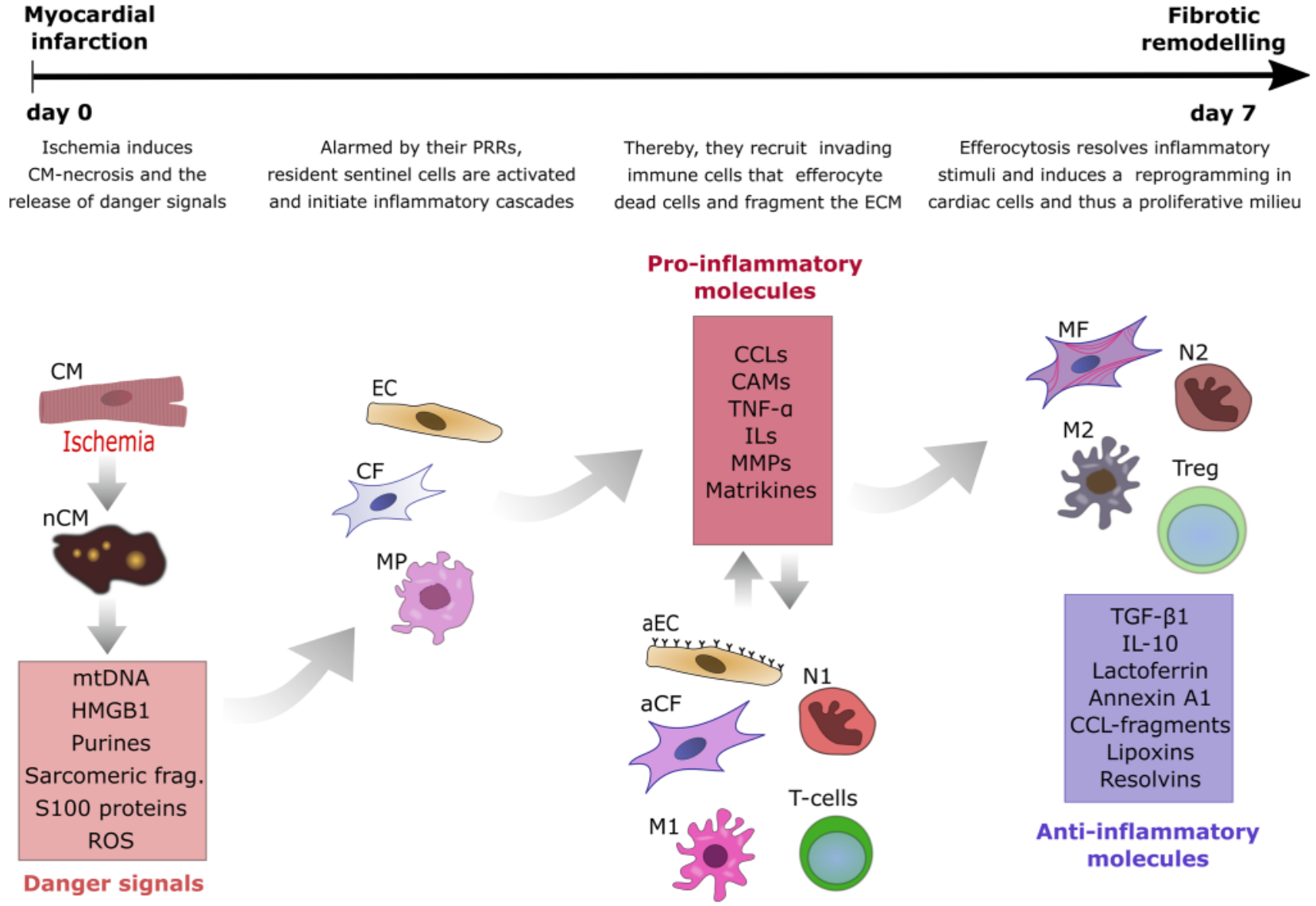

Bacmeister, L., Schwarzl, M., Warnke, S. *et al.* Inflammation and fibrosis in murine models of heart failure. *Basic Res Cardiol* **114**, 19 (2019). https://doi.org/10.1007/s00395-019-0722-5

Infarktový model HF

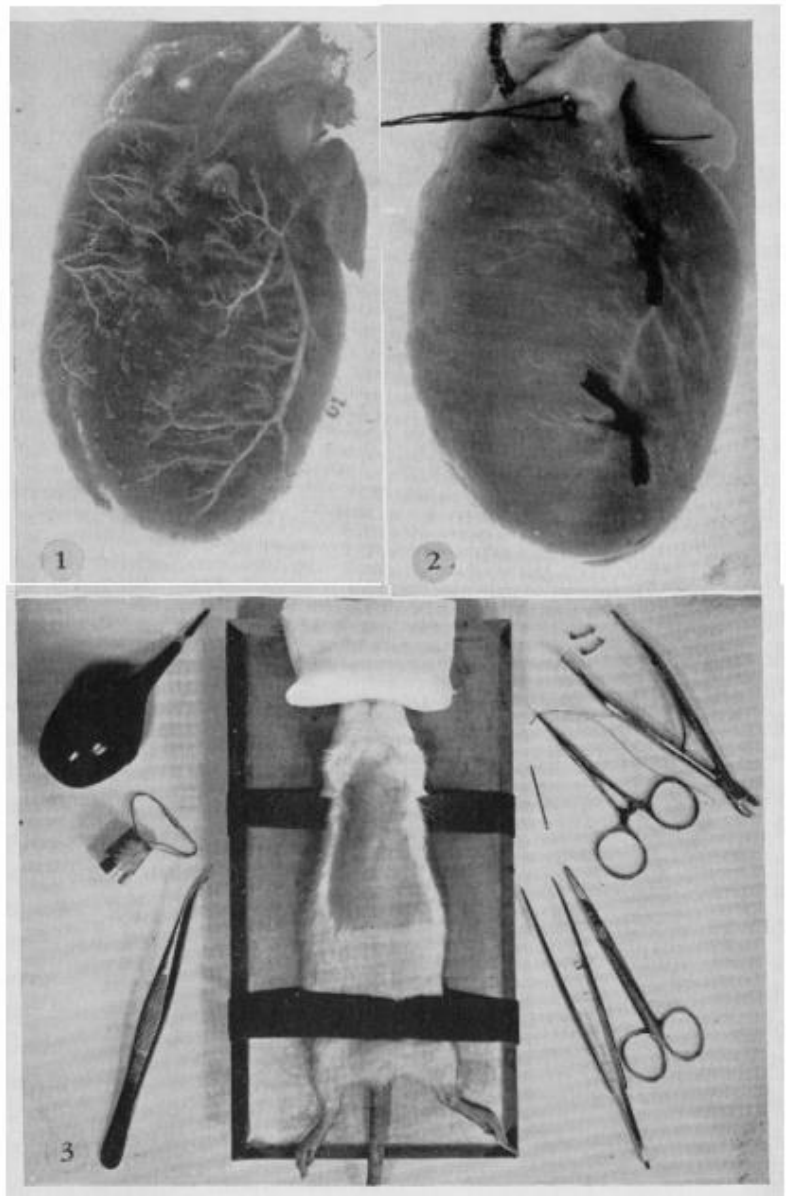

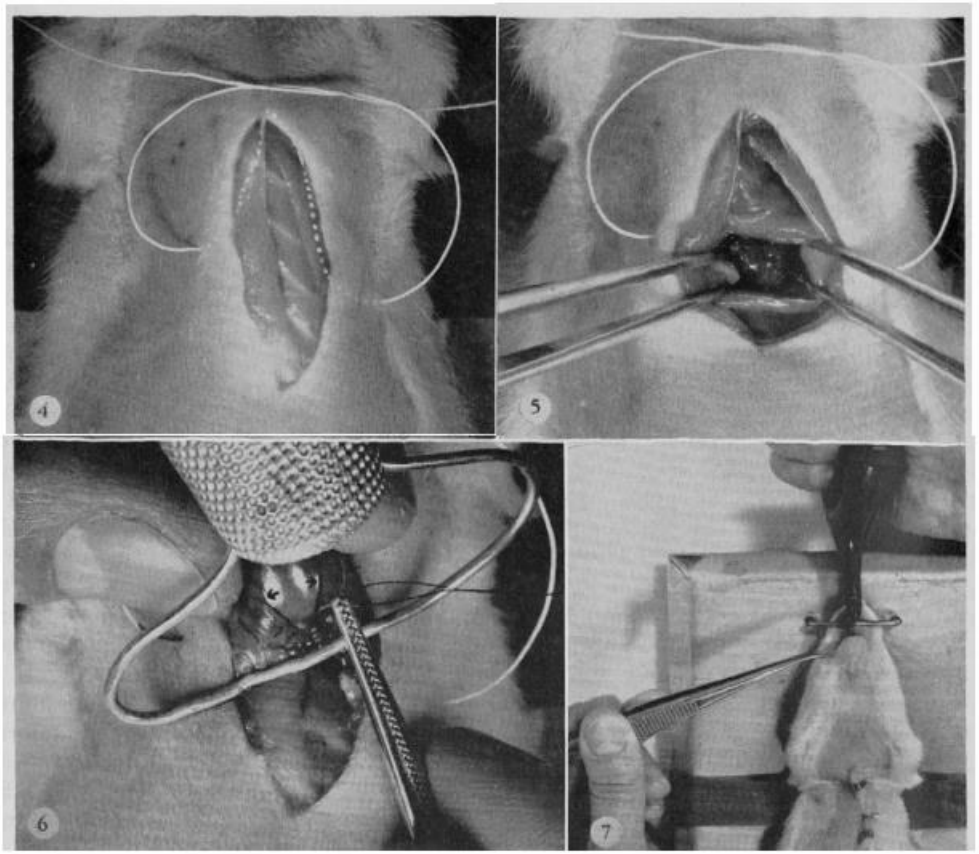

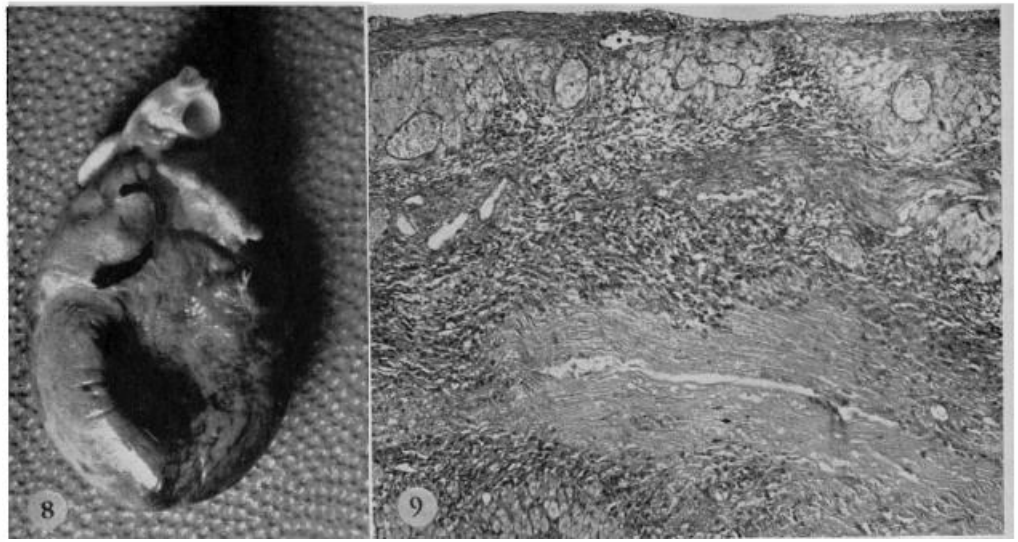

Selye H, Bajusz E, Grasso S, Mendell P. Simple Techniques for the Surgical Occlusion of Coronary Vessels in the Rat. *Angiology*. 1960;11(5):398-407. doi:10.1177/000331976001100505

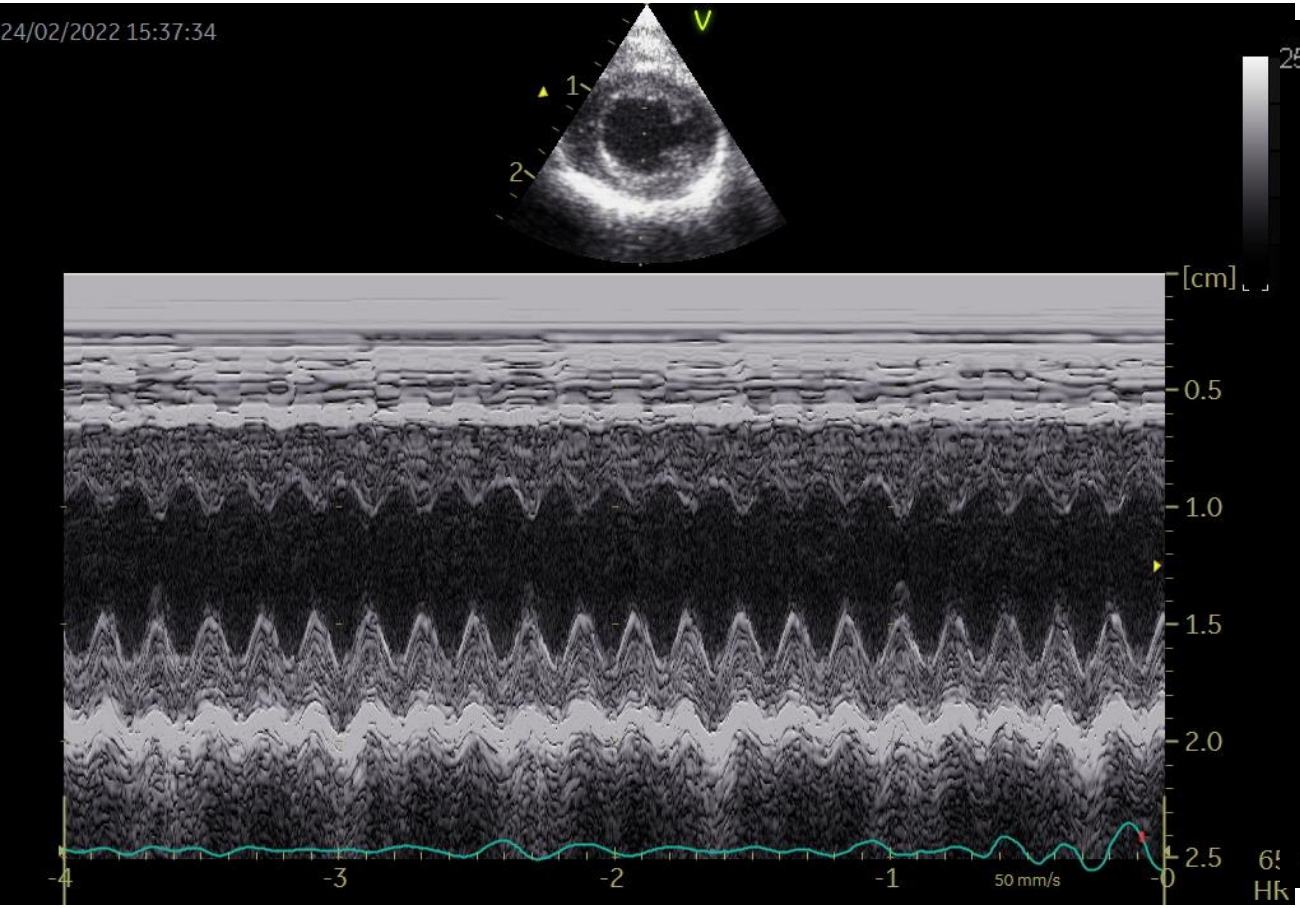
24/02/2022 15:37:34
[cm]
0.5
1.0
1.5
2.0
2.5
-4
-3
-2
-1
-0
50 mm/s

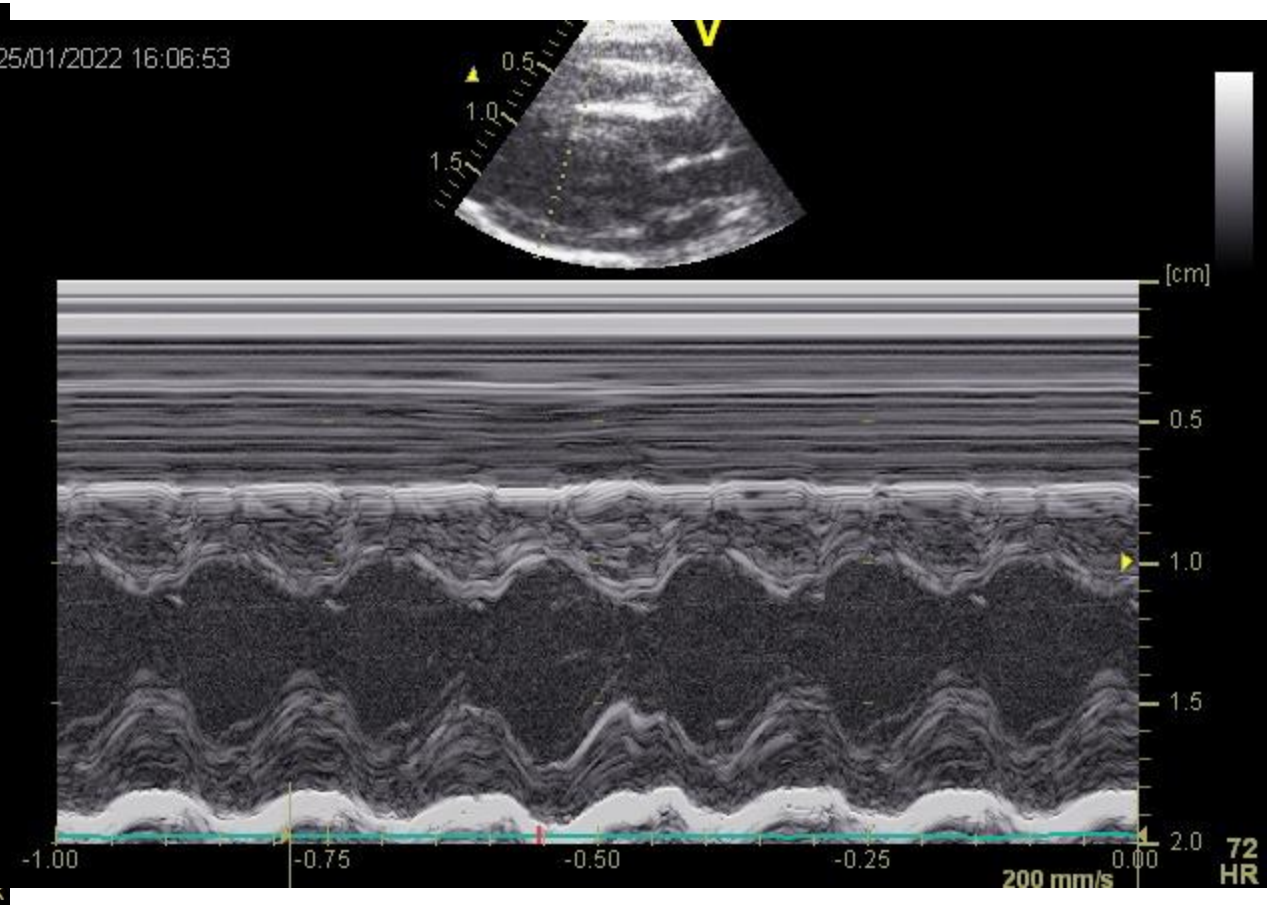
25/01/2022 16:06:53
[cm]
0.5
1.0
1.5
2.0
-1.00
-0.75
-0.50
-0.25
0.00
200 mm/s
72
HR

2weeks after IM

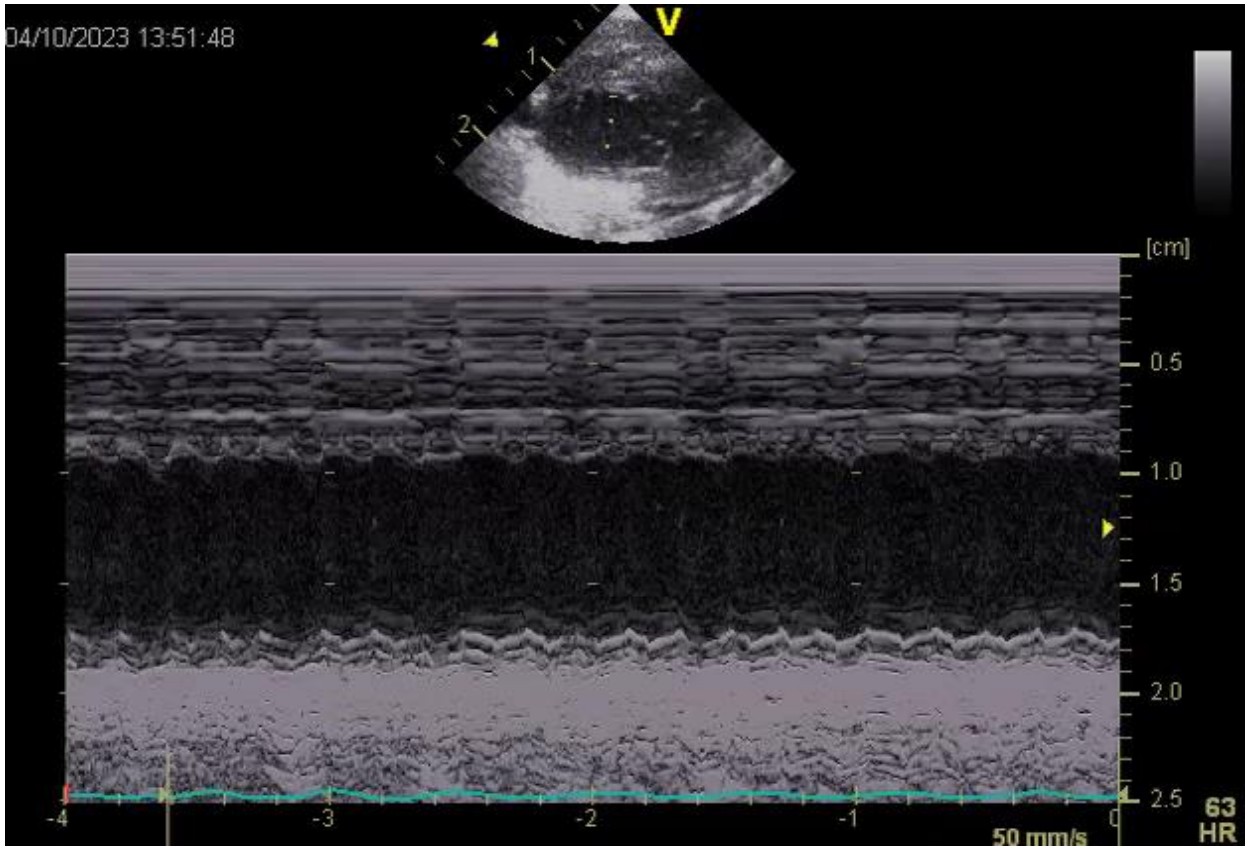

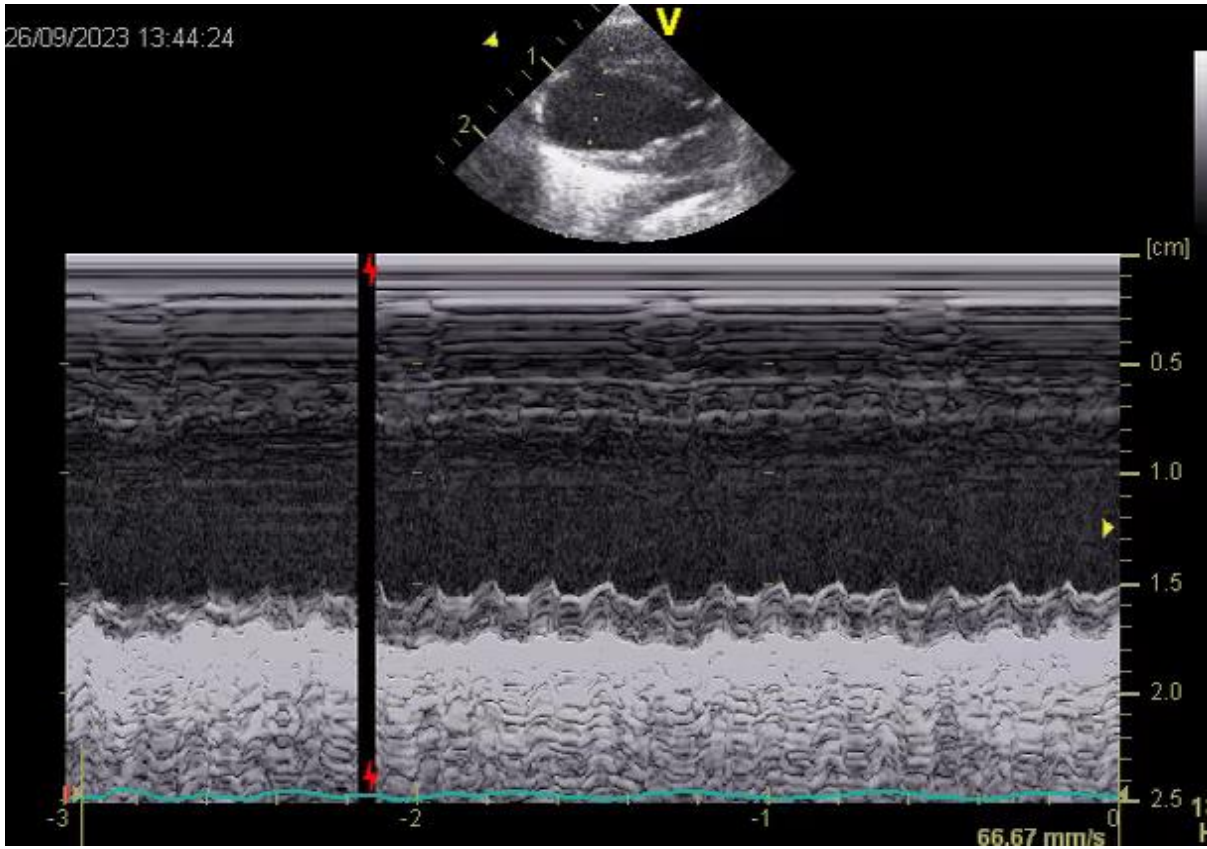

2weeks after IM

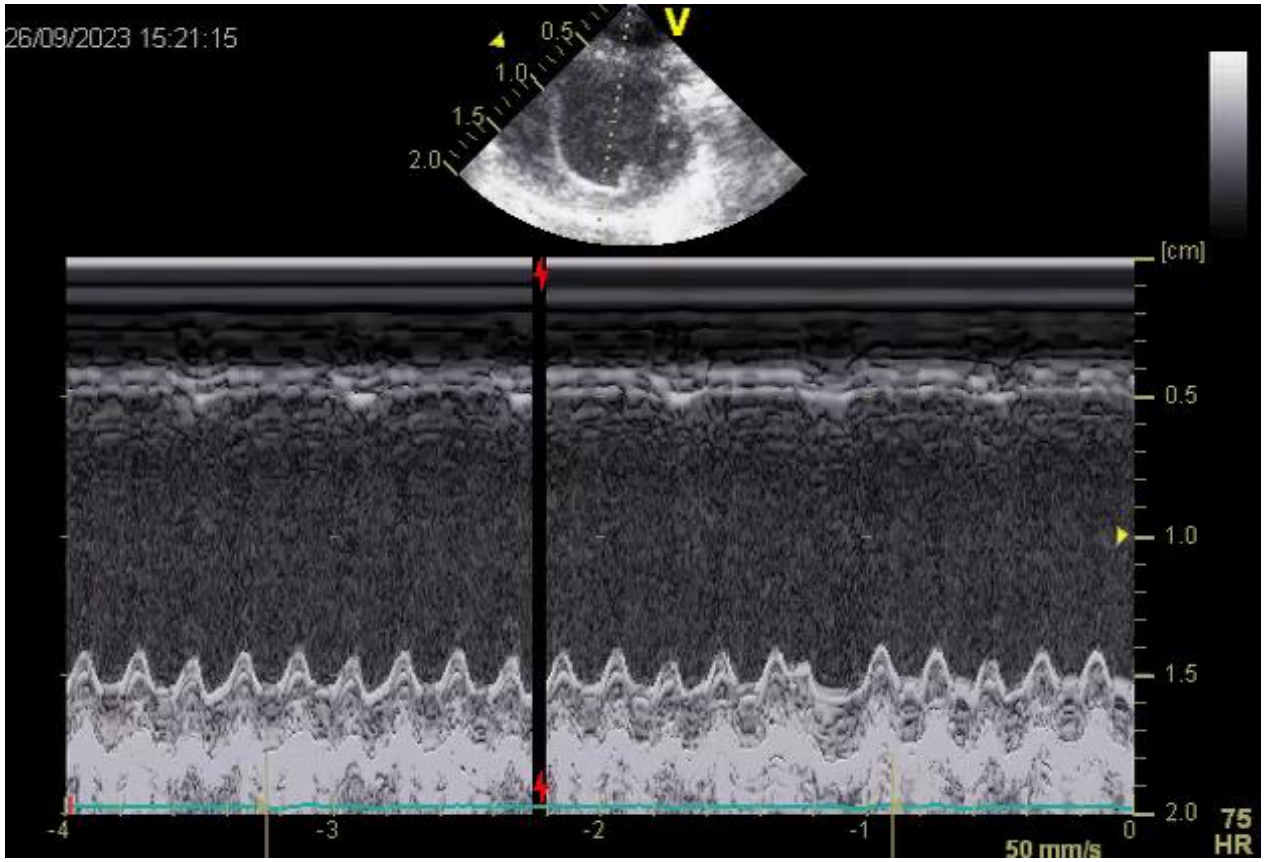

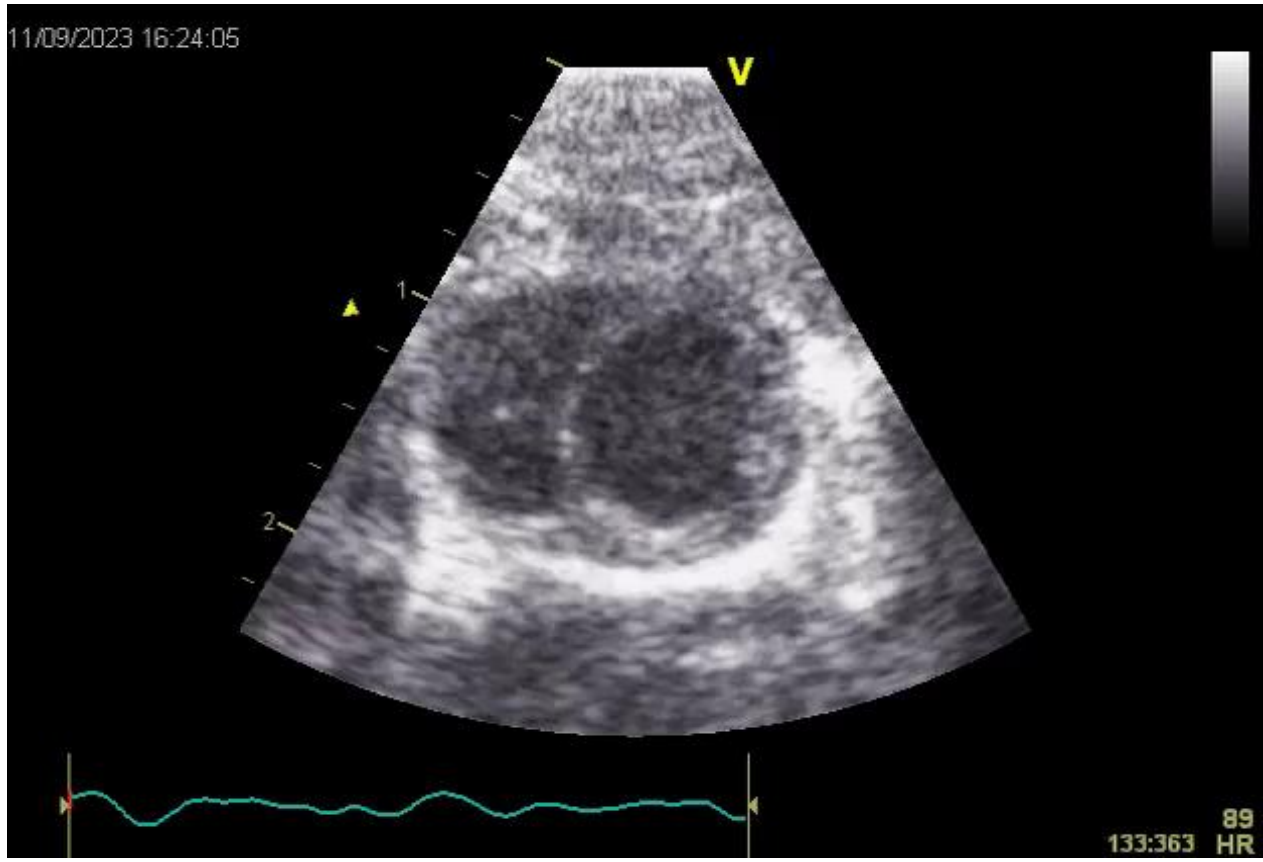

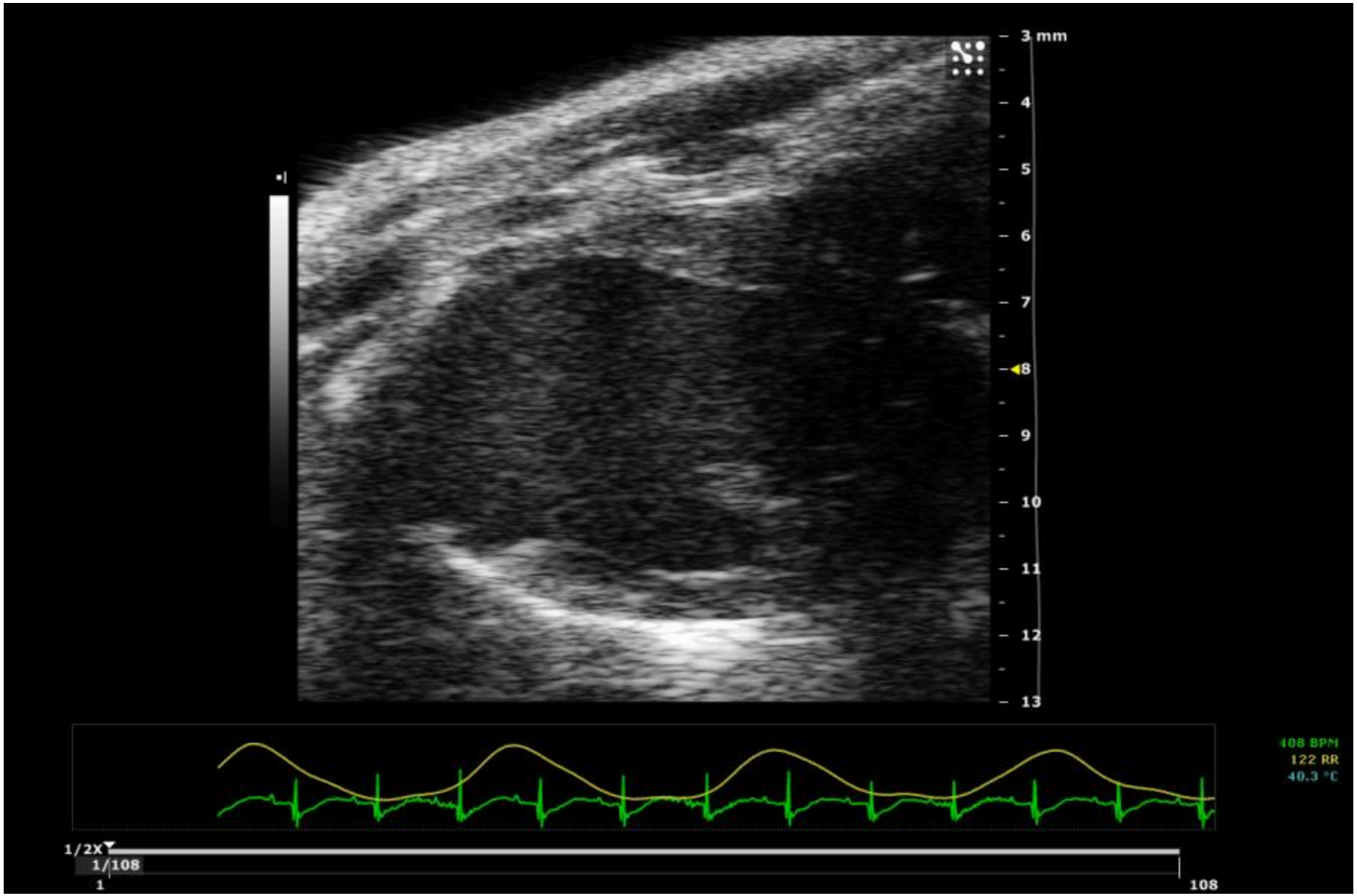
3 mm
4
5
6
7
8
9
10
11
12
13
408 BPM
122 RR
40.3 °C
1/2X
1/108
1
108

SHAM 2 (control)

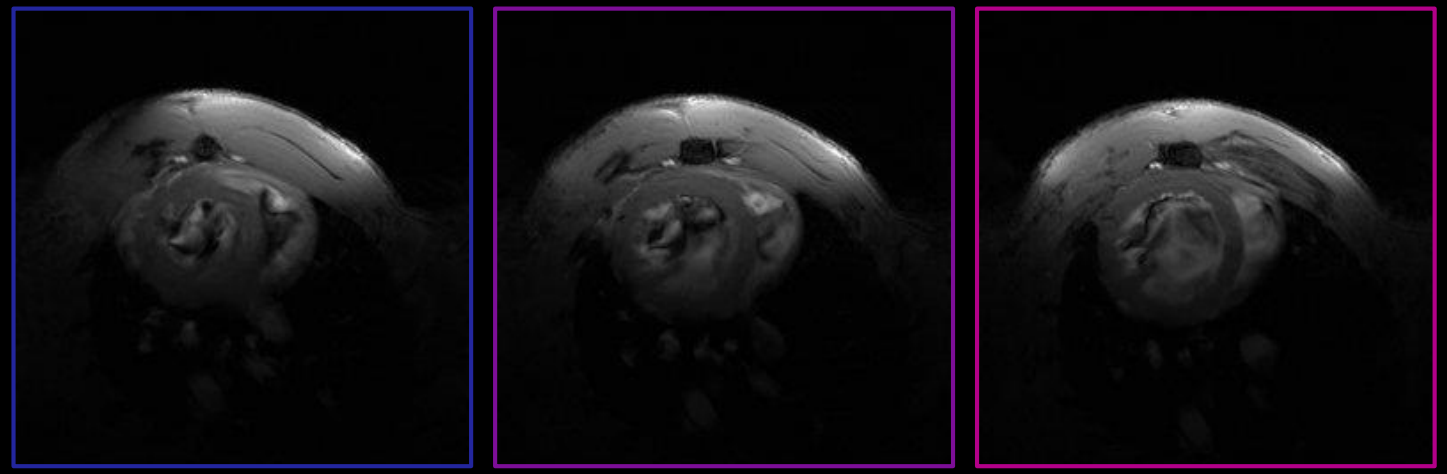

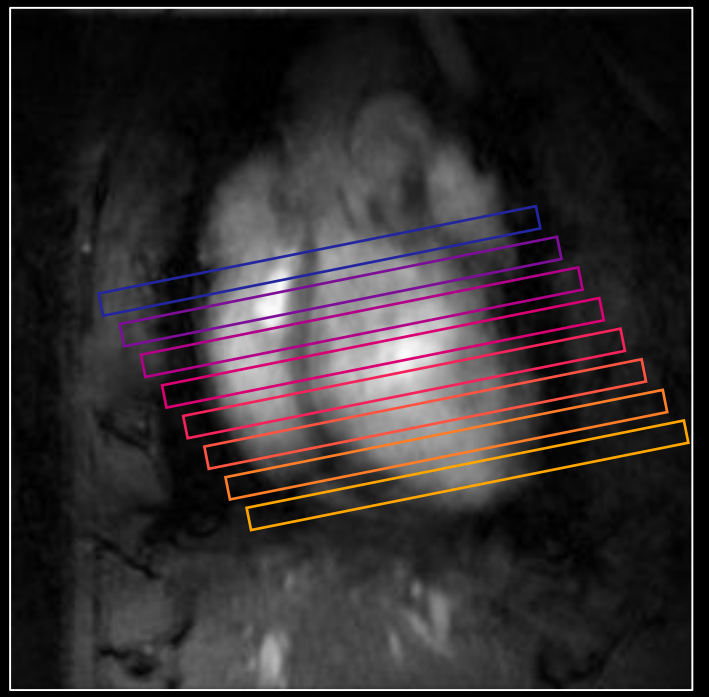

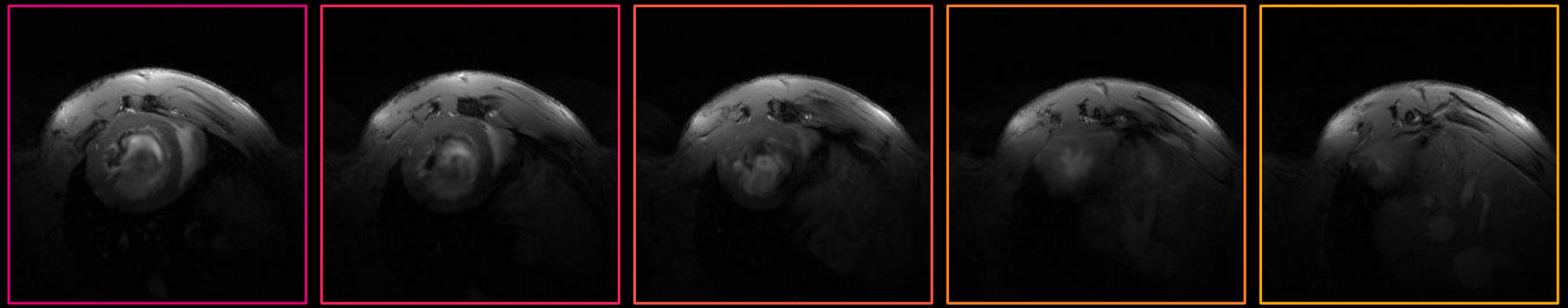

IM 1

- **Ejection fraction: 31 %**
- Evaluated from end-systole and end-diastole from all slices
- Software: Segment Medviso

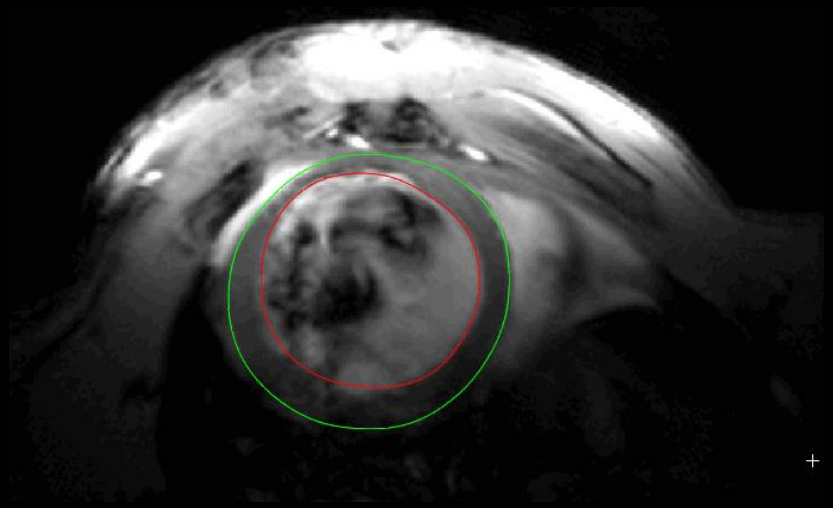

Comparison

SHAM 2

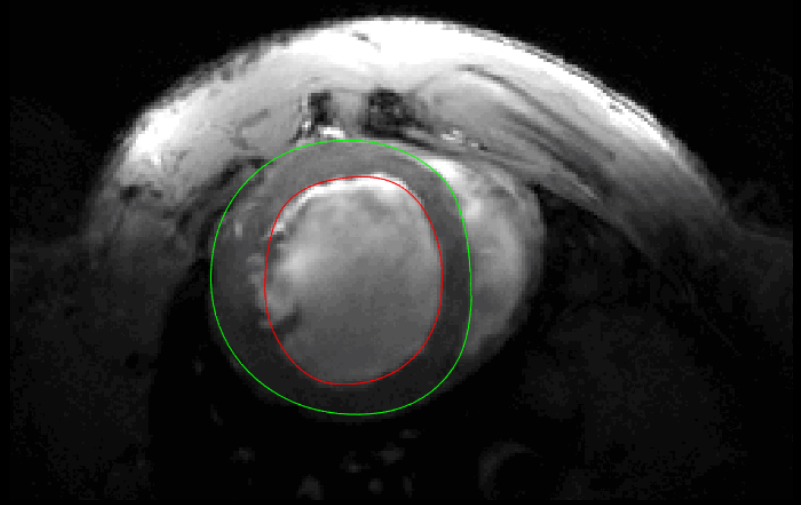

EF: 67 %

IM 1

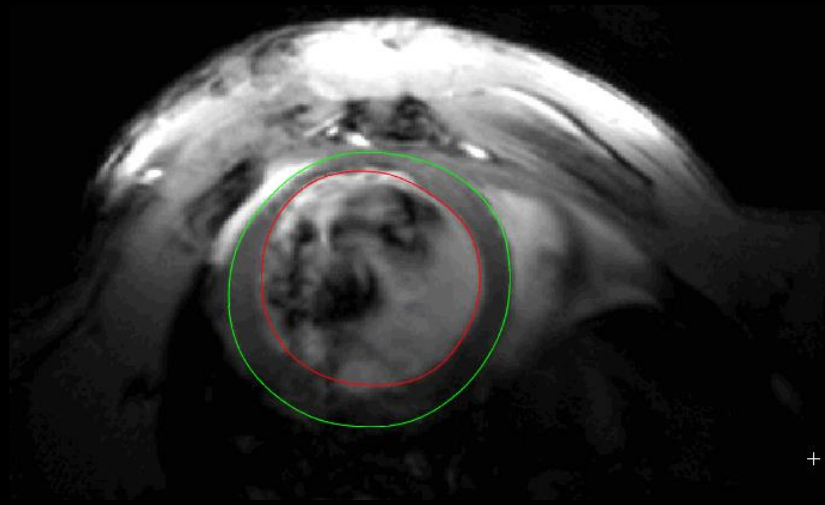

EF: 31 %

Comparison ES

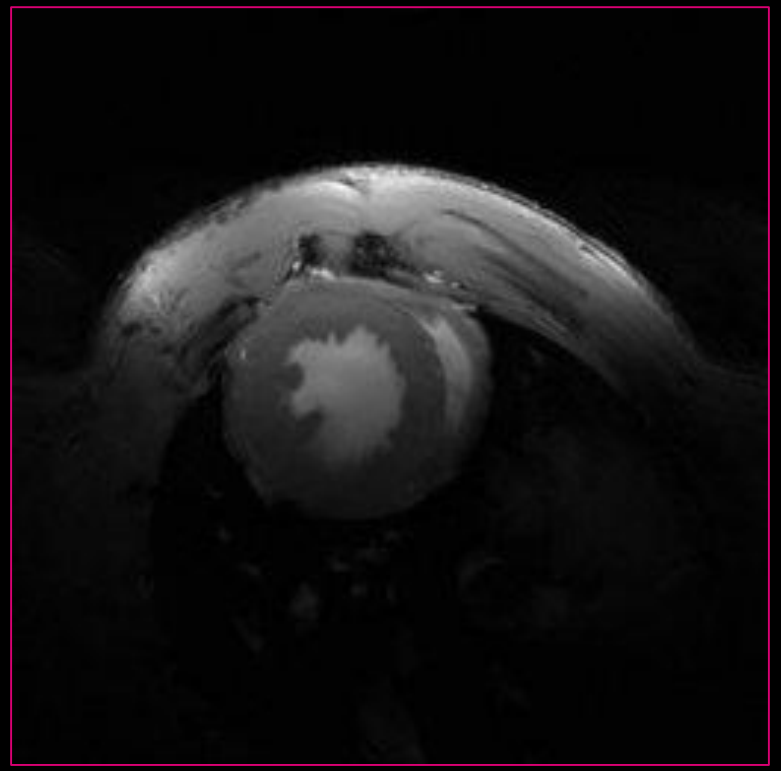

SHAM 2
EF: 67 %

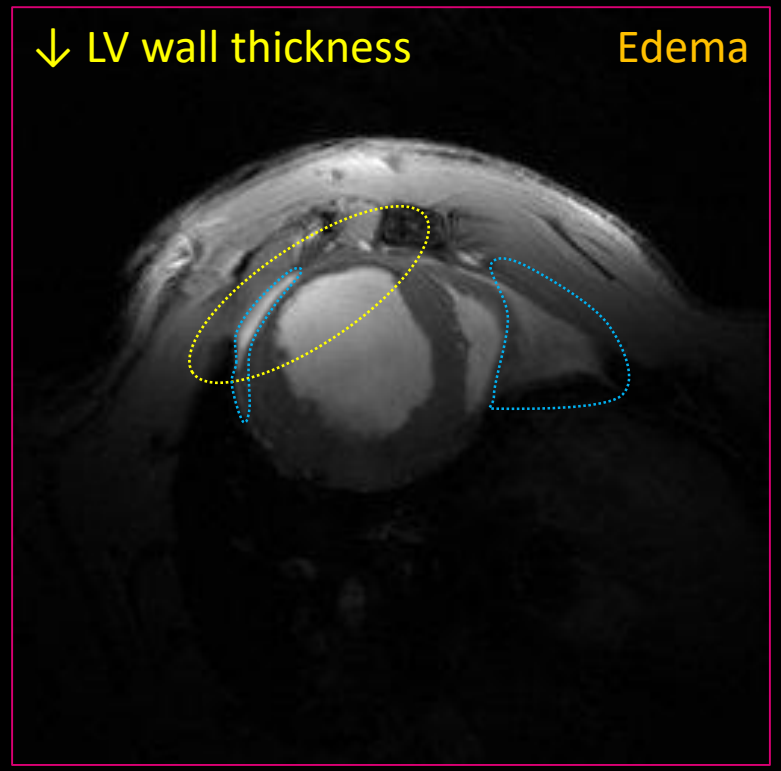

IM 1
EF: 31 %

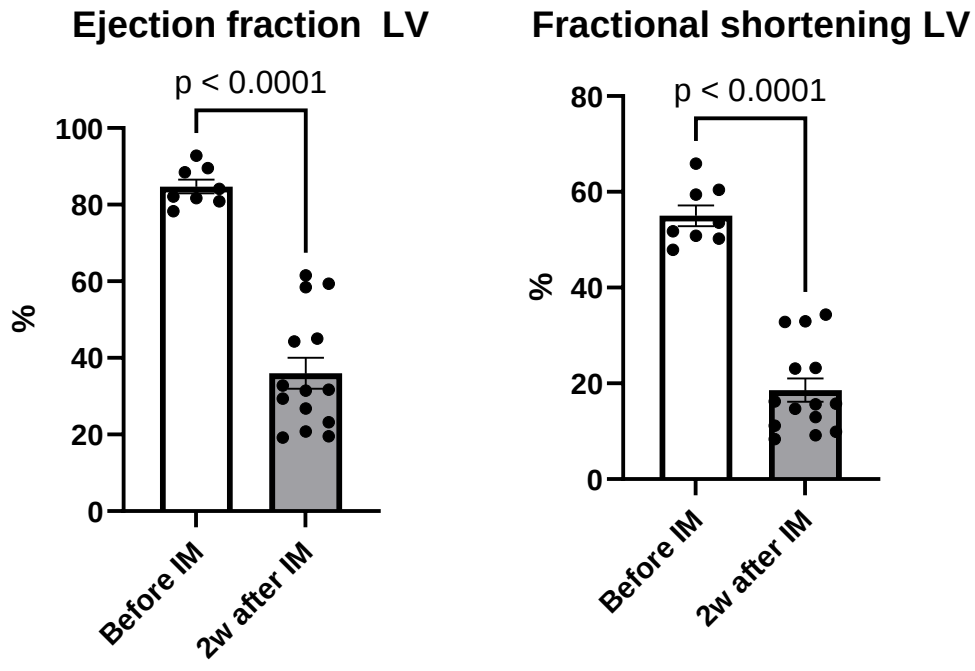
Ejection fraction LV
p < 0.0001
100
80
60
40
20
0
%
Before IM
2w after IM
Fractional shortening LV
p < 0.0001
80
60
40
20
0
%
Before IM
2w after IM

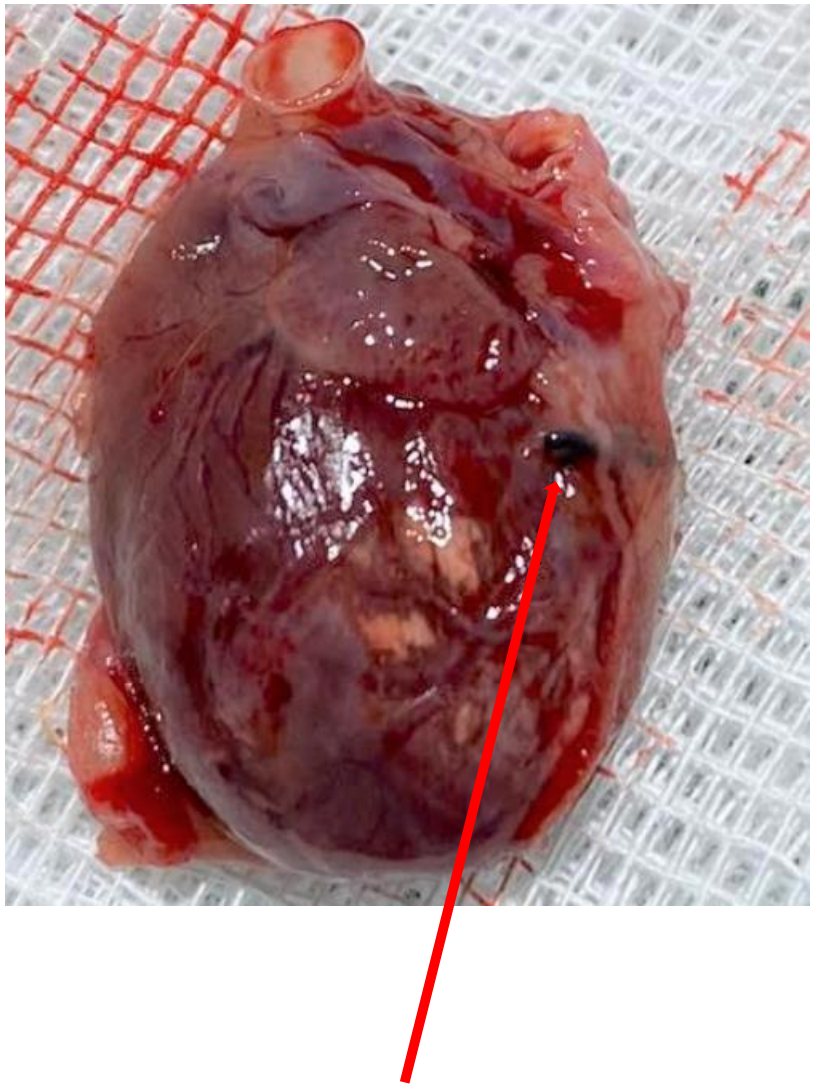

Podväz

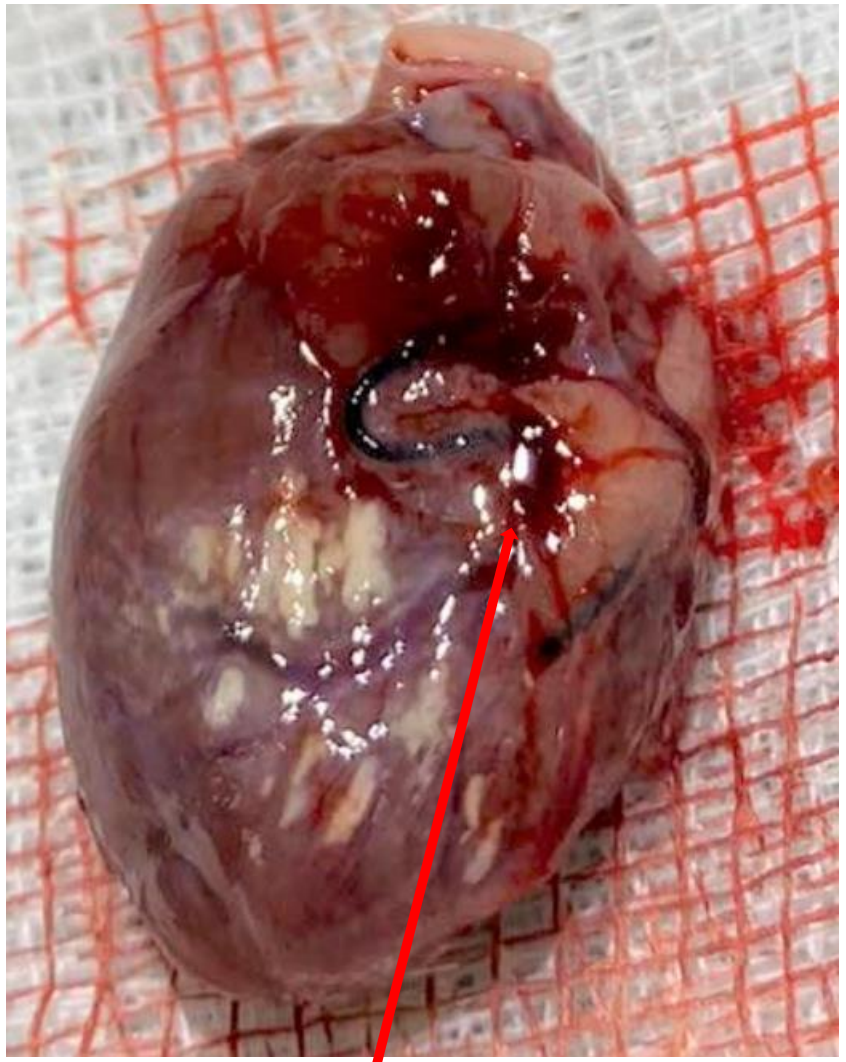

Podväz

Ecg and heart attack, the classic signs

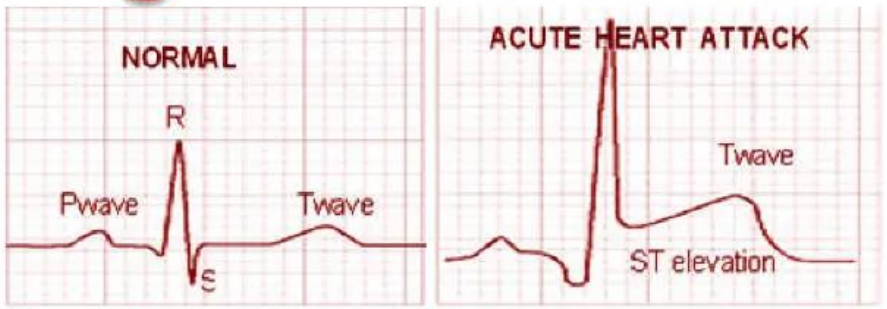

Before IM

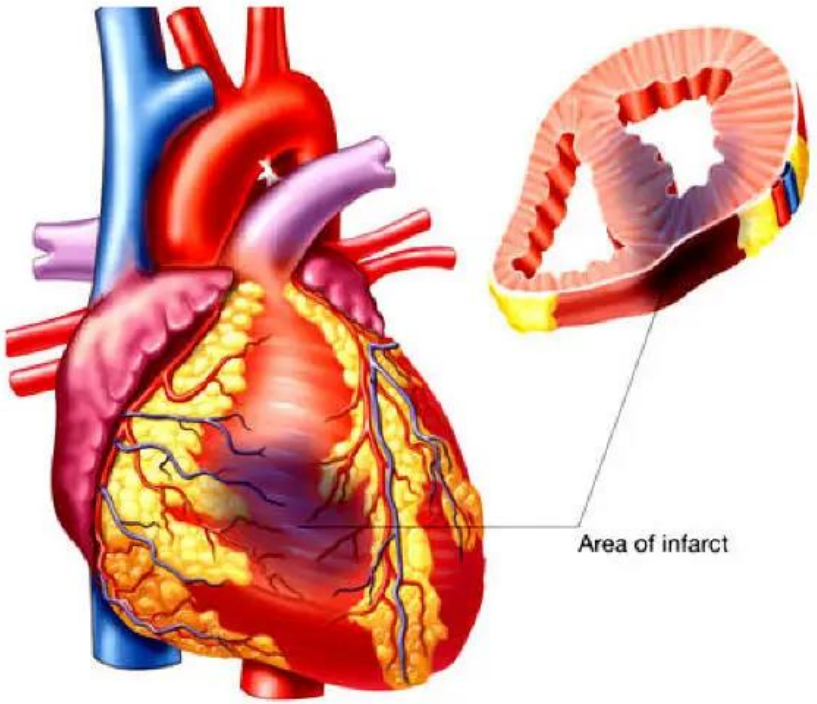

ST-elevation

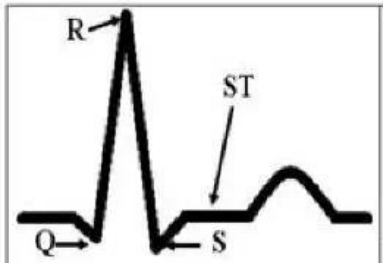			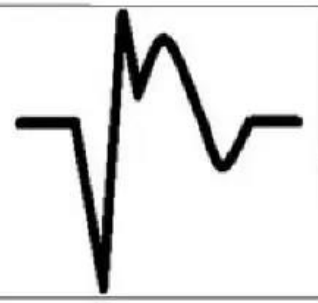		
Cardiac cycle	Minutes after heart arrack starts	Hours later	1-2 days	Several days	Weeks after the attack
Normal	ST shifted	- ST shifted - R dropping - Q appears to be noticeable	- T inverted -Q goes lower	- ST normal - T inverted	- ST and T normal - Q no change


-0.10
-0.15
-0.20
-0.25
-0.30
-0.35
mmHg

-0.10
-0.15
-0.20
-0.25
-0.30
-0.35
mmHg

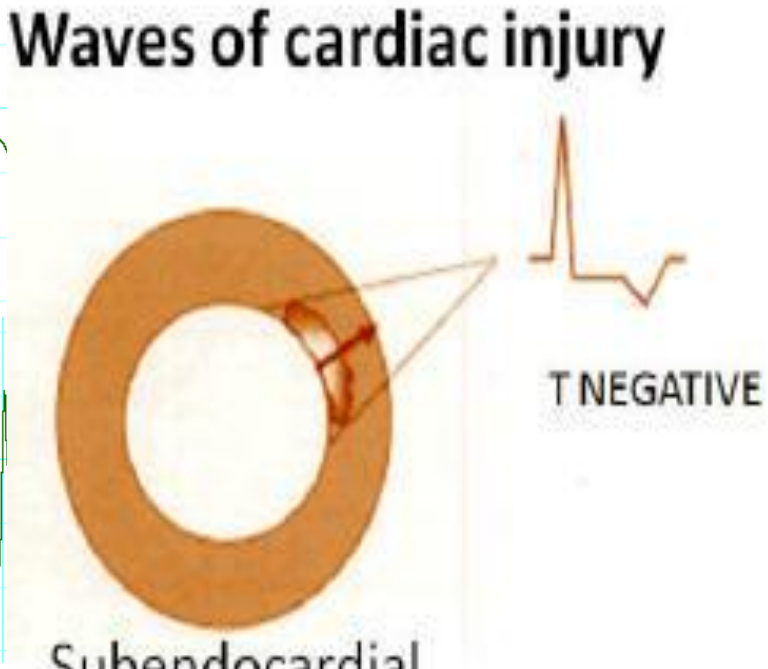
Waves of cardiac injury
T NEGATIVE
Subendocardial
ischemia wave

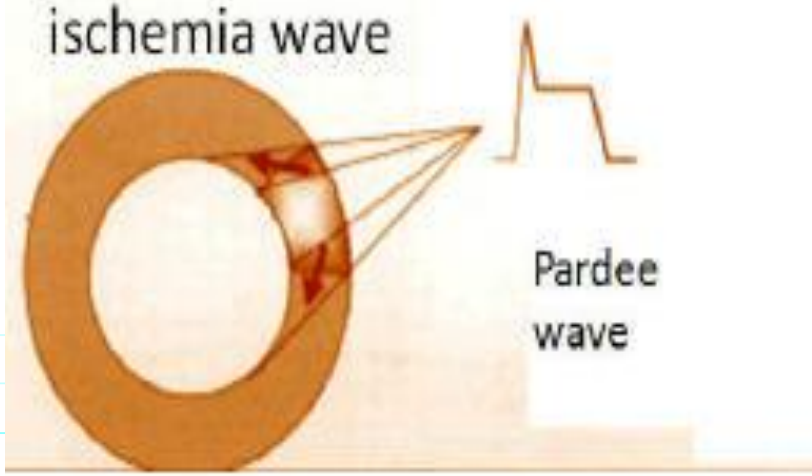
Pardee
wave
Transmural
ischemia wave

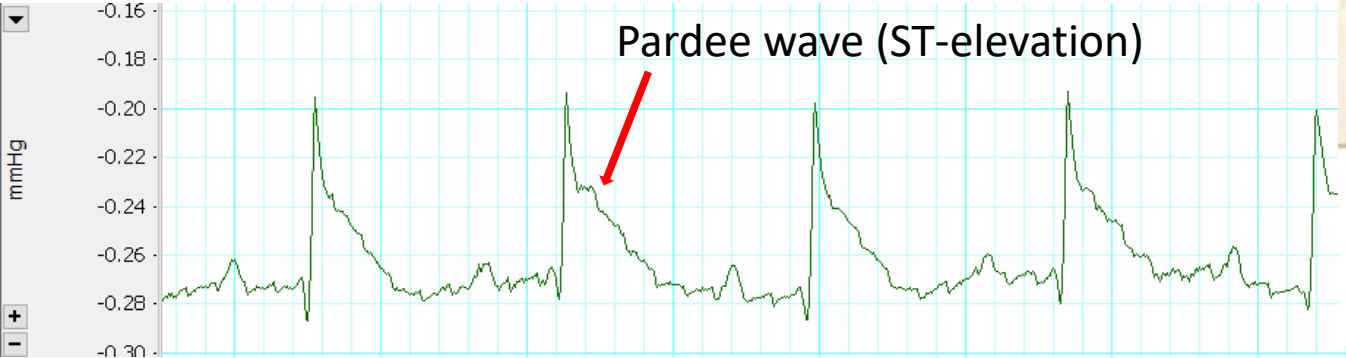
Pardee wave (ST-elevation)
-0.16
-0.18
-0.20
-0.22
-0.24
-0.26
-0.28
-0.30
mmHg

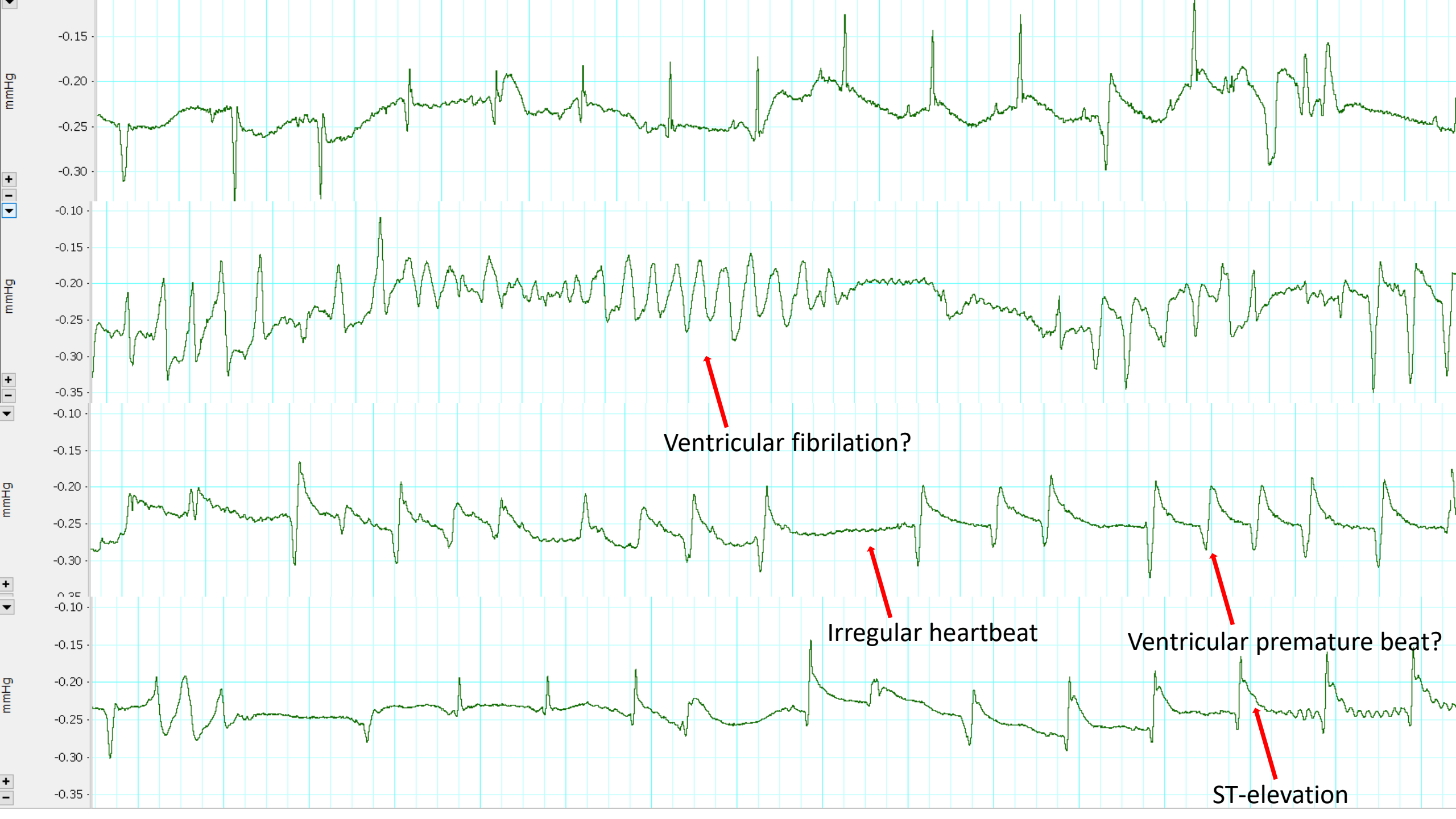
mmHg
-0.15
-0.20
-0.25
-0.30
mmHg
-0.10
-0.15
-0.20
-0.25
-0.30
-0.35
Ventricular fibrilation?
mmHg
-0.10
-0.15
-0.20
-0.25
-0.30
Irregular heartbeat
Ventricular premature beat?
mmHg
-0.10
-0.15
-0.20
-0.25
-0.30
-0.35
ST-elevation

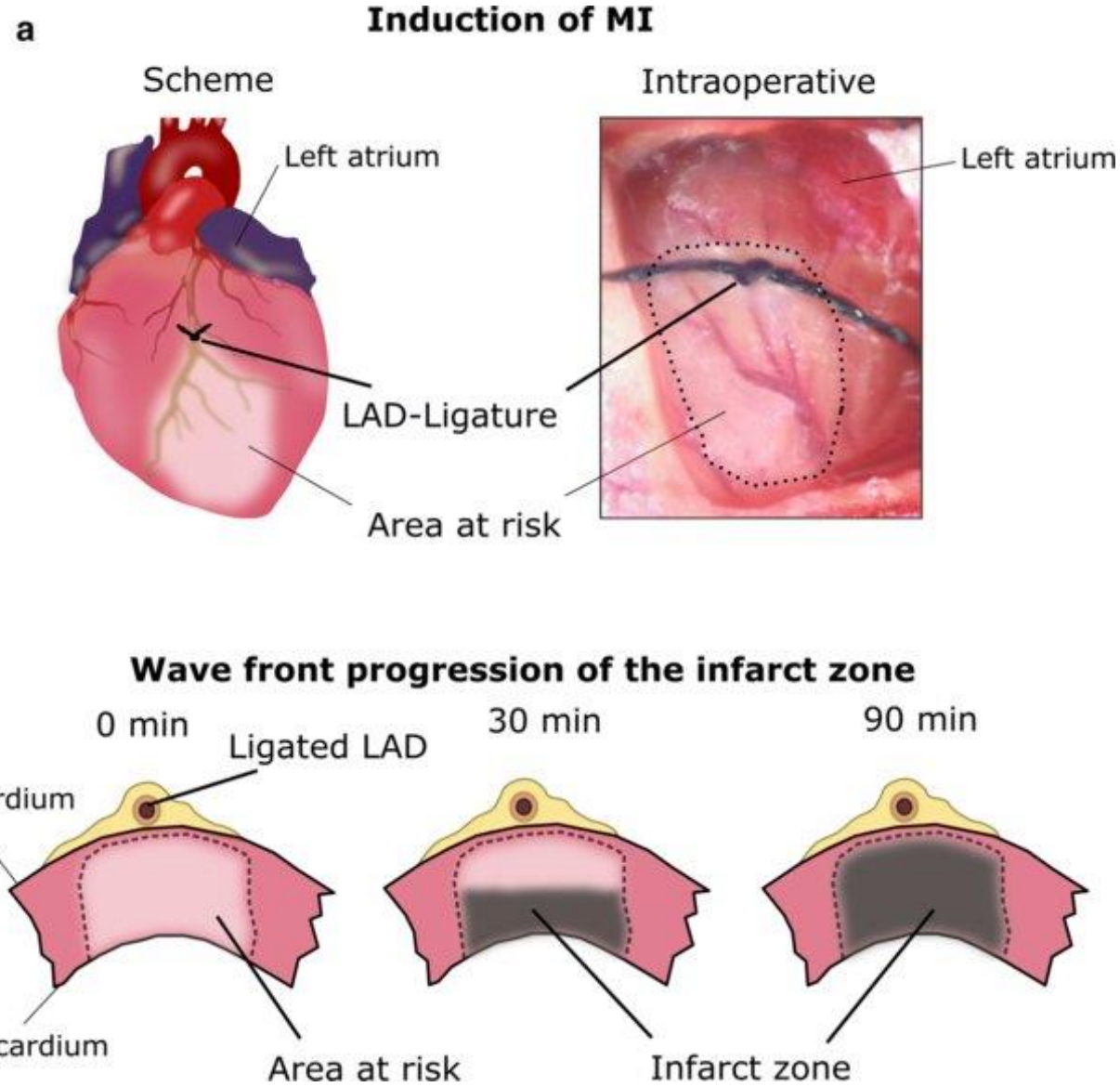
a
Induction of MI
Scheme
Intraoperative
Left atrium
Left atrium
LAD-Ligature
Area at risk
b
Wave front progression of the infarct zone
0 min
Ligated LAD
30 min
90 min
Epicardium
Endocardium
Area at risk
Infarct zone

IM area evaluation (evans blue dye perfusion with subsequent triphenyltetrazolium chloride immersion)

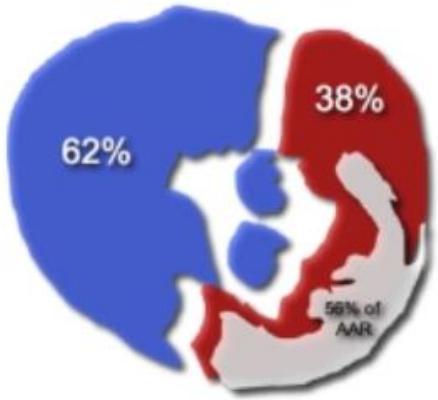

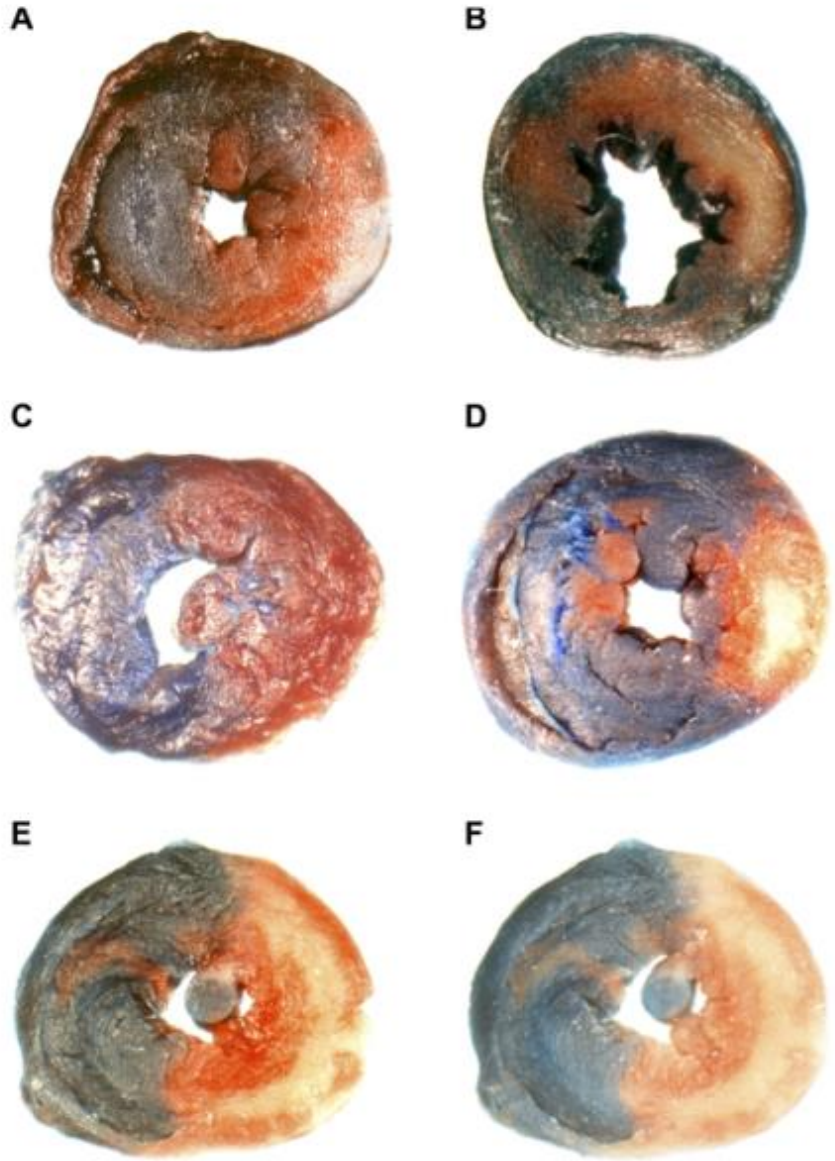

Bohl S, Medway DJ, Schulz-Menger J, Schneider JE, Neubauer S, Lygate CA. Refined approach for quantification of in vivo ischemia-reperfusion injury in the mouse heart. Am J Physiol Heart Circ Physiol. 2009 Dec;297(6):H2054-8. doi: 10.1152/ajpheart.00836.2009. Epub 2009 Oct 9. PMID: 19820193; PMCID: PMC2793132.

Model pravostranného srdcového zlyhania

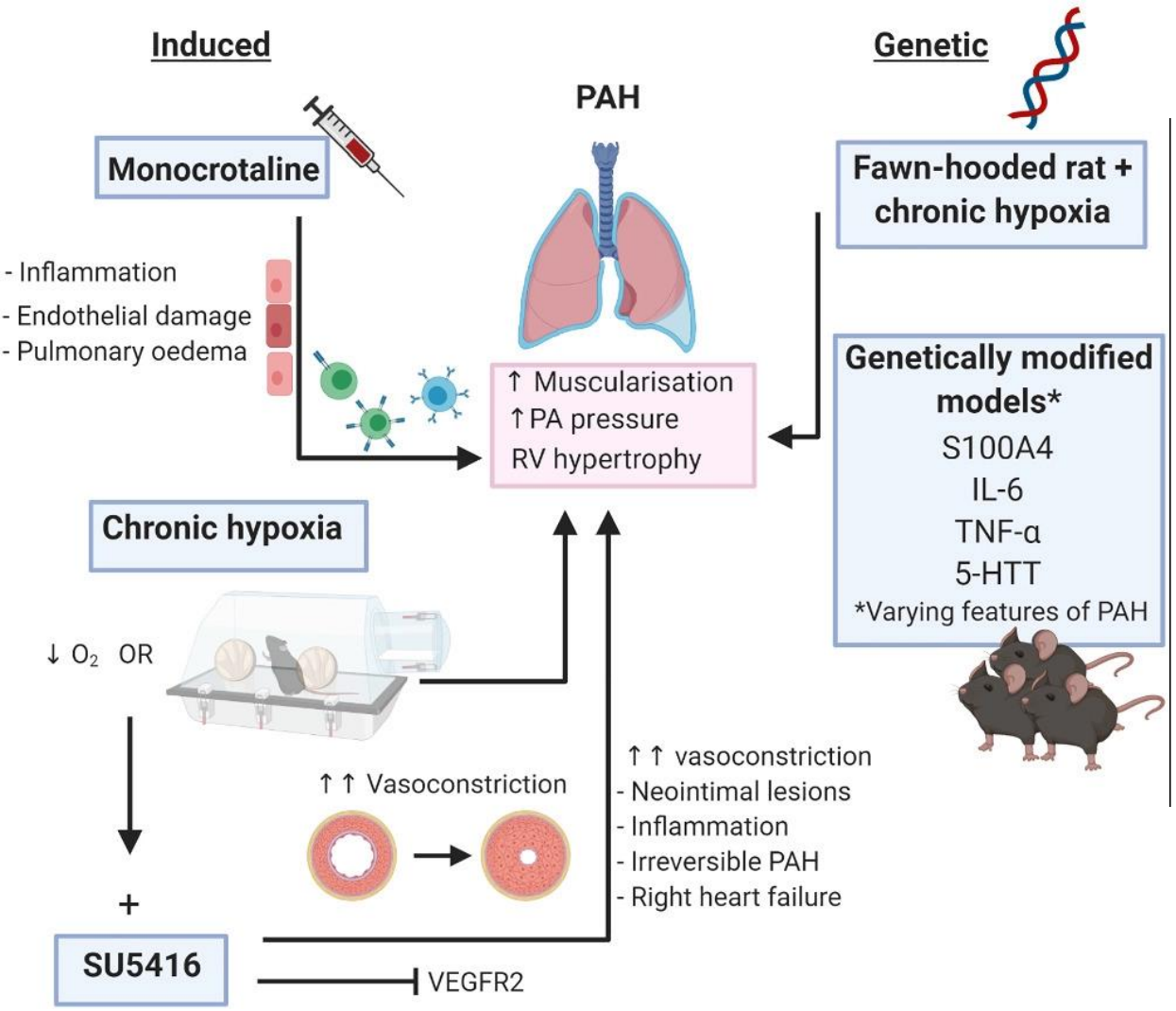

Část 1: optimalizace experimentálního modelu srdečního selhání s plicní vaskulopatií

1. Sham HanSD/placebo
2. IM HanSD/placebo
3. IM HanSD/SU5461

Série 1

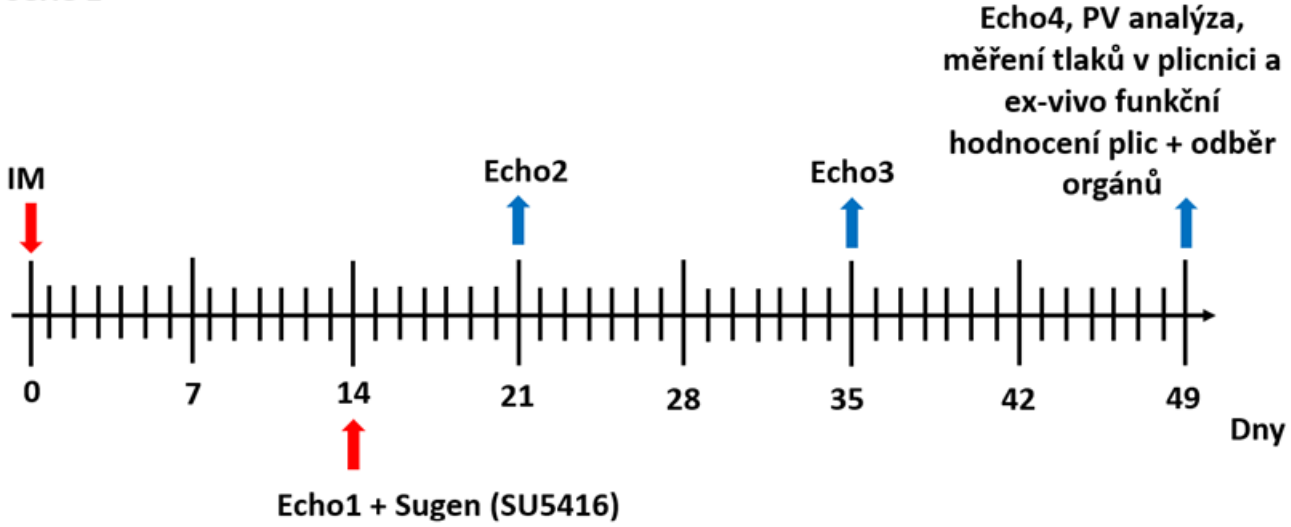

Basal values of arterial pressure

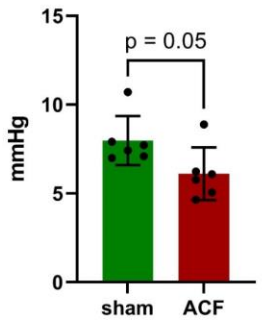

Precapillary resistance
(arterial occlusion)

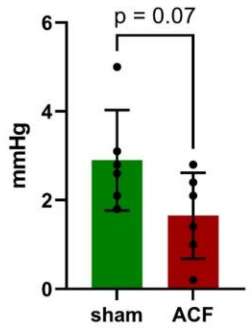

Postcapillary resistance
(venous occlusion)

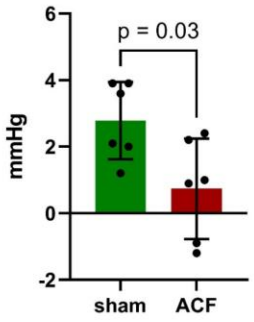

Capillary pressure
(average of arterial and venous pressure after combination of occlusions)

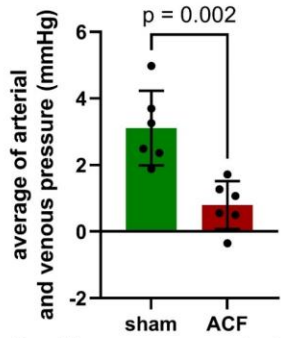

Arterial pressure in hypoxia

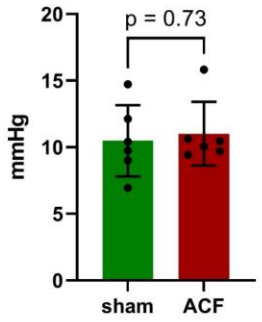

Arterial occlusion in hypoxia

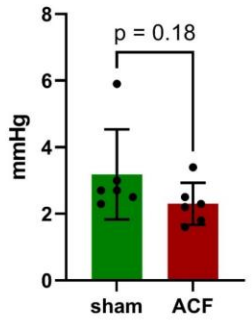

Venous occlusion in hypoxia

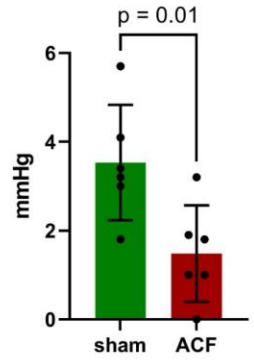

Capillary pressure in hypoxia
(average of arterial and venous pressure after combination of occlusions)

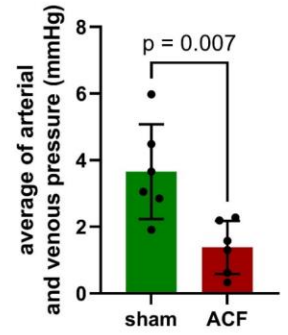

Increase in arterial pressure in hypoxia
(arterial pressure in hypoxia minus basal values)

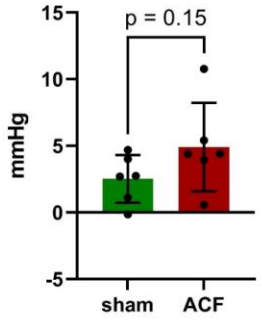

Norepinephrine increase
(pressure values after increase - pressure values before injection)

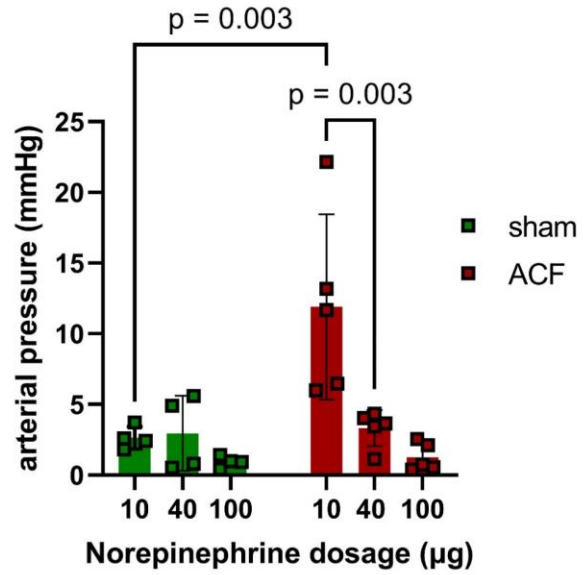

Pressure-flow (P/Q) arterial pressure

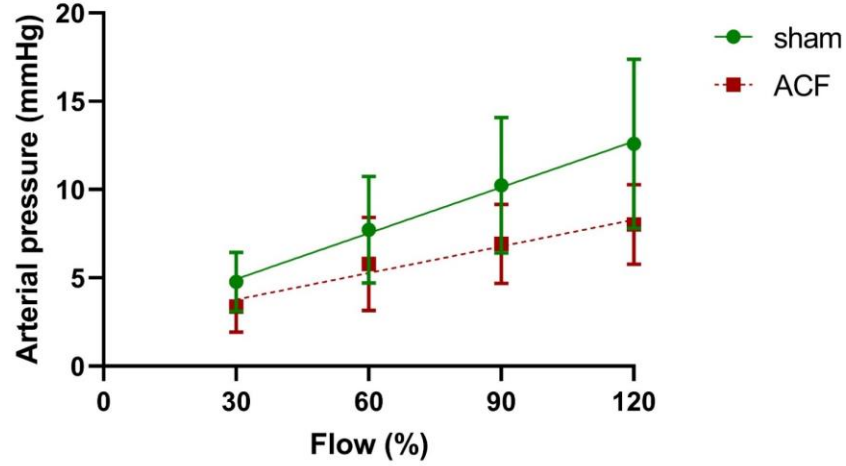

Arterial pressure increase after angiotensin II
(pressure values after increase - pressure values before injection)

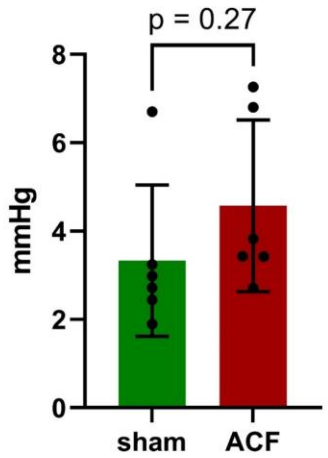

Pressure-flow (PQ) venous pressure

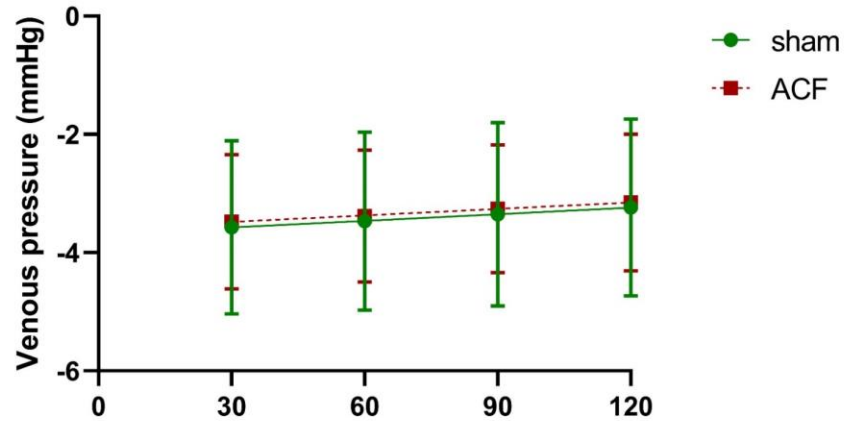

Modely CKD

- Fawn hooded hypertensive rats

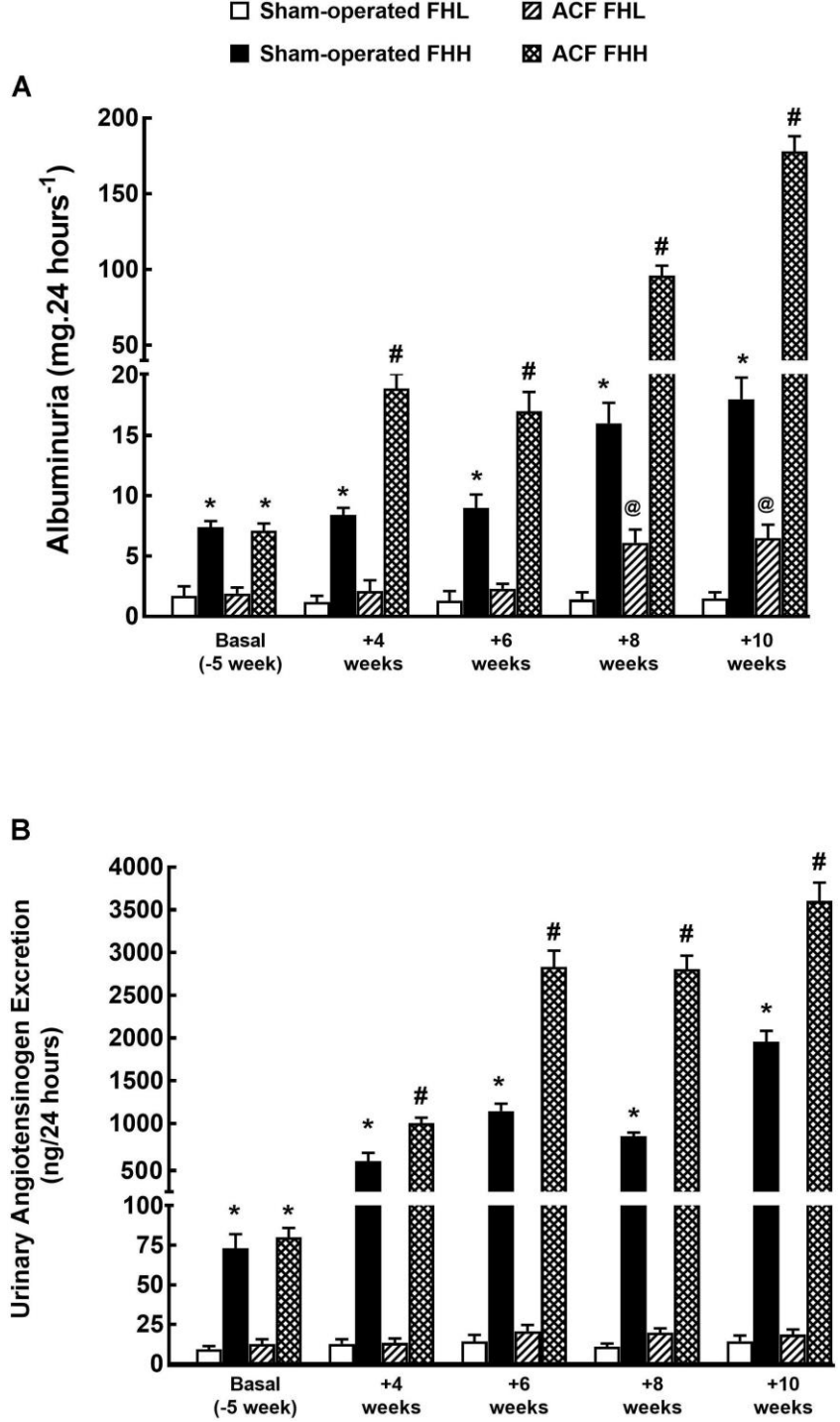

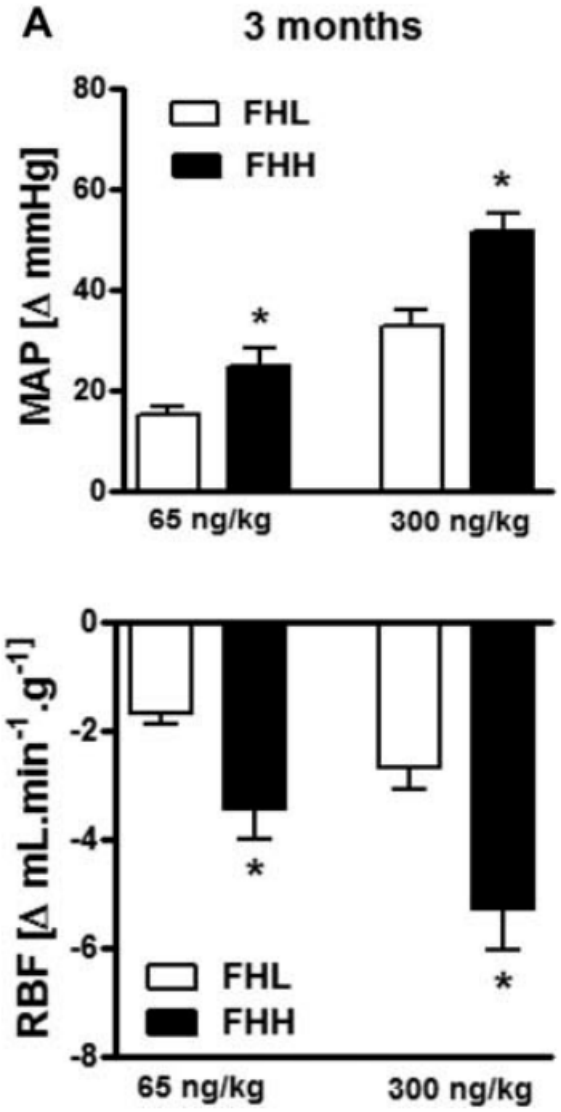

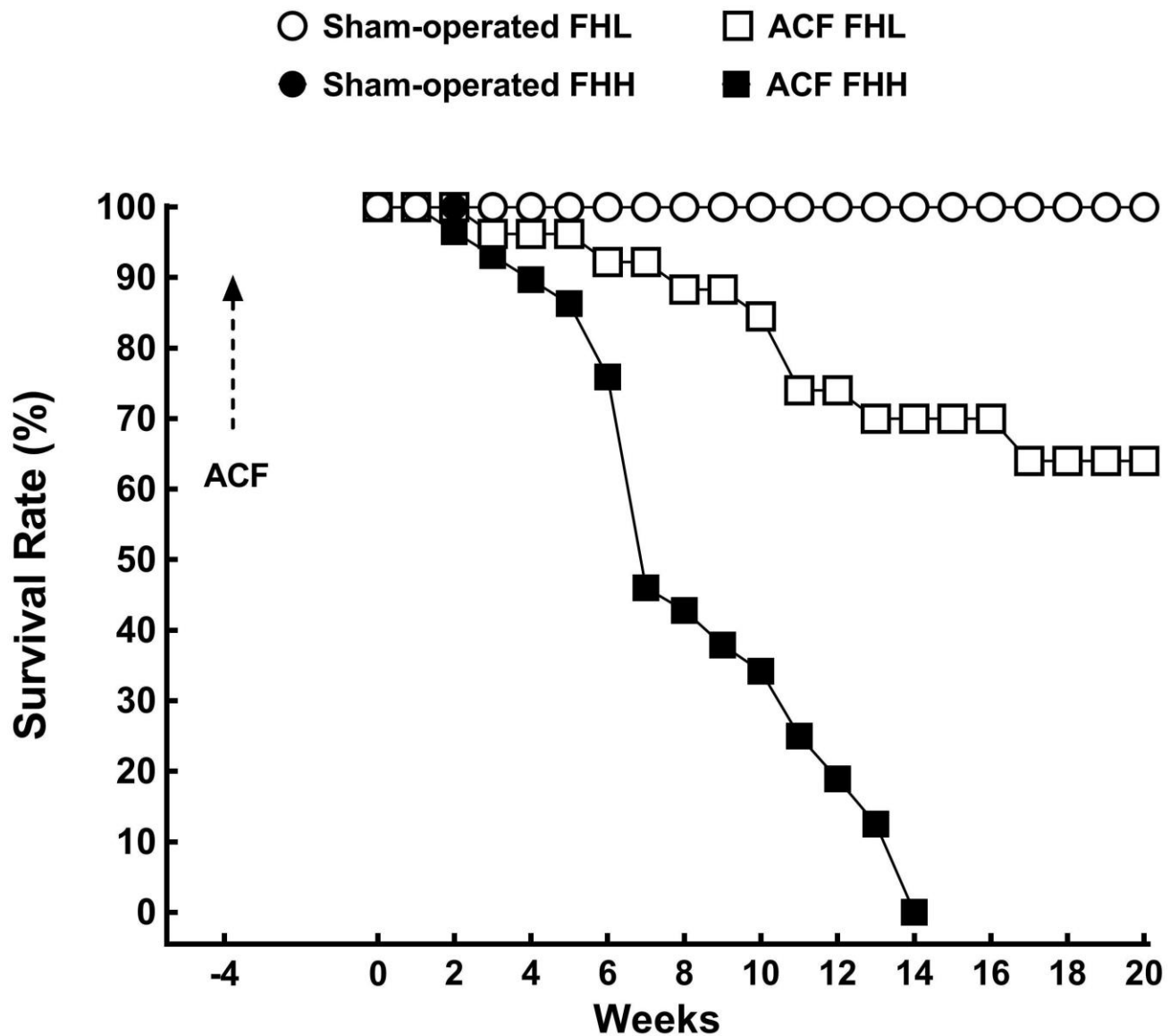

Honetschlagerová, Z., Škaroupková, P., Kikerlová *et al.,* (2021). Effects of renal sympathetic denervation on the course of congestive heart failure combined with chronic kidney disease: Insight from studies with fawn-hooded hypertensive rats with volume overload induced using aorto-caval fistula. *Clinical and experimental hypertension (New York, N.Y. : 1993)*, *43*(6), 522–535. https://doi.org/10.1080/10641963.2021.1907398

Table 1. Agents which cause cardiotoxicity.

Drug	Cardiotoxic effects	Mechanism of cardiac toxicity	Prevalence of cardiotoxicity	Reference
Trastuzumab	• Heart failure	• Damage to mitochondria	1–28%	[10]
Sunitinib, Sorafenib	• Heart failure • Acute coronary syndrome • Hypertension	• Inhibit tyrosine kinase pathway	3–8%	[11]
5-Fluorouracil	• Dilated cardiomyopathy • Ventricular arrhythmia • Sudden cardiac death			
Anthracyclines (Aggregate dose)	• Heart failure	• Production of free radicals	2%	[18]
Doxorubicin (>500mg/m²)				
Liposomal doxorubicin (>900mg/m²)				
Epirubicin (>720mg/m²)				
Imatinib, desatinib, nilotinib	• Heart failure	• Inhibit *ABL* tyrosine kinase in cardiac muscle cells	1.7%	[13]
Bevacizumab	• Hypertension • Congestive heart failure	• Unknown	50%	[14]
Cisplatin	• Hypertension	• Generation of oxidative stress	Unknown	[15]
		• Direct cellular toxicity • Lipid peroxidation	2.3–8%	[16]
		• Unknown	7–28%	[17]
Anthracyclines (Aggregate dose)	• Heart failure	• Production of free radicals	2%	[18]

Sangweni, N. F., Gabuza, K., Huisamen, B., Mabasa, L., van Vuuren, D., & Johnson, R. (2022). Molecular insights into the pathophysiology of doxorubicin-induced cardiotoxicity: a graphical representation. *Archives of toxicology*, *96*(6), 1541–1550. https://doi.org/10.1007/s00204-022-03262-w

Kardiotoxicitou navodené HF

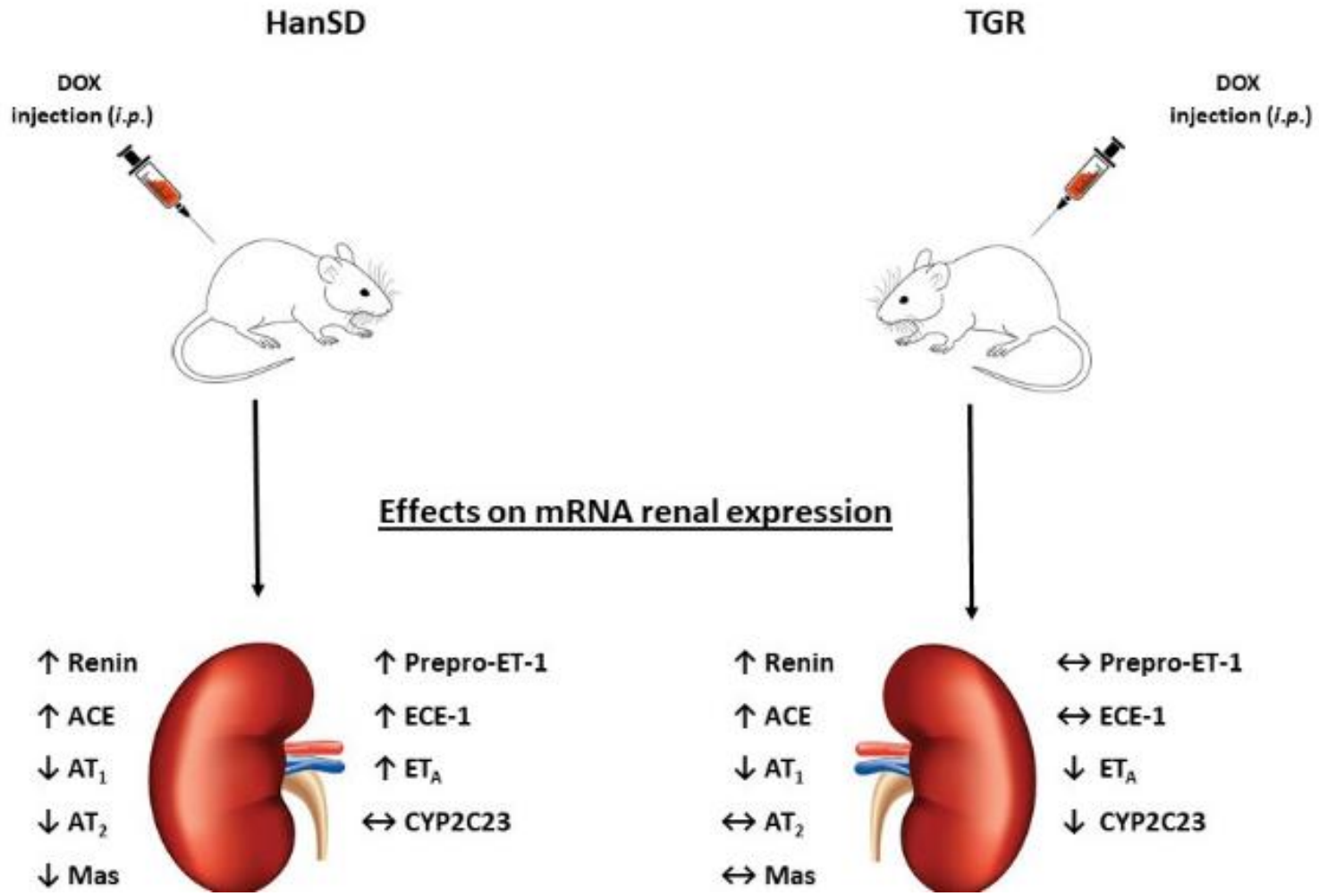

Jíchová, Š., Gawryś, O., Kompanowska-Jezierska, E., Sadowski, J., Melenovský, V., Hošková, L., Červenka, L., Kala, P., Veselka, J., & Čertíková Chábová, V. (2021). Kidney Response to Chemotherapy-Induced Heart Failure: mRNA Analysis in Normotensive and *Ren-2* Transgenic Hypertensive Rats. *International journal of molecular sciences*, *22*(16), 8475. https://doi.org/10.3390/ijms22168475

Doxorubicin model HF

- oxidative stress through cardiac iron overload.
- inflammatory response and resultant.
- mitochondrial dysfunction.
- autophagy.
- apoptosis via the intrinsic pathway.

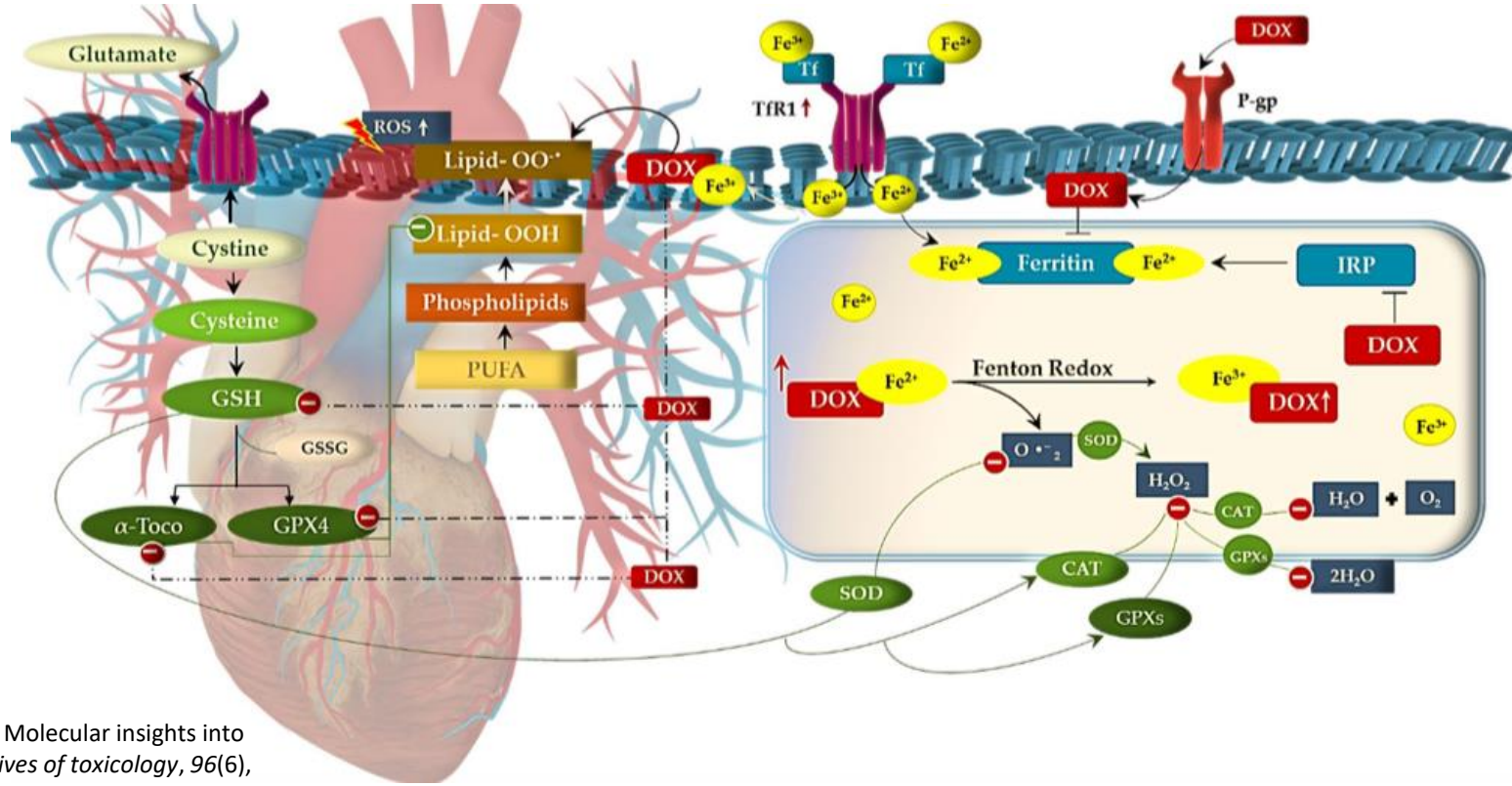

Sangweni, N. F., Gabuza, K., Huisamen, B., Mabasa, L., van Vuuren, D., & Johnson, R. (2022). Molecular insights into the pathophysiology of doxorubicin-induced cardiotoxicity: a graphical representation. *Archives of toxicology*, *96*(6), 1541–1550. https://doi.org/10.1007/s00204-022-03262-w

Control TGR

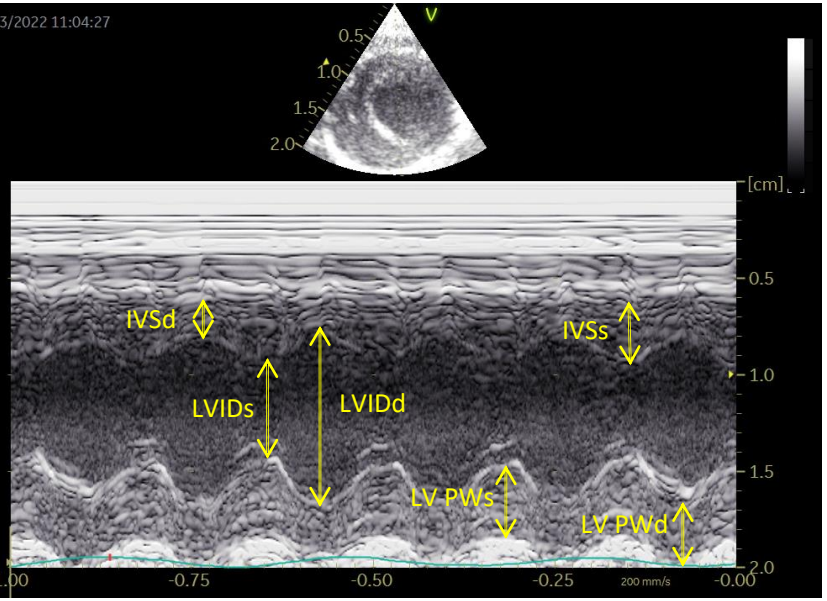

Doxo 2w TGR

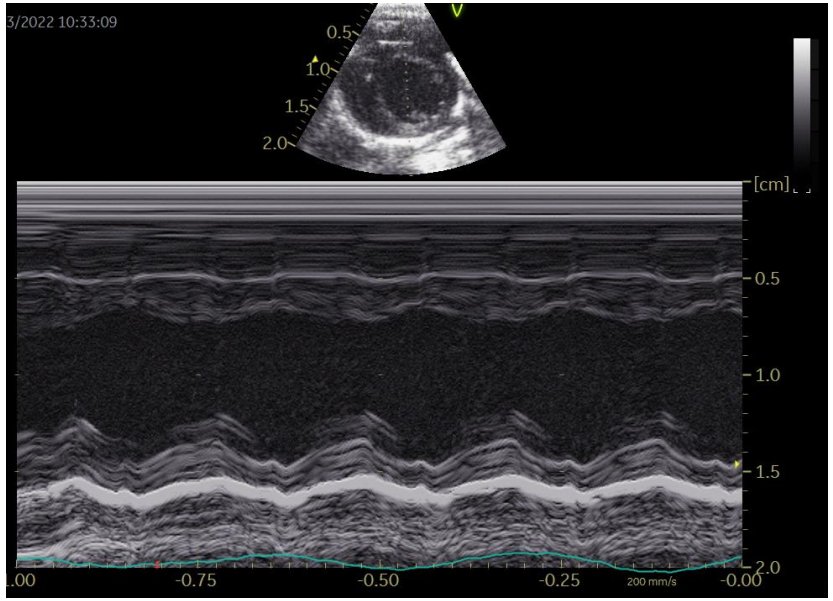

Doxo 5w TGR

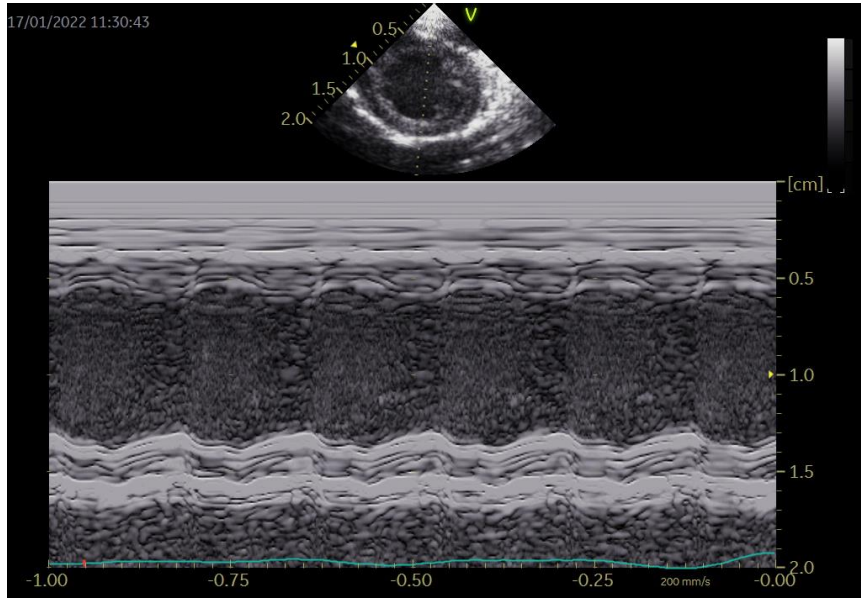

IVSd, IVSs – interventricular septum diameter in end-diastole and systole

LVIDd, LVIDs – left ventricular internal diameter in end-diastole and systole

LV PWd, LVPWs – left ventricular posterior wall diameter in end-diastole and systole

Unpublished data

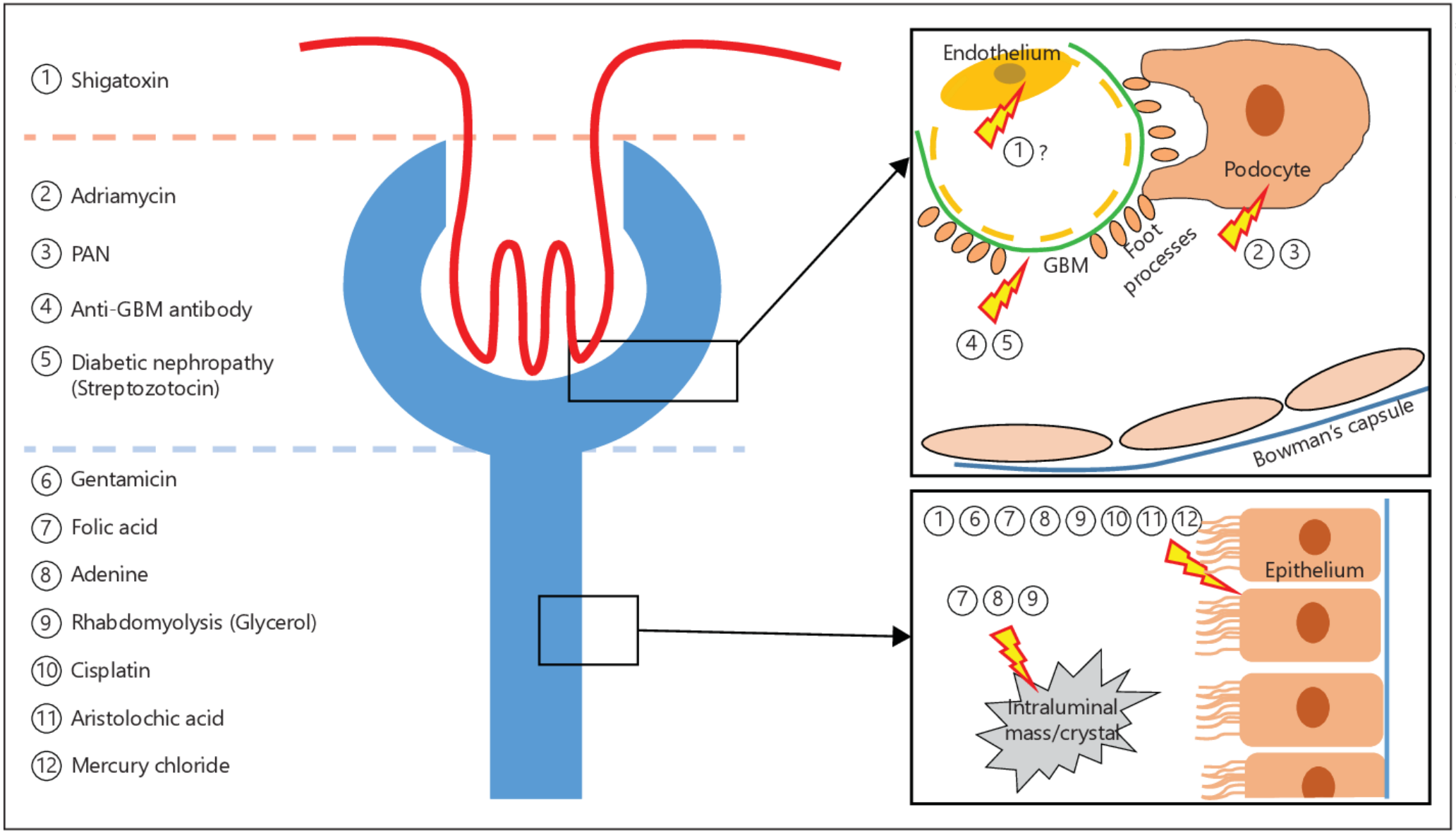

Rabe, Michael and Franz Schaefer. "Non-Transgenic Mouse Models of Kidney Disease." Nephron 133 (2016): 53 - 61.

Experimentálne animálne modely atriálnej fibrilácie

- Pacing induced tachycardia
- Electrically induced AF
- Mono-causal AF

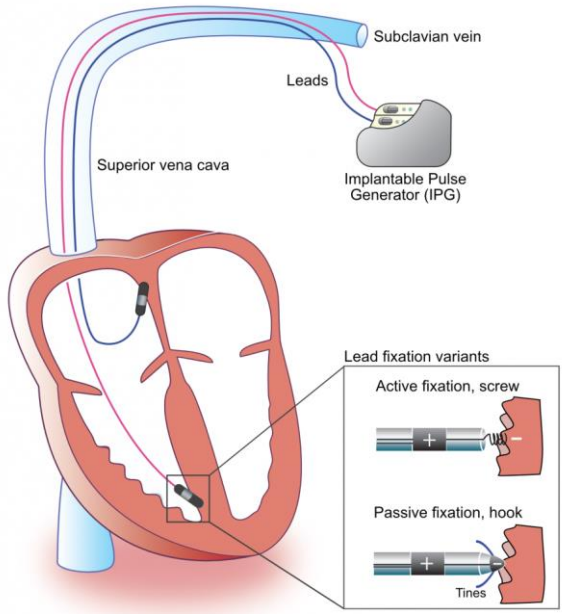

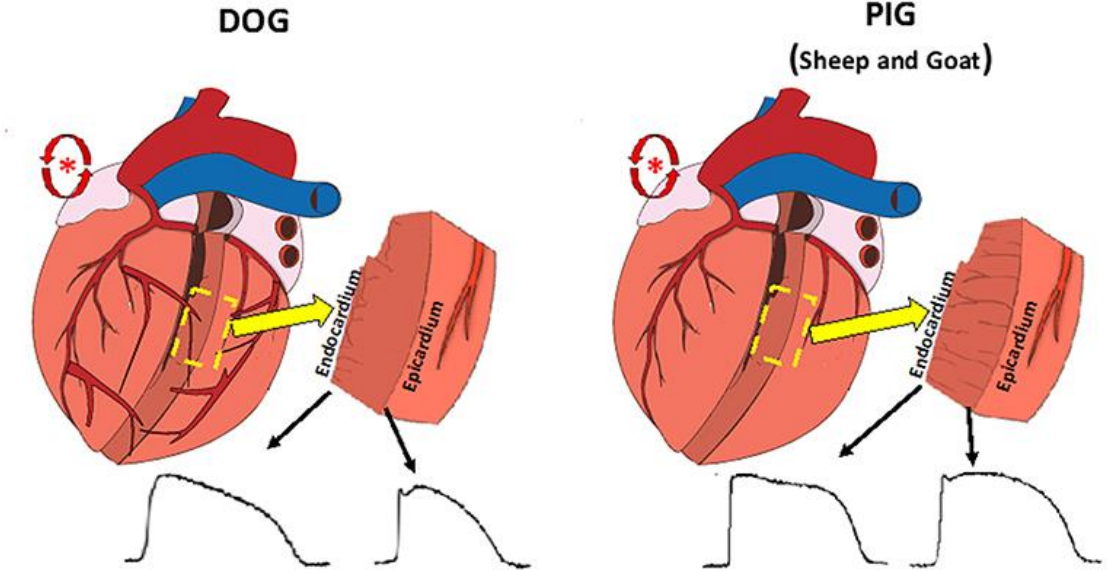

Cardiac Anatomy and Electrophysiology	Dog	Pig	Sheep	Goat
Heart Size vs. man	Similar	Very similar	Similar	Smaller
Coronary Anatomy	Extensive collaterals	Very similar to man	Similar to man but variability between animals	Similar to man and uniform between animals
Purkinje Network	Not transmural: similar to man	Transmural	Transmural	Transmural
Cellular Electrophysiology	Similar APs and ionic currents, maybe more heterogeneous	Similar APs and ionic currents, but lacks I_{to}	Similar APs and transmural heterogeneities	Similar APs to man
VF susceptibility	Similar to man	High	High	
Disease Models				
MI induced VT/VF	++	++	+	+
Cardiac Resuscitation	+	++		
Ischemic Heart Failure	+	++	+	
Non ischemic HF	++	+		
LQTS/Proarrhythmia	++	+		
AF/AFl	++	++		++

Piktel JS, Wilson LD. Translational Models of Arrhythmia Mechanisms and Susceptibility: Success and Challenges of Modeling Human Disease. Front Cardiovasc Med. 2019 Sep 10;6:135. doi: 10.3389/fcvm.2019.00135. PMID: 31552276; PMCID: PMC6748164.

Experimentálne animálne modely chlopňových vád

Kalcifikované ochorenie aortálnej chlopne (Calcific aortic valve disease)

- Mouse: Male Notch1+/− mice fed for 10 months with a Western diet
- New Zealand White rabbits subjected to 1K1C model

Chlopňová nedomykavosť a stenóza

- Pacing-induced heart failure with tricuspidal insufficiency (sheep)
- Supravalvular aortic stenosis by surgical banding of the aorta (Cat, dog, sheep, pig)

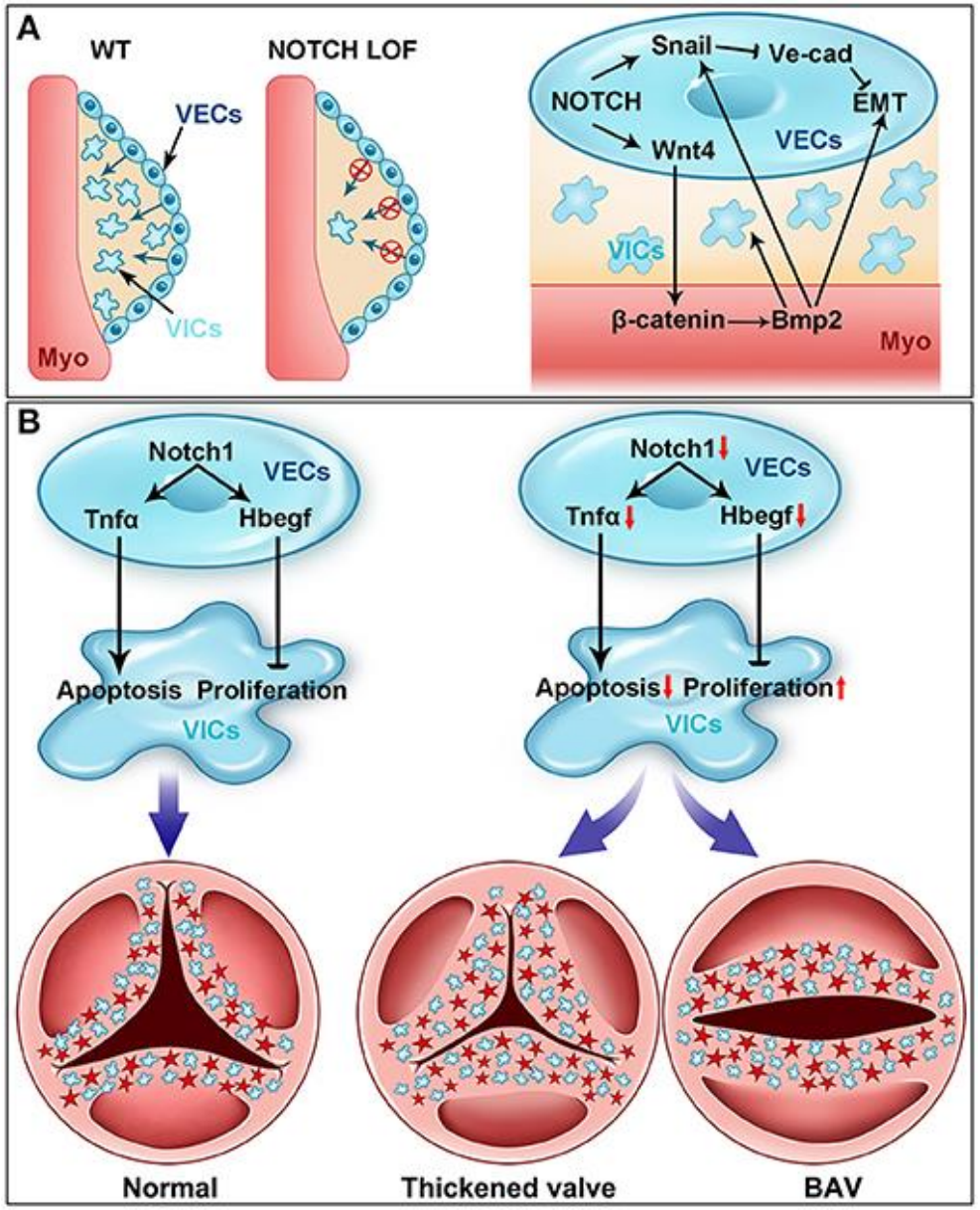

Wang, Y., Fang, Y., Lu, P., Wu, B., & Zhou, B. (2021). NOTCH Signaling in Aortic Valve Development and Calcific Aortic Valve Disease. *Frontiers in cardiovascular medicine*, *8*, 682298. https://doi.org/10.3389/fcvm.2021.682298

Experimentálne animálne modely aterosklerózy

- Familial hypercholesterolaemia (pig)
- Transgenic mice with lack of genes involved in lipid metabolism (LDL-receptor, apolipoprotein E)

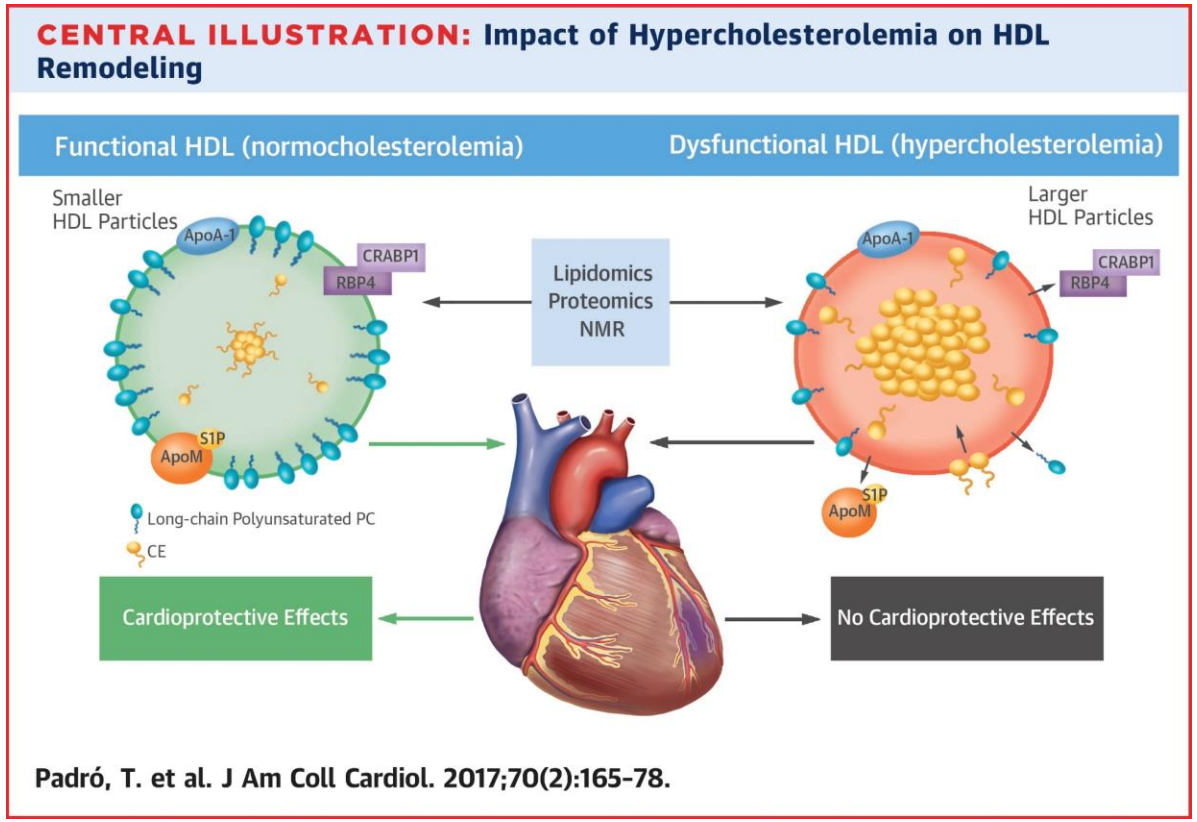

HFpEF a HFrEF

HFpEF vs HFrEF

More Information Online WWW.DIFFERENCEBETWEEN.COM

	HFpEF	HFrEF
DEFINITION	HFpEF is a complex cardiovascular syndrome caused by left ventricular diastolic dysfunction	HFrEF is a complex cardiovascular syndrome caused by left ventricular systolic dysfunction
PHASE	Diastolic phase	Systolic phase
EJECTION FRACTION	Greater than 50%	Lower than 40%
CAUSE	Left ventricle's muscles are too stiff or thickened	Muscles of left side of the heart do not squeeze properly
RESULT	Left ventricle fails to fill with blood properly	Left ventricle fails to pump the amount of blood that body needs
DYSFUNCTION	Left ventricular diastolic dysfunction	Left ventricular systolic dysfunction

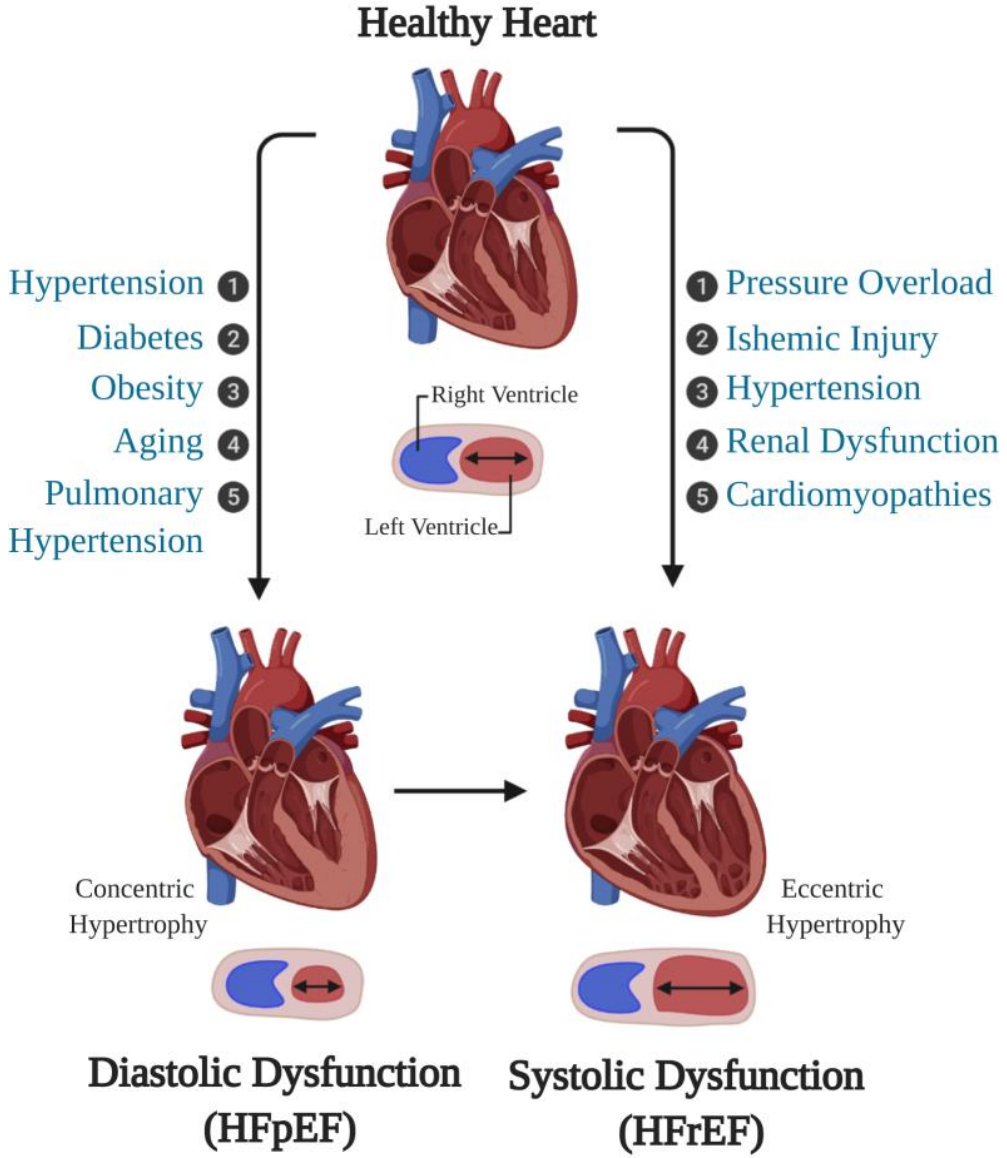

"Heart Failure With Preserved Ejection Fraction (Diastolic Heart Failure)." Heart Failure With Preserved Ejection Fraction (Diastolic Heart Failure) | Michigan Medicine

Noll NA, Lal H, Merryman WD. Mouse Models of Heart Failure with Preserved or Reduced Ejection Fraction. Am J Pathol. 2020 Aug;190(8):1596-1608. doi: 10.1016/j.ajpath.2020.04.006. Epub 2020 Apr 25. PMID: 32343958; PMCID: PMC7416075.

HFpEF experimentálne modely

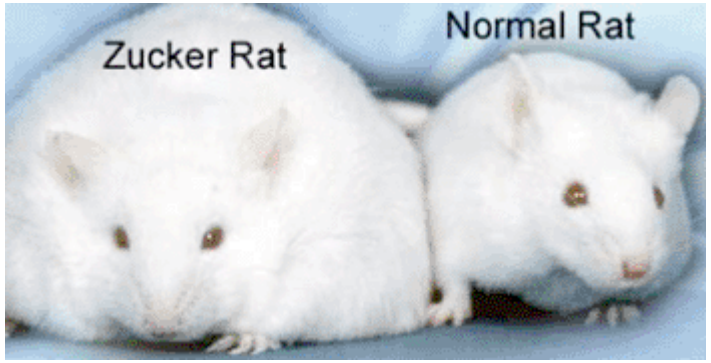

- ZDF (Zucker Diabetic Fatty) rats
- Otsuka Long-Evans Tokushima Fatty rats
- Dahl Salt-sensitive-Obese rats
- Rats with aortic banding
- LV pressure overload by an implantable stent or inflatable aortic cuff in pigs or cats
- L-NAME plus high-fat diet in mice

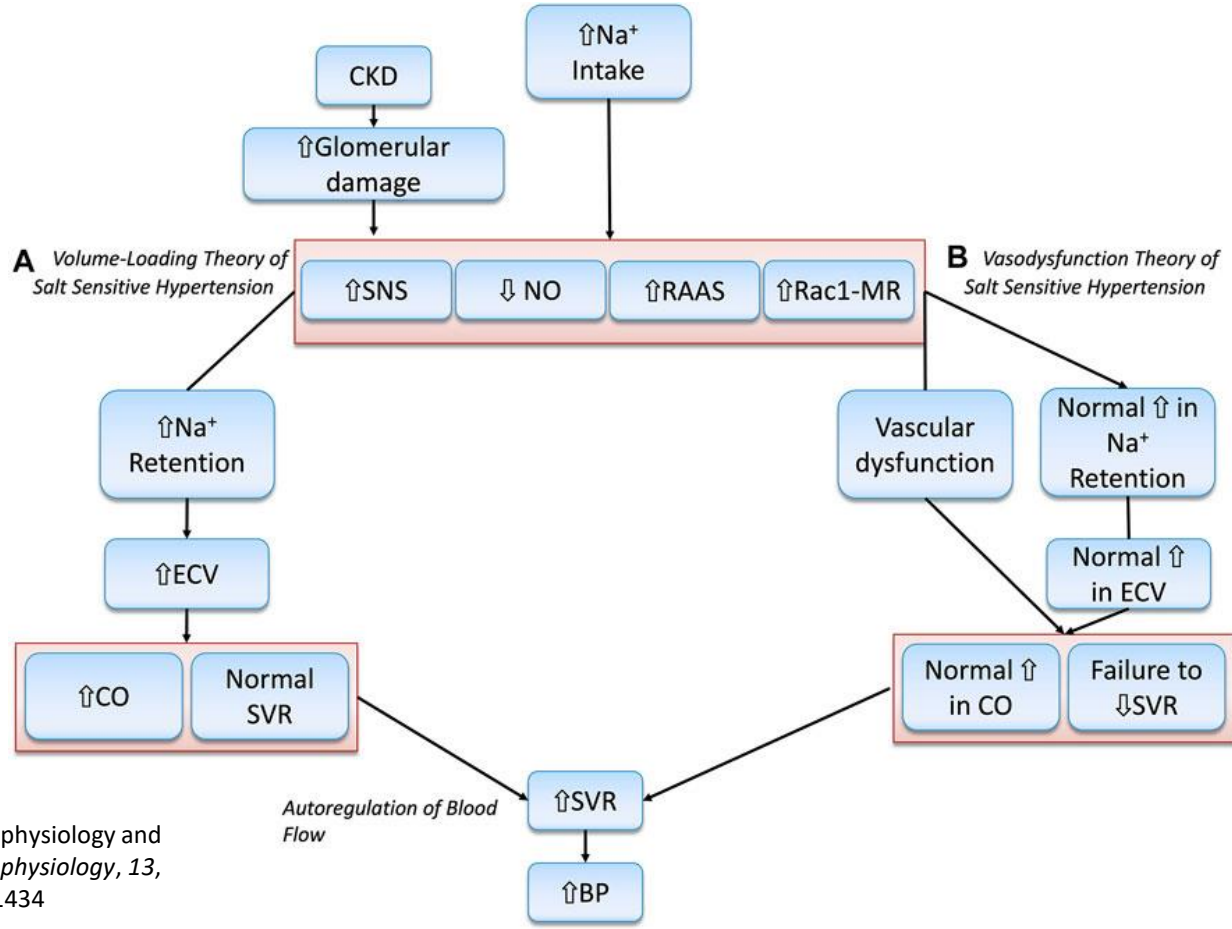

Maaliki, D., Itani, M. M., & Itani, H. A. (2022). Pathophysiology and genetics of salt-sensitive hypertension. *Frontiers in physiology*, *13*, 1001434. https://doi.org/10.3389/fphys.2022.1001434

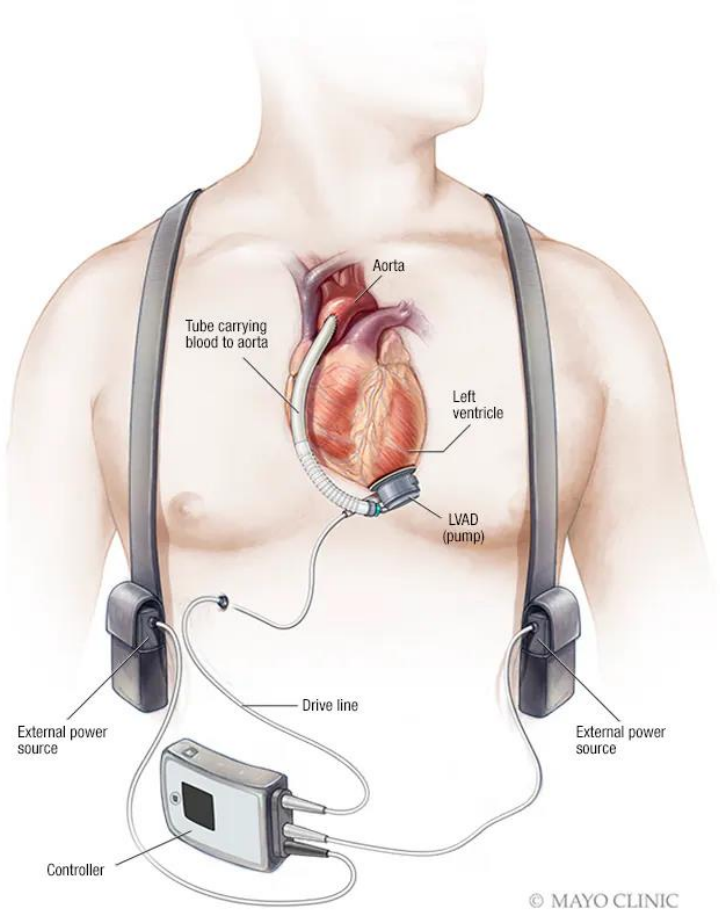

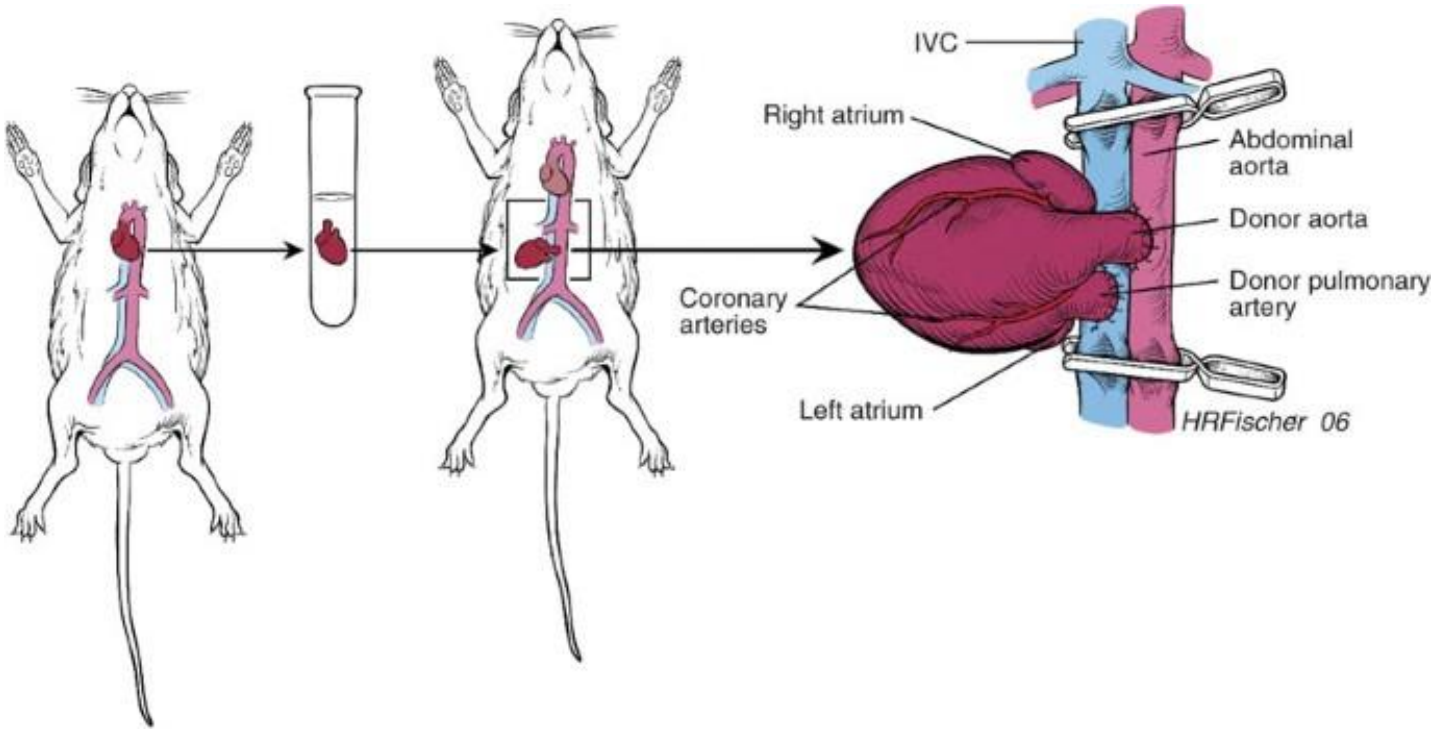

Hasegawa, T., Visovatti, S., Hyman, M. *et al.* Heterotopic vascularized murine cardiac transplantation to study graft arteriopathy. *Nat Protoc* **2**, 471–480 (2007). https://doi.org/10.1038/nprot.2007.48

Množstvo animálnych modelov genetických modifikácii

Gene	Human phenotype	Animal model	Animal phenotype	Pathogenesis
a-MHC	HCM	murine TG R403Q [51]	HCM	myocyte disarray, fibrosis, atrial dilation
Caveolin3	HCM	murine KO [52]	HCM, DCM, cardiac dysfunction	ERK1/2 activation, Src signaling
Caveolin3	HCM	murine TG P104L [53]	HCM, enhanced contractility, apoptosis	nNOS production, altered endoplasmic reticulum (ER) stress response
Caveolin3	HCM	zebrafish KO [54]	cardiac edema	myoblast fusion defects
Titin	DCM, HCM	zebrafish [55]	cardiac edema, poor contraction	blockage of sarcomere assembly
Tropomyosin	HCM	murine TG E180G [56]	HCM, fibrosis and atrial enlargement	increased myofilament sensitivity to Ca^{2+}.
Tropomyosin	HCM	murine TG D175N [57]	HCM, contractility and relaxation reduction	thin filament enhanced Ca^{2+} sensitivity
Troponin T	CM	murine TG MyHC [58]	HCM, reduced number of myocytes	multiple cellular mechanisms
Troponin T	CM	murine TG R92Q [60]	mitochondrial pathology, diastolic dysfunction	induction of ANP and bMHC
Troponin T		zebrafish KO [64]	sarcomere loss and myocyte disarray	dysregulation of thin filament protein expression
Troponin I	HCM	murine TG R145G [65]	HCM, diastolic dysfunction, death.	increased Ca^{2+} sensitivity and hypercontractility
Troponin I	HCM	rabbit TG R145G [66]	HCM and Cx43 disorganization	altered fractal pattern of the repolarization phase
Troponin I	HCM	murine KO [67]	acute HF, shortened sarcomeres	reduced Ca^{2+} sensitivity, elevated resting tension
MyBPC	HCM	murine TG [68]	sarcomere disorganization	stable truncated protein
MyBPC		murine KO [69]	HCM, reduced myofilament stiffness	abnormal sarcomere shortening velocity
MyBPC	HCM	cat TG [70]	sarcomeric disorganization	
Myopalladin	DCM HCM	murine TG Y20C [63]	HCM and heart failure	desmin, DPS, Cx43 and vinculin disruption
CARP	HCM DCM	murine TG αMHC [62]	HCM in response to pressure overload stress	reduced TGF-β, ERK1/2, MEK and Smad3
CARP	HCM DCM	murine KO [71]	No cardiac phenotype	
Talin	HCM	murine CS-KO [61]	HCM, hypercontraction to pressure overload	blunted ERK1/2, p38, Akt, and Gsk3 after stress
SGLT1		Tg CS-siRNA KD [72]	HCM, HF	
Meox1		Tg CS [73]	HCM	
ROCK		murine KO [74]	HCM	re-activation of fetal gene expression
cMyBPC	CM	murine KO [75]	HCM	dysregulation of Xirp2 and Zbtb16
β-MHC		rabbit TG R403Q [76]	HCM	reduced rates of force development and relaxation
CSRP3	HCM	murine KI C58G [77]	HCM	protein depletion via Bag3 and proteasomal overload
MYH7	HCM	pig KI R723G [78]	HCM, HF	myocyte disarray and malformed nuclei
TNNT2		murine R92Q; E163R [79]	HCM	altered myofilament Ca^{2+} sensitivity
αMHC	HCM	murine Arg403Gln [80]	HCM	altered repolarizing voltage-gated K^+(Kv) current
ERBB2		murine Tg [81]	HCM, diastolic dysfunction	ErbB2 signaling

Gene	Human phenotype	Animal model	Animal phenotype	Pathogenesis
Sarcoglycan (delta)	DCM	murine KO [82]	focal necrosis, fibrosis after stress	destabilization of dystrophin glycoprotein complex (DGC), membrane permeability defect, Ca^{2+} imbalance
Sarcoglycan (delta)	DCM	murine KI S151A [83]	mild DCM	
Sarcospan	DMD	murine KO [84]	progressive DMD, extensive degeneration and regeneration.	
Laminin-a2		murine KO [85]	DCM	disruption of extracellular matrix (ECM) - cytoskeleton connection
Dystrophin	XL-DCM	murine [86]	dilated ventricles	destabilization of DGC, sarcolemma-actin connection, Ca^{2+} alteration
Dystrophin	XL-DCM	zebrafish [87]	mutants are less active	
Dystrophin	XL-DCM	canine [88]	DMD and DCM phenotype	
Tropomyosin	DCM	murine KO [89]	homozygous null mice are embryonic lethal (E8-E11.5)	
Tropomyosin	DCM	murine TG E54K [90]	DCM, impaired cardiac function	decrease in Ca^{2+} sensitivity and tension generation
Desmin	DCM	murine TG R173del179 [91]	DCM, intra-sarcoplasmic granular aggregates	blunted response to beta-agonist stimulation
Desmin	DCM	zebrafish [92]	disorganized muscles, small larvae	vulnerability during eccentric work
Desmin	DCM	murine KO [93]	DCM, mitochondrial abnormalities, necrosis	multisystem disruption of muscle architecture
MLP	DCM	murine KO [94]	DCM with hypertrophy and heart failure	altered mechano-sensation
Nebulette	DCM	murine TG [95]	DCM, mitochondrial abnormalities	stretch induced alteration of Z-disk assembly
Nexilin	DCM	zebrafish [96]	Z-disk damage, heart failure	stretch induced Z-disk destabilization
Telethonin	DCM	murine KO [97]	heart failure following biomechanical stress	modulation of nuclear p53 turnover after stress
Telethonin	DCM	zebrafish [98]	deformed muscle structure and impaired swimming ability	disruption of sarcomere-T-tubules ILK
Cypher/ ZASP	DCM	murine KO [99]	DCM, Z disk disruption, muscle weakness	a-actinin or other Z-line components disruption
Filamin C	DCM	medaka zacrofish K1680X [100]	DCM, myocardial wall rupture	Disrupted structure of cardiac and skeletal muscles
Lamin A	DCM	murine KO N195K [101]	nucleo-cytoplasmic shuttling of Mlk1	modulation of actin polymerization via Mlk1
Lamin A	DCM	murine KO [102]	Cardiomyocyte degeneration and mineralization	emerin dislocation
αMHC-cre		CS-Cre [103]	DCM	activated p38, JNK, p53, Bax
Dhcr24 x cTnT R141W		Double Tg Dhcr24 x cTnT [104]	DCM	activation of PI3K/Akt/HKII pathway
MST1 x Gal3		murine TG x KO [105]	DCM, HF	dysregulated transcriptional signaling
MGAT1		CS KO [106]	DCM	altered Ca^{2+} handling
RBM20	DCM	murine KI S637A [107]	DCM	disturbed nuclear localization of RBM20
MLP x MYBPC3	Varied CMs	Double KO [108]	DCM	increased Ca^{2+} sensitivity
FXR1		CS-KO [109]	DCM	altered levels of FCR1
GSK-3β x cTnT		KO, DKO [110]	DCM, HF	myocardial fibrosis, and cardiomyocyte apoptosis
NEXN	DCM	KO [111]	DCM, EFE	collagen and elastin deposits
BIN1		CS-KO [112]	DCM	mislocalization of the Cav1.2

Gene	Human phenotype	Animal model	Animal phenotype	Pathogenesis
cTnI	CMs	murine KO [67]	shortened sarcomeres and elevated resting tension	reduced myofilament Ca^{2+} sensitivity
cTnI	RCM	murine Tg R193H [114]	RCM	increased Ca^{2+} sensitivity
cTnI	RCM	murine Tg R145W [115]	diastolic dysfunction	prolonged force and intracellular Ca^{2+} transients
MYPN	RCM	murine KI Q529X [116]	disrupted intercalated discs, heart failure	desmin, DSP, connexin43 and vinculin disruption
myosin		E143K [117]	RCM	

Gene	Human phenotype	Animal model	Animal phenotype	Pathogenesis
alpha-dystrobrevin	DMD, LVNC	murine KO	Muscle dystrophy, cardiomyopathy	Alteration in cyclic GMP levels
NKX2-5	CHD	murine KI R52G [141]	LVNC, atrial septal anomalies	cardiomyocyte differentiation and heart development
NKX2-5	CHD	inducible Cx40-cre ERT2 [142]	hypertrabeculation, heart failure	cardiomyocyte differentiation and heart development
Fkbp1a		murine KO [143]	DCM, VSD and LVNC	immunoregulation and protein folding and trafficking
Jarid2		murine KO [144]	VSD, LVNC, Double outlet RV	dysregulated embryogenesis
Mest		murine KO [145]	thickness and less dense compact myocardium	dysregulated embryogenesis
Mib1		murine KO [146]	LVNC	dysregulated Notch signaling
BRAF		murine KI Q241R [147]	embryonic/neonatal lethality, LVNC	
CASZ1		murine KO [148]	hypoplasia of myocardium, VSD	abnormal genes expression
ANT2		murine KO [149]	embryonic lethality, LVNC	failure in cardiac developmental
Daam1		murine KO [150]	VSD, LVNC, Double outlet RV	Wnt/PCP signaling
S1PR1		murine KO [151]	LVNC, VSD	S1P signaling
NUMB / NUMBL		murine KO [152]	LVNC	ERBB2, YAP1 STAT5 signaling
RLF		murine KO [153]	LVNC	NOTCH pathway
LRP2		murine KO [154]	LVNC, aortic arch and coronary artery anomalies, VSD	
SLC39A8		murine KO [155]	LVNC, ECM accumulation	decrease MTF1 activity
DTNA		murine Tg N49S [156]	DCM, LVNC, cardiac dysfunction	
SRC-1/3		murine KO [157]	LVNC	up-regulate cyclin E2, cyclin B1 and myocardin
INO80		murine KO [158]	LVNC, defect in coronary vessels	upregulation of E2F-activated genes a
Tafazzin (TAZ)	LVNC	murine KD [159]	Neonatal death, LVNC, VSD	Fatty acid metabolism

https://www.intechopen.com/chapters/68936

Kvantifikácia HF a obličkových funkcií

- Testy renálnych funkcií (GFR, proteinúria, albuminúria)
- Rádiotelemetria

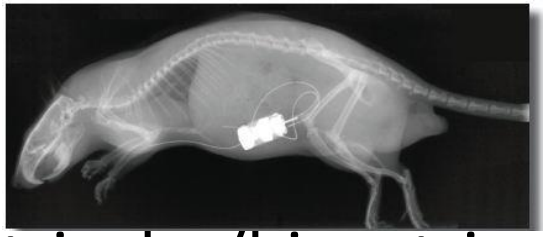

- Echo
- PV analýza (univentricular/biventricular)
- ECG
- Histológia a IHC (IM stress area, fibróza)
- Biochemické markery: Troponín, Nppa, katecholamíny (NA), ANG, sérum kreatinín, kyselina močová
- Génové a proteínové expresie

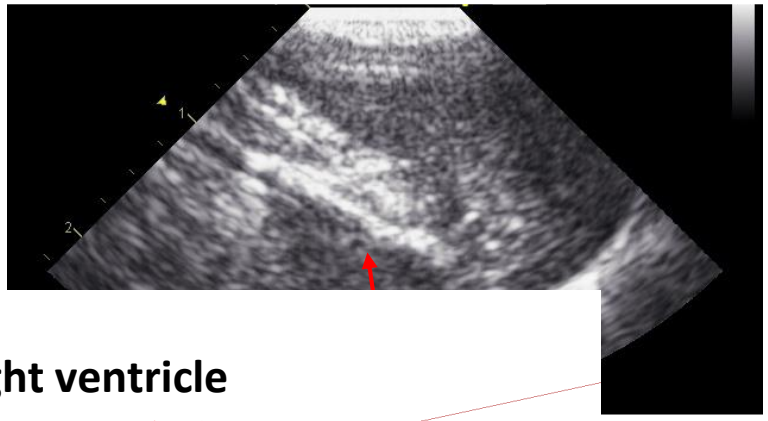

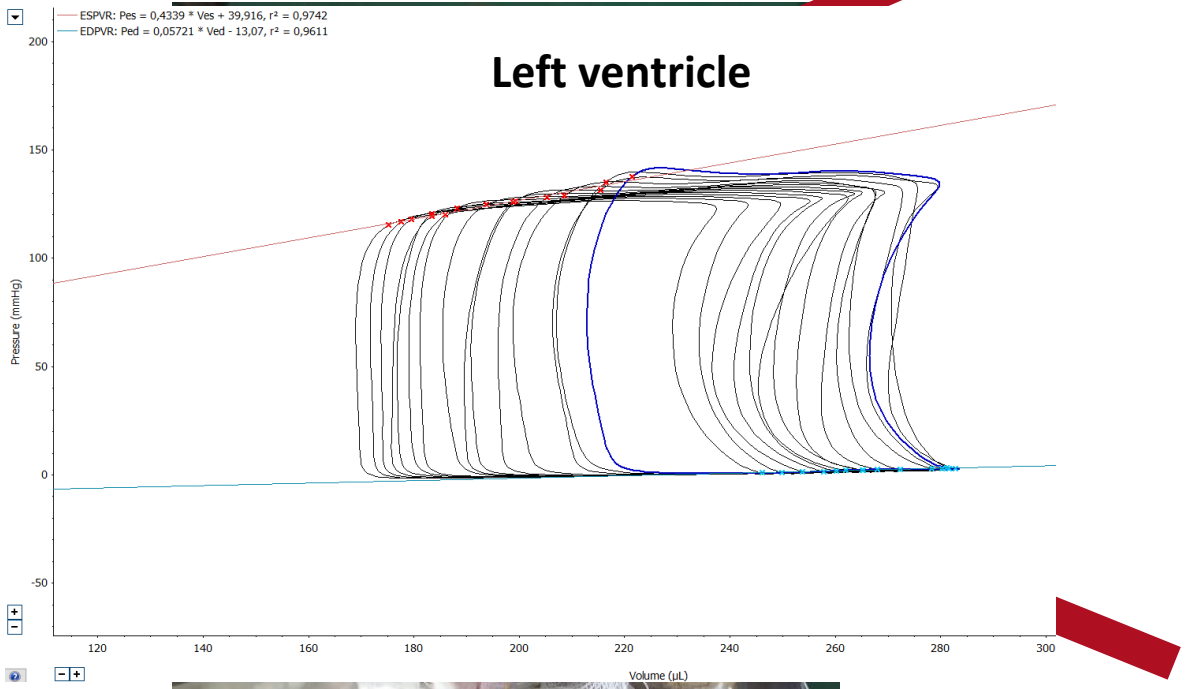

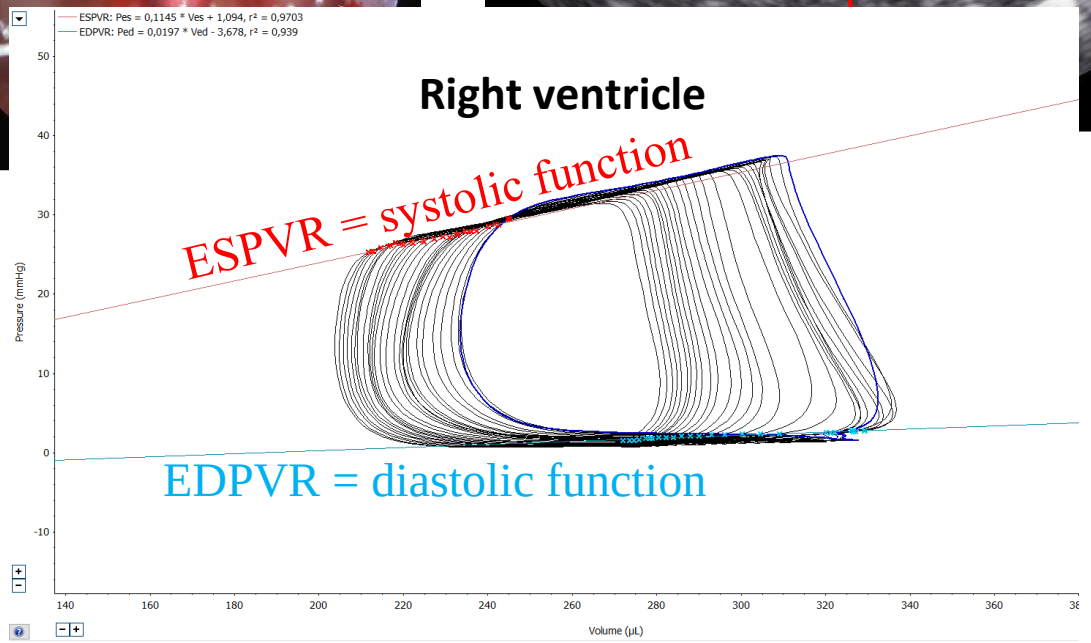

Miklovic, M., Kala, P., & Melenovsky, V. (2023). Simultaneous biventricular pressure-volume analysis in rats. *Journal of physiology and pharmacology : an official journal of the Polish Physiological Society*, *74*(2), 10.26402/jpp.2023.2.02. https://doi.org/10.26402/jpp.2023.2.02

JOURNAL OF PHYSIOLOGY AND PHARMACOLOGY 2023, 74, 2, 131-147
www.jpp.krakow.pl | DOI: 10.26402/jpp.2023.2.02

Original articles

M. MIKLOVIC[1,2], P. KALA[1,3], V. MELENOVSKY[1,4]

SIMULTANEOUS BIVENTRICULAR PRESSURE-VOLUME ANALYSIS IN RATS

[1]Center for Experimental Medicine, Institute for Clinical and Experimental Medicine - IKEM, Prague, Czech Republic; [2]Department of Pathophysiology, 2nd Faculty of Medicine, Charles University, Prague, Czech Republic; [3]Department of Cardiology, University Hospital Motol and 2nd Faculty of Medicine, Charles University, Prague, Czech Republic; [4]Department of Cardiology, Institute for Clinical and Experimental Medicine - IKEM, Prague, Czech Republic

Hypertension Research
https://doi.org/10.1038/s41440-024-01580-3

ARTICLE

Special Features - Renal Denervation and Sympathetic Nerve System

Renal denervation improves cardiac function independently of afterload and restores myocardial norepinephrine levels in a rodent heart failure model

Matúš Miklovič[1,2] · Olga Gawryś[1] · Zuzana Honetschlägerová[1] · Petr Kala[1,3] · Zuzana Husková[1] · Soňa Kikerlová[1] · Zdeňka Vaňourková[1] · Šárka Jíchová[1] · Alena Kvasilová[4] · Misuzu Kitamoto[4] · Hana Maxová[1,2] · Guillermo Puertas-Frias[5] · Tomáš Mráček[5] · David Sedmera[4] · Vojtěch Melenovský[1,6]

Received: 30 June 2023 / Revised: 4 December 2023 / Accepted: 24 December 2023

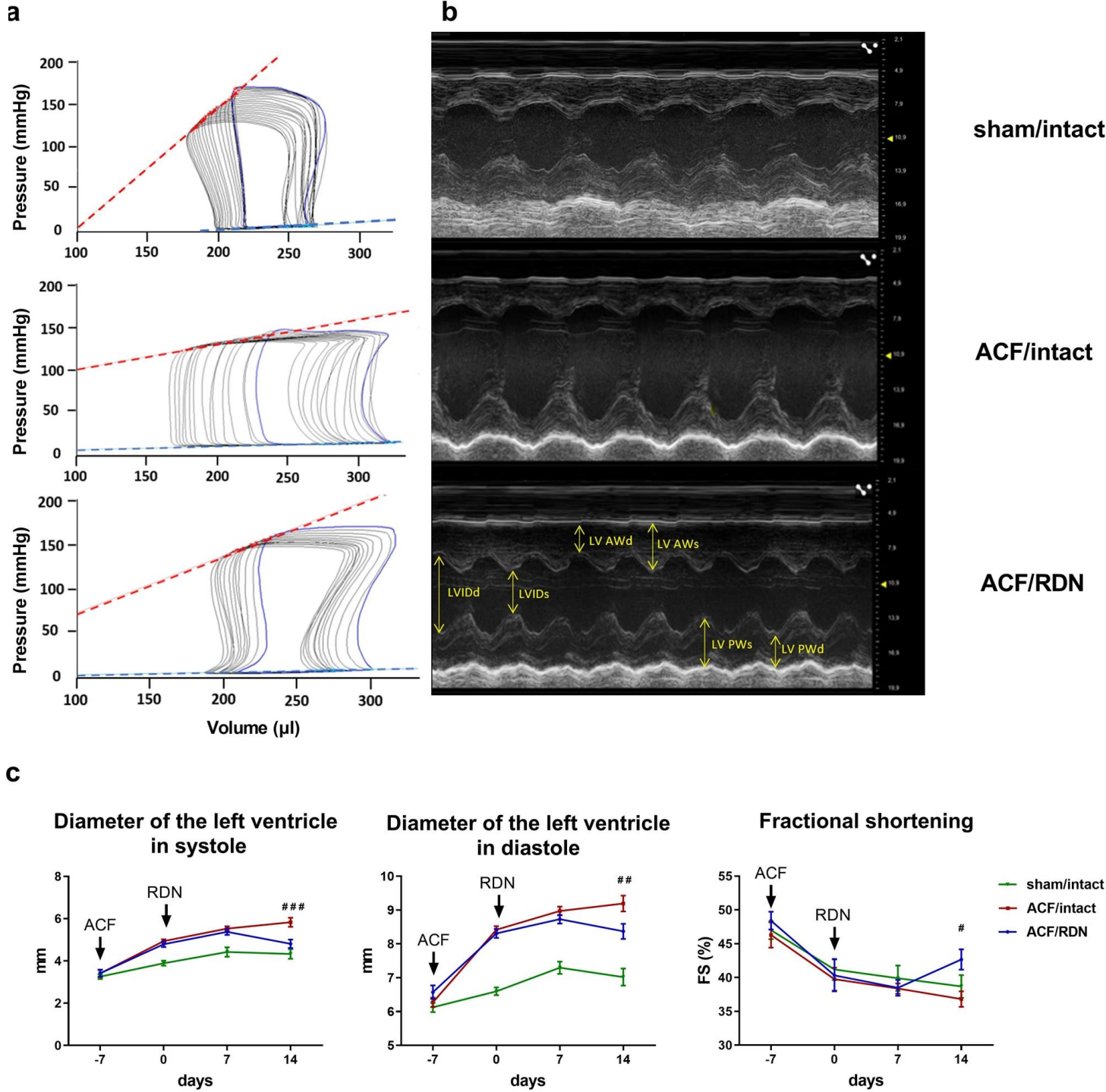

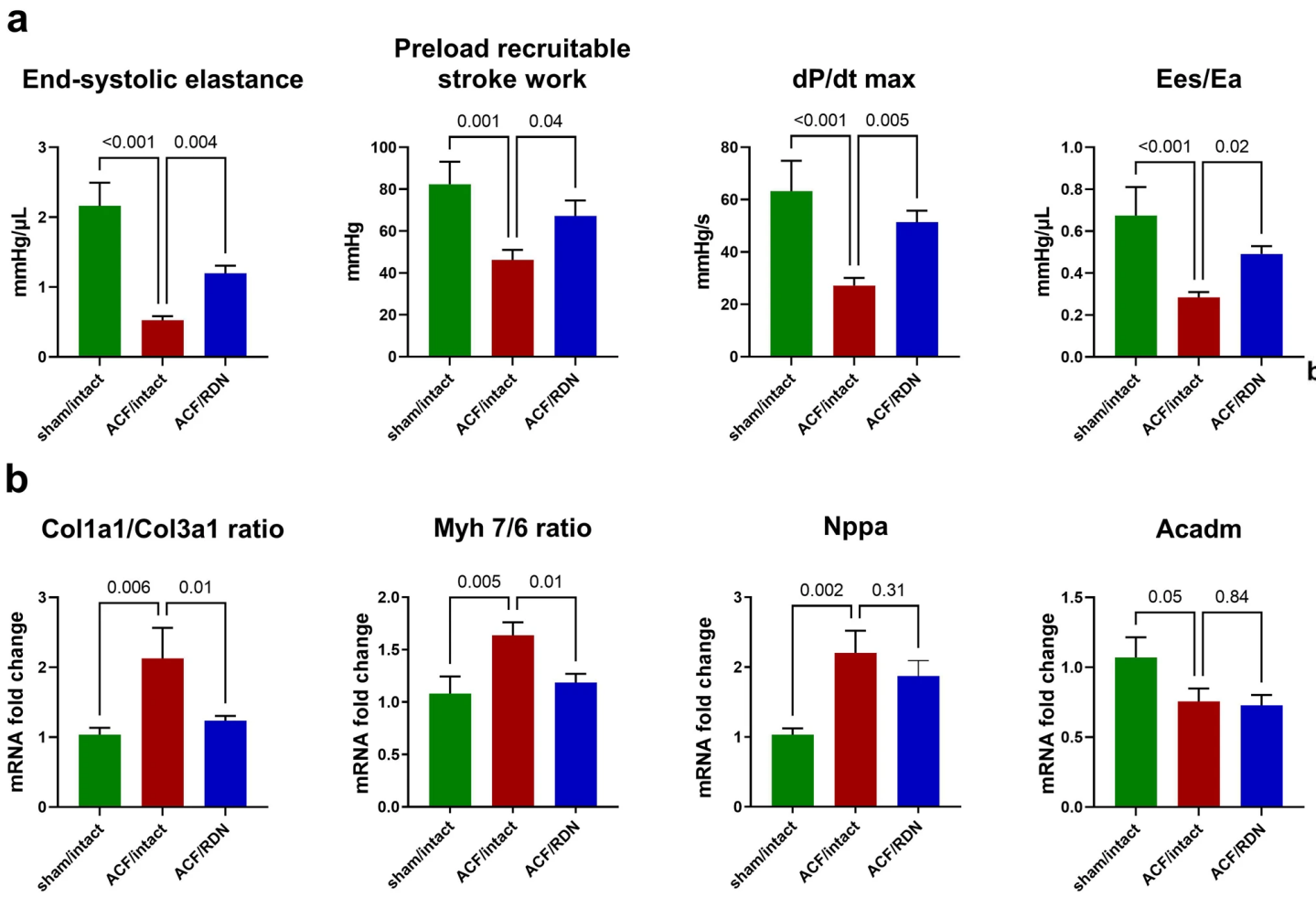

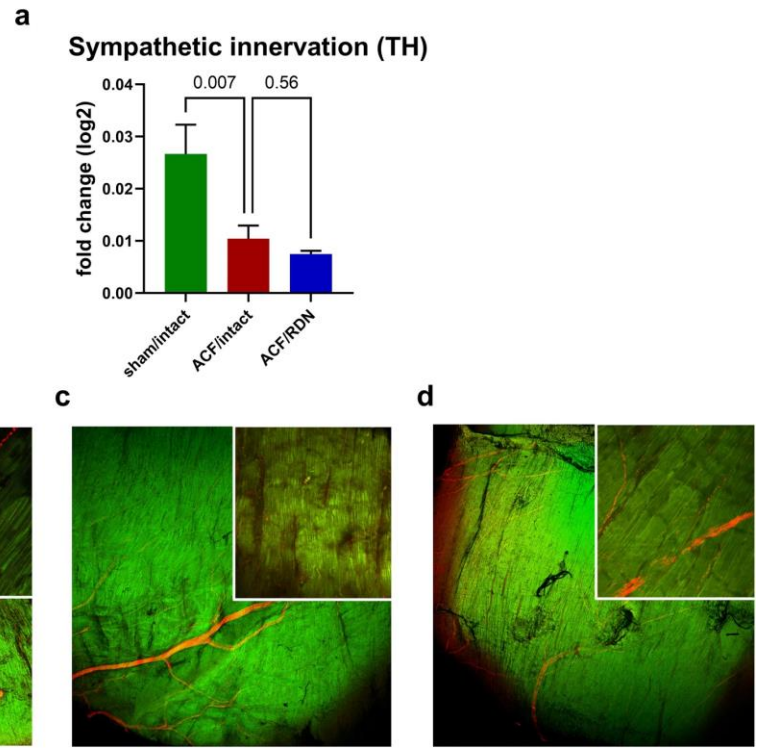

Miklovič, M., Gawryś, O., Honetschlägerová, Z. *et al.* Renal denervation improves cardiac function independently of afterload and restores myocardial norepinephrine levels in a rodent heart failure model. *Hypertens Res* (2024). https://doi.org/10.1038/s41440-024-01580-3

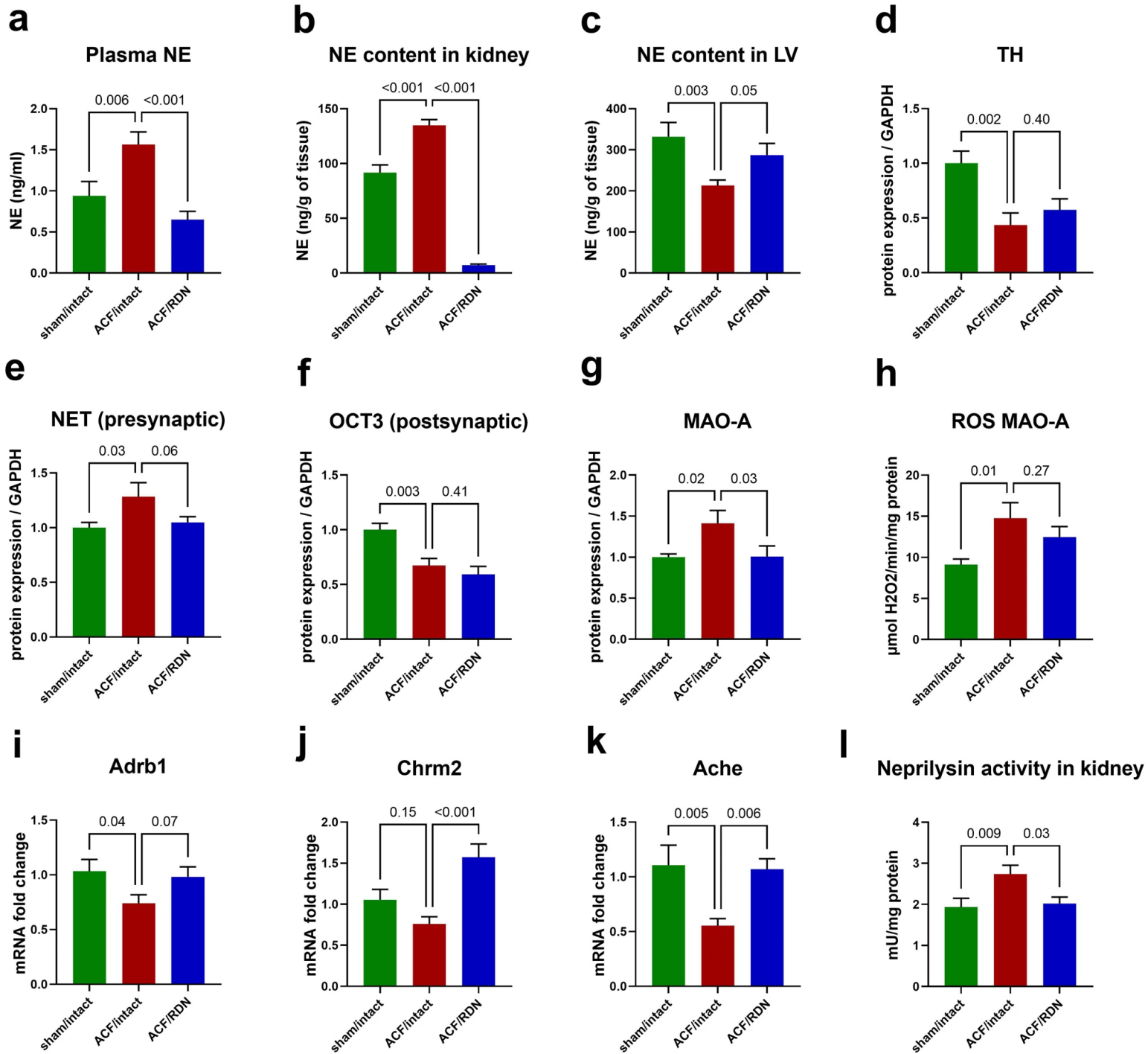
a
Plasma NE
NE (ng/ml)
0.006
<0.001
b
NE content in kidney
NE (ng/g of tissue)
<0.001
<0.001
c
NE content in LV
NE (ng/g of tissue)
0.003
0.05
d
TH
protein expression / GAPDH
0.002
0.40
e
NET (presynaptic)
protein expression / GAPDH
0.03
0.06
f
OCT3 (postsynaptic)
protein expression / GAPDH
0.003
0.41
g
MAO-A
protein expression / GAPDH
0.02
0.03
h
ROS MAO-A
µmol H2O2/min/mg protein
0.01
0.27
i
Adrb1
mRNA fold change
0.04
0.07
j
Chrm2
mRNA fold change
0.15
<0.001
k
Ache
mRNA fold change
0.005
0.006
l
Neprilysin activity in kidney
mU/mg protein
0.009
0.03
sham/intact
ACF/intact
ACF/RDN

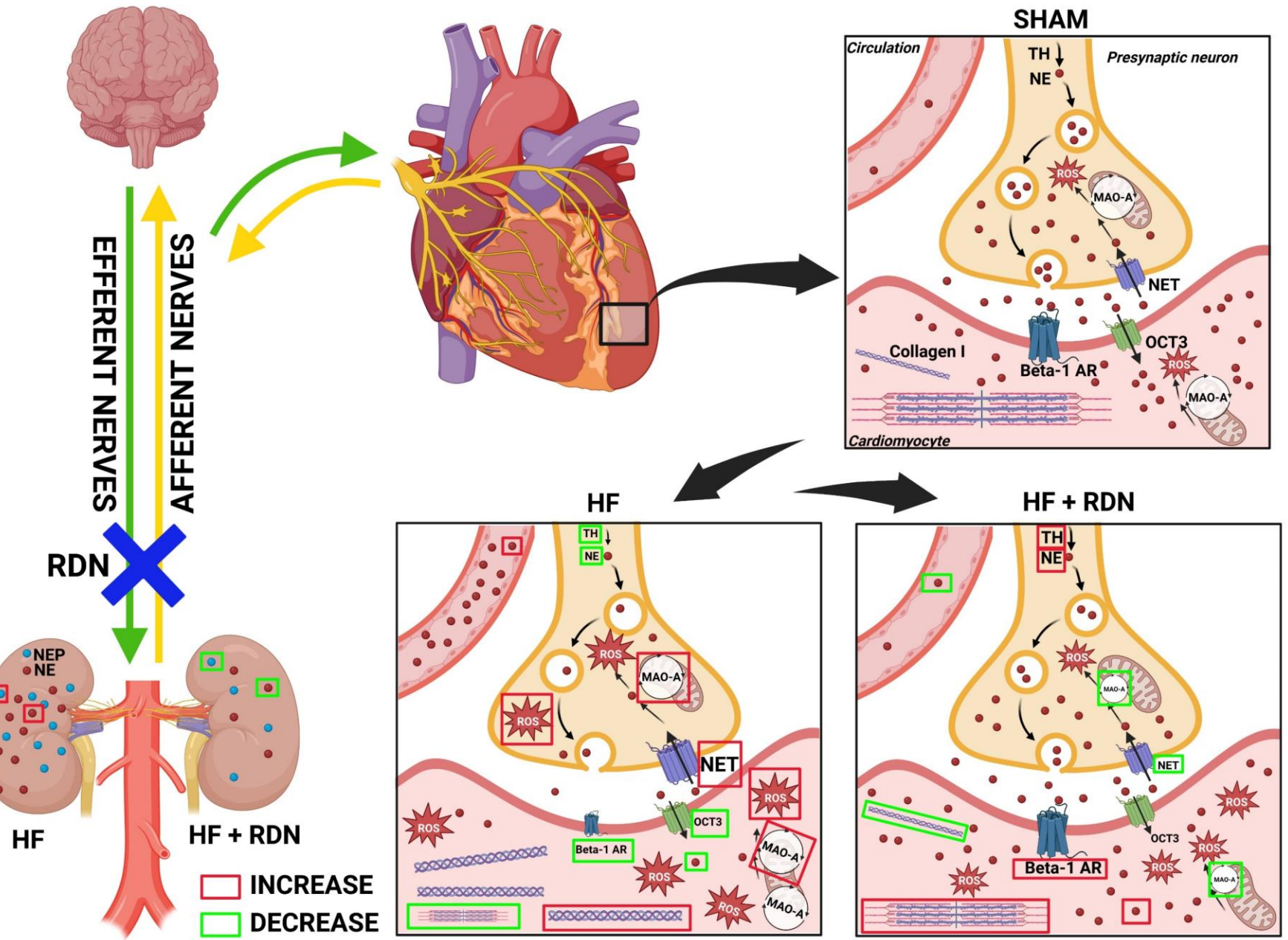

Miklovič, M., Gawryś, O., Honetschlägerová, Z. *et al.* Renal denervation improves cardiac function independently of afterload and restores myocardial norepinephrine levels in a rodent heart failure model. *Hypertens Res* (2024). https://doi.org/10.1038/s41440-024-01580-3

Čo môžu experimentálne štúdie priniesť študentom medicíny/doktorom?

- Pochopenie mechanizmov kardiovaskulárnych ochorení
- Testovanie potenciálnych liečiv – účasť na projektoch základného a preklinického výskumu a translačného výskumu
- Vlastný projekt - množstvo skúseností, spoluúčasť/písanie grantu
- Experimentálna kardiochirurgia-zručnosť
- Prezentovanie výsledkov, práca v tíme, rozšírenie obzorov a metodík
- Publikovanie v impaktovaných časopisoch, účasť na konferenciách
- Šanca objaviť doposiaľ nepoznané patofyziologické mechanizmy a prispieť k poznaniu závažných KVS chorôb

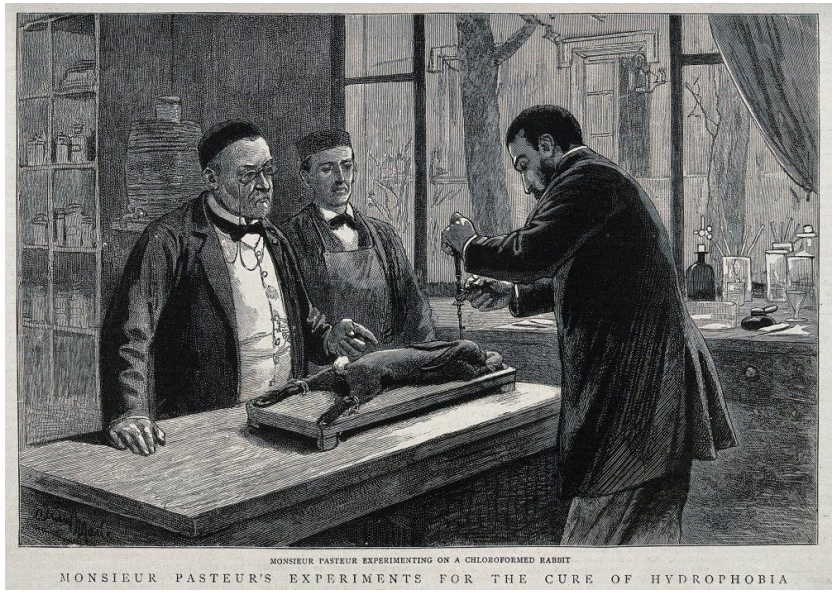

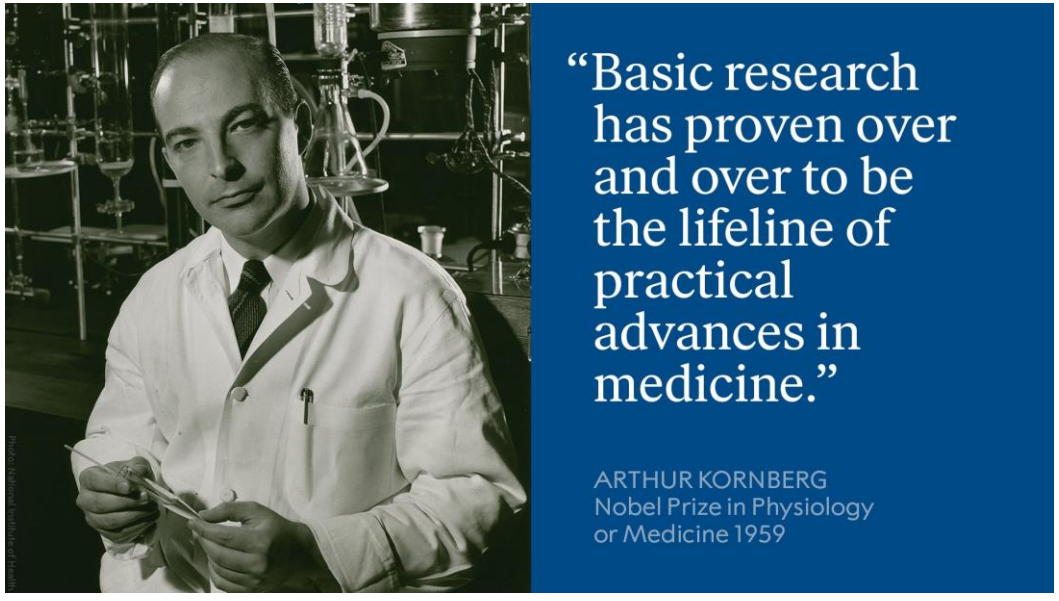

prof. MUDr. Vojtěch Melenovský, CSc.

prof. MUDr. Luděk Červenka, CSc. MBA

Doc. MUDr. Hana Maxová, PhD.

Mgr. Olga Gawryś, PhD.

MUDr. Petr Kala, PhD.

Mgr. Matej Molnár

Mgr. Šárka Jíchová, PhD.

Mgr. Soňa Kikerlová

Ing. Zdenka Vaňourková, PhD.

Bc. Petra Škaroupková

MVDr. Zuzana Honetschlägerová, PhD.

Mgr. Markéta Adamová, PhD.

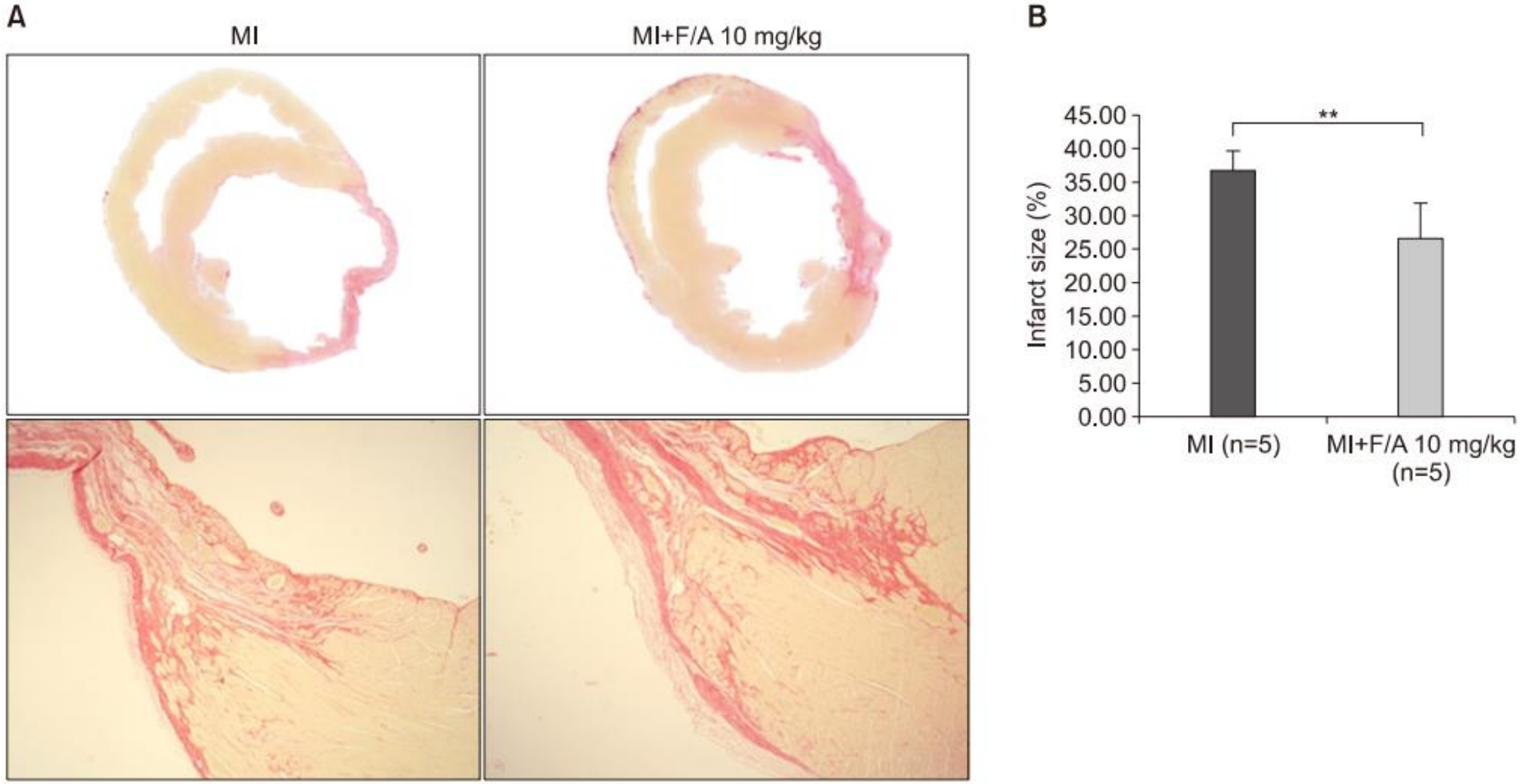

FIG. 3. (A) Picrosirius red stain and (B) measurement of infract size (%). MI: myocardial infarction, F/A: fimasartan/amlodipine. **p<0.01.